

ABSTRACT

Title of Document: MRP5/ABCC5, A CONSERVED ABC TRANSPORTER, REGULATES METAZOAN HEME HOMEOSTASIS

Tamara Korolnek, Doctor of Philosophy, 2014

Directed By: Professor Dr. Iqbal Hamza, Department of Animal and Avian Sciences

Hemes are metalloporphyrins used by nearly all organisms as cofactors for proteins involved in respiration, binding and sensing gases, and as catalysts for various reactions. Despite extensive knowledge about heme biosynthesis and catabolism, the pathways for transporting heme between cells and within cells remain poorly understood. *C. elegans* serves as a unique animal model for uncovering these pathways, as it is unable to synthesize its own heme and depends on the uptake of dietary heme for growth and reproduction. Functional RNAi screens implicated *mrp-5* as a potential heme transporter in *C. elegans*. This gene encodes a membrane-bound ABC transporter that localizes to the basolateral intestinal membrane and is required for worm growth and reproduction. Depletion of *mrp-5* activates heme deprivation signals within the worm, protects worms from toxicity associated with a toxic heme analog, and results in worms accumulating the fluorescent heme analog, zinc mesoporphyrin IX, in intestinal cells. Taken together, these results indicate a defect in

heme export from the intestine when MRP-5 activity is lost. Functional assays in yeast support the hypothesis that MRP-5 is capable of exporting heme across cell membranes, and that this function is conserved in the human ortholog. Knockdown of *mrp5* in zebrafish embryos results in developmental defects and decreased blood formation, indicating that this transporter likely regulates heme homeostasis in vertebrates. Loss of Mrp5 in mammalian cells leads to decreased heme transport into the secretory pathway as measured by activity of a Golgi-targeted heme-dependent enzyme. Furthermore, macrophages from mice lacking Mrp5 are unable to activate a number of cellular responses when undergoing erythrophagocytosis, the process whereby the heme-iron in senescent red bloods is recycled. Altogether, our results implicate MRP-5 as a key heme transporter in *C. elegans*, and point to an evolutionarily conserved role for MRP5 proteins in regulating heme homeostasis.

MRP5/ABCC5, A CONSERVED ABC TRANSPORTER, REGULATES
METAZOAN HEME HOMEOSTASIS

By

Tamara Korolnek

Dissertation submitted to the Faculty of the Graduate School of the
University of Maryland, College Park, in partial fulfillment
of the requirements for the degree of
Doctor of Philosophy
2014

Advisory Committee:
Professor Iqbal Hamza, Chair
Dr. Caren Chang
Dr. Eric Haag
Dr. Michael Krause
Dr. Heven Sze

© Copyright by
Tamara Korolnek
2014

Dedication

*When I heard the learn'd astronomer,
When the proofs, the figures, were ranged in columns before me,
When I was shown the charts and diagrams, to add, divide, and measure them,
When I sitting heard the astronomer where he lectured with much applause in the
lecture room,
How soon unaccountable I became tired and sick,
Till rising and gliding out I wander'd off by myself,
In the mystical moist night-air, and from time to time,
Look'd up in perfect silence at the stars*

Walt Whitman
"When I Heard the Learn'd Astronomer"

To my teachers and mentors,
Who taught me proofs, figures, charts, and diagrams,
And to those who taught me to appreciate the perfect silence of wonder

Acknowledgements

The work presented in this dissertation would not have been possible without the support and guidance of my committee, my advisor, my lab mates, my previous teachers and mentors, and my friends and family. I am incredibly thankful for the time and effort that others have spent helping me through the past six years and I could not have accomplished this without them.

I would like to thank the faculty and staff of both the MOCB program and the Animal Sciences department. Dr. Leslie Pick spoke to me the day that I interviewed at the University of Maryland and warmly welcomed me to the MOCB program. Dr. Lisa Taneyhill accepted me as a rotation student and her wonderful lab was a great introduction to the Animal Sciences department. Dr. Ian Mather's membrane trafficking course was the most challenging, interesting, and enjoyable science course I have ever taken. Dr. Tom Porter and Dr. Byung Eun Kim have constantly expressed their support for me. Dr. Liqing Yu was always available to discuss the nuances of ABC transporters.

Thank you to my committee members, Dr. Heven Sze, Dr. Michael Krause, Dr. Caren Chang, and Dr. Eric Haag. In science, time is incredibly precious, and I appreciate all the time and effort you have put in to see me through this degree. I appreciate the thoughtful questions, comments, and suggestions that have pushed me to be a better scientist.

I would also like to thank my previous teachers and mentors who have contributed to my training in the biological sciences. In grade school, Dr. Joel Goodman asked me where plants came from and I was delighted to answer correctly. He then asked me what pH was, and I had no clue what he was talking about. (This was great preparation for a career in science.) In high school, Mrs. Goodwill made biology both demanding and fun. At Hebrew University, Dr. Yoram Milner encouraged me, even as a junior, to enroll in his graduate course, taught it English specifically for me, and wrote me a beautiful letter of recommendation. May his memory be blessed. Dr. John McDermott accepted me as an undergraduate student into his lab, and Dr. Rob Perry transformed me from a scientific *tabula rasa* into a molecular biologist. The summer in that lab was one of the happiest times in my life. Many thanks to Dr. Ajit Kumar, Dr. Krishna Banaudha, and Deborah McIlwain for your support and guidance during my Master's thesis work.

Thank you to Steam Café for sheltering me, feeding me, and providing me with WiFi as I studied for graduate courses and wrote my dissertation proposal. I would like to thank the owners, staff, and patrons of Kangaroo Boxing Club and the now-defunct Polly's. Mary Daly was the first to welcome me into the Polly's family, and our friendship that began with a mutual love of hockey and working at the bar has lasted to this day. Thank you to Mary, Chris, Victor, Book, Erik, Bo, Gema, Frank, Ronnie Jackson and all the other staff and regulars for the friendship and happy times. After the demise of Polly's, KBC stepped up to fill the void with lots and lots of barbecue. Thank you Peyton, Trent, Robin, Chris, Josh, Adam, Kat, Carrie, Sarah, Alex, Shawn, Alfonso, Angel, John, Zack, Josh, Malcolm, Sammy, Katie, Maria,

Erikka, and fine, even Greg, for being friends and family and a home away from home. I have to give Amy Robinson and Amber Webb a shout-out, although sadly, Ivy & Coney and Showtime are too far away from my home to serve as regular refuges.

I would like to thank all the Chimneys for being my family in DC (and Salem and Kansas and LA and now Portland.) Thank you Jamie, Hector, Tisha, Larisa, Dr. Denisha Jones, Scary Mary, Stacey, Eddie, Jason, Timmy, Errol, Iris, Scott, Matt, Laura Wood, Jim Barkley, Randy, Lisa Accokeek, Big Tom, Lauren, Stephanie, Brian, Mary Rice, Anna, Bob Scott, Theron, Steve, Jen, and Anacani. I must give a huge thank you to Michael and Catrina for their insane amounts of generosity and hospitality, and Tara Bunch, for the free weekly massages that got me through this past year. I have never laughed as hard and as long as when I am with y'all and I could not have done this without your support.

I would like to thank all the past and current members of the Hamza lab, who in addition to providing the groundwork for my project and helping train me as a scientist, have provided an enormous amount of emotional support for the past few years. Scott was the first person to train me and I will never forget his patience, kindness, and sense of humour. Thank you to Caiyong, who was my first bench neighbour, and who was always happy to serve as my positive control. Thank you to Tamika for the mental and scientific support. Thank you Xiaojing, Jason, and Jianbing for being wonderful fellow graduate students. Thank you to Jon, Haifa, and Simon for being wonderful friends and coworkers. I must reserve a special thank you for Caitlin and Kate for being the backbones of our lab.

Thank you to my mentor, Dr. Iqbal Hamza, for your guidance and belief in my abilities. Thank you for the excellent training in molecular and cellular biology and genetics, for giving me the opportunity to improve my writing and presentation skills, and for your love of heme (which was indeed contagious). Because of your training, I feel eager and ready to move onto the next stage of my scientific career.

Lastly, there are a few incredibly special people in my life that I would be honoured to acknowledge. Thank you to Josh, for being there from my first day working in a lab, through my Master's degree and then when I was applying to graduate school. Thank you for your love and support of my ambitions as a scientist. Thank you to Aliza and Michal for your love and friendship. Thank you to Lia, for being one of my oldest and best friends. I am so grateful for our friendship and for the support you've given me for the past fifteen (!) years. Thank you to Jenny, for being my pillar ever since I met you. I will never forget morning coffee on the porch at Tilted Acres and when I need a dial-a-scientist, I will always think of you. Thank you to Kevin, for being my other pillar. You listened to me every night, and my joy was your joy and my troubles were your troubles. I love you so so much.

Thank you to Mary Lou, Matt, and Mike. I am so grateful to have you in my life. Thank you to John. I am so grateful to have met you and I will miss you very much. May your memory be blessed. Thank you to my grandparents, Louis Feintuch and Harry and Mary Korolnek, for leaving me with wonderful memories and a beautiful legacy to uphold. May your memories be blessed. Thank you to my grandmother, Rose Feintuch, for inspiring me with your intelligence and fierceness. I did this degree, Bubby, partly because I know how much school meant to you, and to

try to make up for how the world took away your chance at an education. Thank you to my brother and sister-in-law, Mickey and Shira, for your constant love, support, and acceptance. Thank you to my parents for understanding who I am and why I needed to do this. I really, really, really could not have done this without your support, and not a day goes by where I don't appreciate your enormous love for me.

This is for all of you, and I hope you are proud.

Table of Contents

Dedication	ii
Acknowledgements	iii
Table of Contents	viii
List of Figures and Tables	xi
List of Abbreviations	xiii
Chapter 1: Introduction	1
The Biological Requirement for Heme Trafficking Molecules	1
Delivery of Heme to Subcellular Compartments	3
Heme Requirements in the Mitochondria	3
Heme Requirements in the Cytosol	8
Heme Delivery to Cytosolic Proteins	9
Heme Requirements in the Secretory Pathway	12
Heme Delivery to the Secretory Pathway	14
Heme Trafficking During Physiological Processes	16
Heme Mobilization During Erythrophagocytosis	16
Heme Trafficking During Embryogenesis	19
ABC Transporters	22
ATP Hydrolysis by Nucleotide Binding Domains	22
Mechanism of Transport	25
ABC Transporter Structure	27
Multidrug Resistance Protein 5 (MRP5)	30
Problem Statement	Error! Bookmark not defined.
Chapter 2: Materials and Methods	33
Worm Methods	33
Worm Culture	33
Synchronization of Worms	33
Worm Strains	34
Gateway Cloning	34
Generation of Transgenic Worms	34
Single Worm PCR	35
RNA Extraction, cDNA Synthesis, and Quantitative Real Time PCR	35
RNA Interference	36
Heme Analog Assays	36
Quantification of Fluorescence using COPAS BioSort	37
Growth Assays	37
Yeast Methods	38
Strains and Growth	38
Cloning and Transformation	38
Growth Assays	39
β -Galactosidase Assay	40
Ferric Reductase Assay	40
Immunofluorescence	41

Mammalian Methods	41
Mouse Strains and Care	41
Generation of Immortalized Fibroblasts	42
Mammalian Cell Culture.....	42
DNA Cloning.....	43
Immunofluorescence.....	43
Immunoblotting.....	44
Horseradish Peroxidase Assay	44
Preparation of Red Blood Cells and <i>In Vitro</i> Erythrophagocytosis.....	45
RNA Isolation, cDNA Synthesis and Quantitative RT-PCR.....	46
General Procedures	47
Preparation of Hemin Chloride.....	47
Microscopy	47
Bioinformatics and Statistics	47
Chapter 3: Delineating the role of <i>mrp-5</i> in <i>C. elegans</i> heme homeostasis.....	48
Summary.....	48
Results.....	49
Identification of <i>mrp-5</i> as a regulator of heme homeostasis in <i>C. elegans</i>	49
MRP-5 is essential for embryonic development and larval growth.....	53
<i>C. elegans</i> development requires intestinal MRP-5.....	60
MRP-5 is an intestinal heme exporter.....	68
HRG-3 overexpression cannot rescue MRP-5 loss-of-function phenotypes	73
Discussion.....	76
Chapter 4: Conserved Heme Transport by Metazoan MRP5 Proteins	82
Summary.....	82
Results.....	83
MRP5 is conserved in metazoans	83
MRP5 expression alters heme homeostasis in a heterologous system	88
MRP5 is a conserved heme transporter	94
Discussion.....	97
Chapter 5: The Role of MRP5 in Mammalian Heme Homeostasis.....	102
Summary.....	102
Results.....	103
<i>Mrp5</i> ^{-/-} mice do not have hematological defects.....	103
MRP5 regulates heme availability in the secretory pathway.....	106
<i>Mrp5</i> ^{-/-} macrophages have an altered response during erythrophagocytosis	107
Discussion.....	118
Chapter 6: Discussion	125
Conclusions.....	125
Future Directions	130
Structure/Function Analysis of MRP5 Proteins.....	130
Interacting Partners and Other Heme Trafficking Mechanisms	132
Zebrafish Mutant Analysis.....	133
Heme Transport Assays	133
Analysis of <i>Mrp5</i> Knockout Mice	134
Significance.....	135

Appendix I	138
Appendix II	139
Appendix III.....	140
Appendix IV.....	142
Appendix V.....	144
Appendix VI.....	146
Appendix VII	148
Appendix VIII.....	150
References.....	152

List of Figures and Tables

Chapter 1

Table 1.1: List of selected eukaryotic hemoproteins	4
Figure 1.1: Presumptive pathways for delivery of heme to hemoproteins in eukaryotic cells.	6
Figure 1.2: Heme transport pathways during erythrophagocytosis.	17
Table 1.2: List of Eukaryotic ABC Importers	23
Figure 1.3: Conserved Motifs in Nucleotide Binding Domains.	24
Figure 1.4: Sav1866 Structure.	28

Chapter 3

Figure 3.1: Current model of heme homeostasis in <i>C. elegans</i>	50
Figure 3.2: <i>mrp-5</i> is involved in heme homeostasis in <i>C. elegans</i>	52
Figure 3.3: Loss of <i>mrp-5</i> , and no other <i>mrp</i> , results in a heme depletion signal in the heme sensor strain, IQ6011.....	54
Figure 3.4: Gene structure and protein topology of <i>mrp-5</i>	55
Figure 3.5: Loss of <i>mrp-5</i> results in embryonic lethality and larval arrest.	57
Figure 3.6: Heme-dependent rescue of the <i>mrp-5(ok2067)</i> mutant.	59
Figure 3.7: <i>mrp-5</i> is expressed in multiple tissues in <i>C. elegans</i>	61
Figure 3.8: MRP-5 localizes to the basolateral membrane of the intestine.	63
Figure 3.9: Loss of <i>mrp-5</i> specifically in the intestine causes embryonic lethality....	66
Figure 3.10 Loss of <i>mrp-5</i> leads to intestinal accumulation of a heme analog.	69
Figure 3.11: <i>VC1599 (mrp-5/+)</i> worms exhibit haploinsufficiency phenotypes.....	70
Figure 3.12: Loss of <i>mrp-5</i> results in an extraintestinal heme depletion signal.	71
Figure 3.13: Ectopic expression of <i>hrg-3</i> cannot rescue <i>mrp-5</i> -associated lethality..	74
Figure 3.14: Proposed model of heme transport pathways in <i>C. elegans</i>	78

Chapter 4

Table 4.1: Pairwise Alignment Scores (% Identity) of MRP5/ABCC5 Homologs....	84
Figure 4.1: Phylogenetic analysis of MRP and ABCC proteins.	85
Figure 4.2: Expression of MRP5 inhibits growth of a heme synthesis-deficient yeast strain.....	89
Figure 4.3: Expression of MRP5 inhibits growth in a heme-dependent manner.	92
Figure 4.4: Ectopic expression of MRP5 in yeast alters heme availability in the cytosol and the secretory pathway.	95
Figure 4.5: MRP5 localizes to intracellular membranes in yeast.	98

Chapter 5

Figure 5.1: Generation of <i>Mrp5</i> ^{+/+} and <i>Mrp5</i> ^{-/-} fibroblasts.....	104
Figure 5.2: Localization of human MRP5 in polarized MDCKII cells.	108
Figure 5.3: Localization of MRP5 in immortalized mouse embryonic fibroblasts. .	110
Figure 5.4: MRP5 localizes to the secretory pathway and alters heme levels in this compartment.	112
Figure 5.5: MRP5 is upregulated during erythrophagocytosis in bone marrow-derived macrophages.	115
Figure 5.6: MRP5 does not localize to the phagolysosomal membrane during erythrophagocytosis in bone marrow-derived macrophages.	117
Figure 5.7: MRP5 is required for an appropriate cellular response to phagocytosed red blood cells during EP.	119
Figure 5.8: Proposed model for MRP5 function in mammalian cells.	121

List of Abbreviations

ABC	ATP-binding cassette
ADP	Adenosine diphosphate
ALA	δ -aminolevulinic acid
ALAS	δ -aminolevulinic acid synthase
ANOVA	Analysis of variance
ATP	Adenosine triphosphate
AU	Arbitrary units
BMDM	Bone marrow-derived macrophage
BSA	Bovine serum albumen
CFTR	Cystic fibrosis transmembrane conductance regulator
COX	Cytochrome C oxidase
CYC	Cytochrome C
CYP	Cytochrome P450
DAPI	4',6-diamidino-2-phenylindole
DIC	Differential interference contrast
DMEM	Dulbecco's modified Eagle's medium
DMT	Divalent metal transporter
ECL	Extracellular loop
EDTA	Ethylenediaminetetraacetic acid
EE	Early endosome
EP	Erythrophagocytosis
ER	Endoplasmic reticulum
ERC	Endocytic recycling complex
ERMES	ER-mitochondrion encounter structure
FBS	Fetal bovine serum
FLVCR	Feline leukemia virus, subgroup C, receptor
Fpn	Ferroportin
FRE	Ferric reductase
Ftn	Ferritin
FVB	Friend virus B
GalT	1,4-galactosyltransferase
Gapdh/gpd	Glyceraldehyde 3-phosphate dehydrogenase
GaPPIX	Galium protoporphyrin IX
GFP	Green fluorescent protein
HA	Hemagglutinin
HBP	Heme-binding protein
HCCS	Holocytochrome C synthase
HD	Heme-depleted serum

HMOX	Heme oxygenase
HRG	Heme-responsive gene
HRP	Horseradish peroxidase
ICL	Intracellular loop
ICS	Intercistronic sequence
IMM	Inner mitochondrial membrane
IMS	Intermembrane space
IPTG	Isopropyl β -D-1-thiogalactopyranoside
IRES	Internal ribosome entry site
LB	Luria-Bertani
LCM	L-929 cell-conditioned media
LCR	Locus control region
LE	Late endosome
MAM	Mitochondrial-associated membrane
mCeHR	Modified <i>C. elegans</i> Habitation and Reproduction
MDCK	Madin-Darby canine kidney
MDR	Multidrug resistance
MDV	Mitochondria-derived vesicles
MEF	Mouse embryonic fibroblasts
MO	Morpholino
MPO	Myeloperoxidase
MRP	Multidrug resistance-associated protein
MSD	Membrane-spanning domain
M ϕ	Macrophage
NBD	Nucleotide-binding domain
NGM	Nematode growth medium
NTCP	Na ⁺ -taurochlorate co-transporting polypeptide
OD	Optical density
OMM	Outer mitochondrial membrane
ORF	Open reading frame
PBS	Phosphate buffered saline
PCR	Polymerase chain reaction
P-gp	P-glycoprotein
PM	Plasma membrane
ppm	Parts per million
PUG	Protoporphyrin uptake gene
qRT-PCR	Quantitative real-time polymerase chain reaction
RBC	Red blood cell
RES	Reticuloendothelial system
RHBP	<i>Rhodnius</i> heme-binding protein
RNAi	RNA interference
SA	Succinyl acetone
SC	Synthetic complete
SDS-PAGE	Sodium dodecyl sulfate polyacrylamide gel electrophoresis
SEM	Standard error of the mean
SLC	Solute carrier

SREBP	Steroid response element-binding protein
SYN	Syntaxin
TGN	Trans-Golgi network
TMD	Transmembrane domain
UTR	Untranslated region
WGA	Wheat germ agglutinin
WT	Wild-type
YFP	Yellow fluorescent protein
YPD	Yeast extract-peptone-dextrose
ZnMP	Zinc mesoporphyrin

Chapter 1: Introduction

Heme is an iron-containing porphyrin that functions as a cofactor in a huge array of cellular processes. Heme is also a major source of bioavailable iron in the human diet. By the end of the 20th century, the pathways for heme biosynthesis had been well elucidated and the structures of many heme-containing proteins have been solved. Indeed, Max Perutz and John Kendrew were awarded the Nobel Prize in chemistry in 1962 for their crystal structures of hemoglobin and myoglobin (1, 2). While the synthesis of heme has been well-characterized, the pathways for inter- and intra-cellular heme transport remain poorly understood. This gap in our knowledge is largely due to the inability to uncouple the processes of heme biosynthesis and heme transport, as well as the ability of heme to promiscuously bind to proteins. Progress in this field can be contrasted with the fields of iron and copper trafficking, which have not suffered similar setbacks and have progressed steadily over the past decade.

The Biological Requirement for Heme Trafficking Molecules

The terminal step of heme biosynthesis, which occurs in the mitochondrial matrix, is the insertion of iron into protoporphyrin IX. Heme is then targeted to both soluble and membrane-bound hemoproteins. Heme must be able to cross membranes, yet also be delivered to soluble proteins in the cytosol. Heme's amphipathic nature means that it is able to function in both milieus, but not without the assistance of

protein partners. Due to the hydrophobicity of the porphyrin ring, heme is not readily soluble in aqueous solutions. When heme is at neutral pH and is in the ferrous state it has no net charge, as the negative charges of the propionate groups balance the positive charges of the chelated iron. While this form of heme readily inserts into and diffuses through lipid bilayers, the hydrophilic propionate head groups hinder the flipping of heme from one leaflet to another (3-5). Heme exit from the membrane is inefficient without the presence of soluble heme binding proteins (6).

In addition to the difficulties posed by heme's dual chemical nature, its peroxidase activity and capacity to generate reactive oxygen species combined with its ability to intercalate into membranes and bind many proteins nonspecifically renders heme highly toxic. The deleterious effects of heme have been reviewed extensively in mammalian cells and other systems (7-12). Thus, even though heme is able to diffuse into membranes and be extracted by heme-binding proteins, it is unlikely that this process would be unregulated, as peroxidation of membrane lipids would result in severe damage, especially during a process such as erythropoiesis, with each red cell processing the heme required for over 300 million hemoglobin molecules. Additionally, many heme synthesis precursors and heme breakdown products are also toxic, and thus careful control of heme synthesis, trafficking, and degradation is a prerequisite.

Given these chemical and biochemical properties of heme, it is apparent that a system of transporters and chaperones would be necessary to efficiently and specifically distribute heme to hemoproteins found in various compartments in the cell, all the while preventing adventitious heme toxicity.

Delivery of Heme to Subcellular Compartments

Heme Requirements in the Mitochondria

Most of the mitochondrial respiratory chain complexes rely on the redox capability of a heme prosthetic group (Table 1). Heme is present in these complexes in the *a*, *b*, or *c* forms. Heme *b* is the most common form of heme. It is the form synthesized by ferrochelatase, containing a C2 vinyl group and C8 methyl group, and is attached to proteins via noncovalent coordination of the heme iron with amino acid side chains (13, 14). Heme *a* is modified from heme *b* and its porphyrin ring contains a C2 hydroxyethylfarnesyl and a C8 formyl side group (14). Heme *c* is found covalently linked to proteins; the two vinyl side chains are converted to thioether linkages to cysteine residues in the apoprotein (15).

The biogenesis and cofactor requirements of the mitochondrial respiratory complexes have recently been reviewed, but will be briefly discussed here with regard to heme transport and trafficking (16-18). The cytochrome *bc*₁ complex (also known as coenzyme Q-cytochrome *c* reductase or Complex III) is a multi-subunit protein located with the other electron transport complexes in the inner mitochondrial membrane (IMM). The cytochrome *bc*₁ complex includes two heme *b*-containing cytochromes as well as a heme *c*-containing cytochrome, and interacts with another hemoprotein, the electron carrier cytochrome *c*, for the purpose of generating a proton gradient along the IMM. Cytochrome *c* is soluble in the intermembrane space (IMS) of mitochondria and is found loosely associated with the IMM, as it carries an electron from the cytochrome *bc*₁ complex to cytochrome *c* oxidase. Cytochrome *c*

Table 1.1: List of selected eukaryotic hemoproteins

Hemoprotein	Function	Subcellular Localization
Succinate Dehydrogenase (Complex II)	Electron Transport	Mitochondrial (IMM)
Cytochrome <i>bc</i> ₁ complex (Complex III)	Electron Transport	Mitochondrial (IMM)
Cytochrome <i>c</i>	Electron Transport	Mitochondrial (IMS)
Cytochrome <i>c</i> oxidase (Complex IV)	Electron Transport	Mitochondrial (IMM)
CYP11A1	Steroid Synthesis	Mitochondrial (matrix)
Hemoglobin	Gas Binding	Cytosolic
Myoglobin	Gas Binding	Cytosolic
Neuroglobin	Gas Binding	Cytosolic
Cytoglobin	Gas Binding	Cytosolic
Nitric Oxide (NO) Synthase	NO Signalling	Cytosolic
Soluble Guanylyl Cyclases	NO and Ca ²⁺ Signalling	Cytosolic
Hap1p	Transcription Factor	Nuclear
Bach1	Transcription Factor	Cytosolic/Nuclear
Rev-erb- α	Transcription Factor	Nuclear
DGCR8	miRNA Processing	Nuclear
mPer2	Circadian Rhythm	Cytosolic/Nuclear
Cytochrome <i>b</i> ₅	Electron Carrier	Cytosolic
P450 Cytochromes	Oxidation of Metabolites and Xenobiotics	ER membrane (active site is cytosolic)
Prostaglandin Synthases (COX1 and COX2)	Autocrine/Paracrine Signaling	ER
Myeloperoxidase	Microbicide	Lysosome-like azurophil granules
Catalase	Antioxidant	Peroxisomes
Thyropoxidase	Thyroid Hormone Synthesis	Plasma Membrane
Ferric Reductase	Iron Transport	Plasma Membrane
Lactoperoxidase	Microbicide	Secreted
Ligninase	Nutrient Breakdown	Secreted
Heme-Containing Chloroperoxidase	Haloperoxidase	Secreted
Peroxidasin	Extracellular Matrix Synthesis	Secreted
HRG-3	Heme Mobilization	Secreted
<i>Rhodnius</i> heme binding protein (RHBP)	Heme Mobilization	Secreted

oxidase (also known as Complex IV) includes two heme *a*-containing cytochromes, which also participate in electron transfer and proton translocation into the IMS. Succinate dehydrogenase (Complex II) also contains a heme *b* moiety, which is required for stability of the complex (19). The heme *b* in succinate dehydrogenase may also be involved in electron transport, but the exact function of this heme remains unclear (16).

In eukaryotes, the cytochrome *bc*₁ complex (Complex III) is composed of seven or eight nuclear-encoded subunits that function together with three catalytic core proteins encoded in the mitochondrial genome (20-22). Cytochrome *b* is a membrane-bound core protein that contains two heme groups, each of which has a unique redox potential (23). Heme *b*_H, the high potential heme, is bound in an accessible cavity on the matrix side of the protein. Heme *b*_L, the low potential heme, is found within the IMS portion of cytochrome *b*. Heme *b*_H can be inserted into cytochrome *b* without having to traverse a membrane; it is unknown whether or not a chaperone assists in this process (24). It is unclear if heme *b*_L is acquired in the matrix, or if this heme is inserted in the IMS, thus necessitating movement of heme across the IMM (Figure 1, Pathway 1). Cytochrome *c*₁, being nuclear encoded, is targeted to the mitochondria after being translated in the cytosol. Its heme cofactor is covalently attached in the IMS by the heme lyases Cyc3 and Cyt2 in yeast or holocytochrome *c* synthase (HCCS) in mammals (25). In addition to the heme in cytochrome *c*₁ and possibly the heme *b*_H of cytochrome *b*, the soluble respiratory protein cytochrome *c* also acquires its heme in the IMS from HCCS (25).

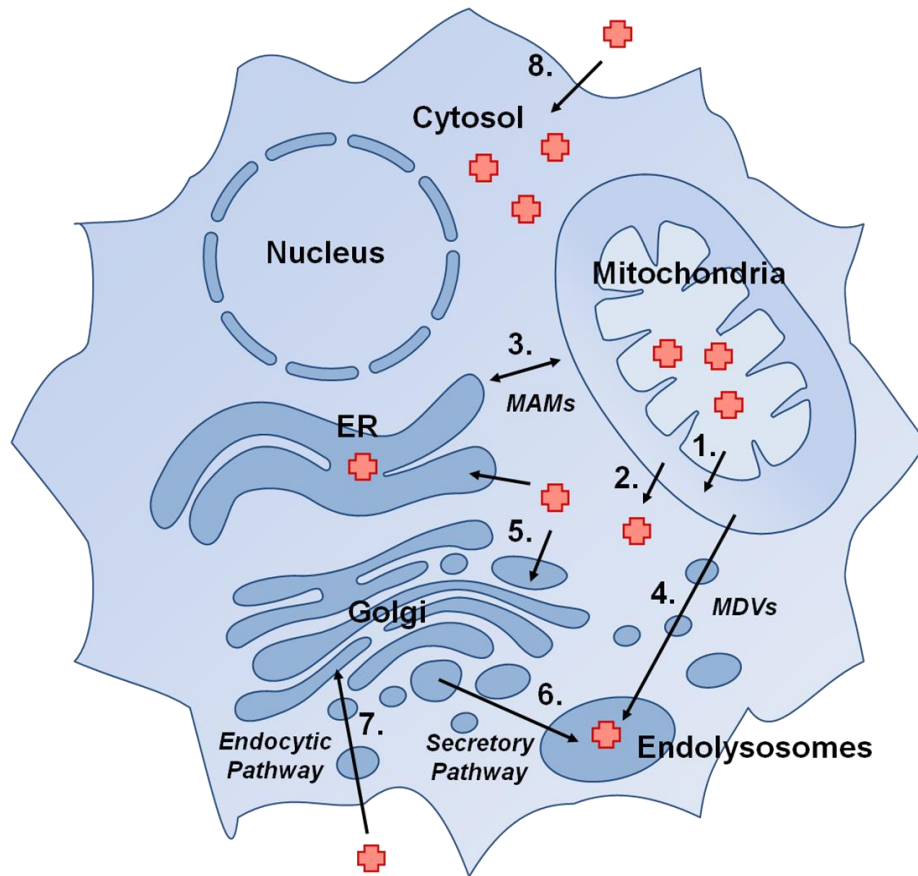


Figure 1.1: Presumptive pathways for delivery of heme to hemoproteins in eukaryotic cells.

Pathways are numbered as follows: 1) Heme transport across the inner mitochondrial membrane, 2) Heme transport across the outer mitochondrial membrane, 3) Direct heme trafficking from the mitochondria to the ER via mitochondria-associated membranes (MAMs), 4) Trafficking of heme from mitochondria to endolysosomal compartments via mitochondrial-derived vesicles (MDVs), 5) Transport of cytosolic heme into the secretory pathway by a heme exporter, 6) Trafficking of heme in ER/Golgi to endolysosomal compartments, 7) Import of heme into the cell via an endocytic pathway, and 8) Import of heme via a plasma membrane heme importer.

The biogenesis of cytochrome *c* oxidase (Complex IV) is highly conserved in eukaryotes (18). Heme *a* in cytochrome *c* oxidase (COX) is bound to the mitochondrial-encoded COX1 subunit. Heme *a* is synthesized via the conversion of heme *b* to the intermediate heme *o* by the farnesylation of the C2 position by COX10 (heme *o* synthase), and the subsequent oxidation of the C2 methyl side chain to formyl by COX15 (heme *a* synthase) (14, 18). Both COX10 and COX15 are integral membrane proteins located in the IMM. Studies have indicated that insertion of heme *a* into COX1 occurs post-translationally, as early intermediates of the cytochrome *c* oxidase assembly do not contain heme *a* and are able to form in the absence of heme *a* biosynthesis (26). This is in contrast with later intermediates, which do not form without the presence of heme *a*. It remains unclear if heme chaperones exist to shuttle heme *b* from its site of synthesis to COX10, or to deliver heme *a* to the COX1 subunit. By contrast, multiple mitochondrial chaperones, including COX17, SCO1, and COX11, have been shown to act as chaperones for delivery of copper to the cytochrome *c* oxidase complex [Also reviewed in (18)].

In addition to the respiratory chain complex proteins, another cytochrome, cytochrome P450 side-chain cleavage enzyme (also known as CYP11A1), is also found in the mitochondrial matrix. This enzyme is expressed in steroid-synthesizing tissues such as the brain and adrenal glands and functions to convert cholesterol to pregnenolone, a precursor for mineralocorticoids, glucocorticoids, androgens, and estrogens (27). CYP11A1 catalyzes this first step in steroid synthesis by initiating three sequential monooxygenase reactions of the cholesterol side chain: hydroxylation of C20 and C22 and then cleavage the C20-C22 bond to generate the

steroid precursor pregnenolone and isocaproic aldehyde. While the crystal structures of both bovine and human CYP11A1 have recently been solved, nothing is known regarding how the heme cofactor is inserted into this important hemoprotein (28, 29).

Heme Requirements in the Cytosol

While heme moves from the mitochondrial matrix into the IMS for insertion into particular cytochromes, heme must also exit the mitochondria for insertion into hemoproteins which acquire heme in the cytosol (Table 1). The most well-known cytosolic hemoproteins are the gas-binding globins, including hemoglobin, myoglobin, neuroglobin, and cytoglobin. Adult hemoglobin consists of two α and two β chains, each bound to a molecule of heme. Hemoglobin can be generated *in vitro* (for example, by heterologous expression in *E. coli*, or by recombining purified apo-hemoglobin with heme) indicating that no specific chaperone is required for heme insertion. Because of its asymmetric side chains, each heme can be incorporated into hemoglobin in two orientations. The term “heme disorder” refers to mixtures of these two orientations within a subset of hemoglobin molecules (30). Interestingly, the amount of heme disorder differs between hemoglobin synthesized *in vivo* or *in vitro* (31). This is a possible indication that stereoselective insertion of heme into hemoglobin occurs, although the mechanism for this phenomenon remains unclear.

Other hemoproteins that must acquire their heme in cytosol include nitric oxide synthases and the soluble guanylyl cyclases (a nitric oxide receptor), nuclear heme-binding proteins including Hap1p, DGCR8, mPer2, Bach1 and Rev-erb- α , as well as the soluble form of cytochrome *b*₅. Even P450 cytochromes, the most well-known hemoproteins in the ER, are anchored in the ER membrane with their heme-

containing globular domain facing the cytosol (32, 33). Thus, cytochrome P450 proteins may acquire their heme from the cytosolic face of the membrane.

Heme Delivery to Cytosolic Proteins

Cytosolic hemoproteins can acquire their heme from two possible sources: heme synthesized *de novo* in the mitochondria, or heme imported from outside the cell. Heme synthesized in the mitochondria exits the active site of ferrochelatase in the matrix. It is possible that this heme immediately intercalates into the IMM and then is removed into the IMS by a heme binding chaperone, or is actively transported across the IMM, and then moved across the outer mitochondrial membrane (OMM) by a high affinity heme transporter (Figure 1, Pathways 1 & 2).

The sole mitochondrial heme exporter identified to date is the mitochondrial isoform of Flvcr1 (34, 35). Flvcr1, a member of the major facilitator superfamily of transporters, was initially identified as a plasma membrane heme exporter. Cats infected with feline leukemia virus, subgroup C (FeLV-C) develop aplastic anemia, with failure of erythropoietic blast-forming units to mature into colony-forming units, as binding of the virus to its receptor, Flvcr1, resulted in its internalization and inactivation (34). Early experiments showed that Flvcr1 could mediate the cellular export of heme and the heme analog, zinc mesoporphyrin (34). Mice lacking Flvcr1 die either at E7.5 or between E14.5 and E16.5 due to impaired erythropoiesis, in keeping with *in vitro* studies showing that K562 cells fail to differentiate into erythroid-like cells when infected with FeLV-C (35).

Recently, Chiabrando *et al* identified a mitochondrial isoform of Flvcr1, termed Flvcr1b (36). While Flvcr1a encodes a plasma membrane-localized

transporter, Flvcr1b contains an alternative transcription start site, resulting in a shortened amino terminus containing a mitochondrial targeting signal. Depletion of Flvcr1b in HeLa cells results in accumulation of mitochondrial heme, indicating that Flvcr1b plays a role in heme export from the mitochondria (36). Specific deletion of Flvcr1a in mice resulted in death at E14.5 and birth due to hemorrhage, edema, and skeletal abnormalities; however, erythropoiesis in these mice is normal (36). Thus the authors conclude that the lethality of the original Flvcr1 knockout mice was due to lack of heme export from the mitochondria by Flvcr1a, as that deletion targeted both Flvcr1 isoforms.

Numerous questions regarding heme exit from the mitochondria remain unanswered. It is not yet known if Flvcr1b resides on the mitochondrial IMM or OMM, with the possibility of another distinct mitochondrial heme exporter yet to be found. It is also unclear whether Flvcr1b is actually located within the mitochondria or is associated with membranes that tether the mitochondria to other organelles. If mitochondrial heme export is indeed attenuated, how do *Flvcr1*^{-/-} embryos even survive until E14.5? Does Flvcr1b only function in some cell types? No specific heme chaperones have been found to bind heme in the IMS, or to deliver heme to cytosolic hemoproteins. A number of cytosolic heme-binding proteins have been identified, including 22- and 23-kDa heme-binding proteins (HBPs) and the HBP homolog, SOUL (37-39). These proteins could serve as “sponges” for heme exiting the mitochondria, simultaneously protecting the cell from heme’s cytotoxicity and also delivering heme to target hemoproteins. It remains unclear whether multiple non-

specific porphyrin-binding molecules perform the role of chaperoning heme in the cytosol, or if there are heme- and/or hemoprotein-specific pathways.

Presumably, heme imported into the cell, rather than solely heme exported from the mitochondria, could be bound by cytosolic heme chaperones and delivered to newly forming hemoproteins (Figure 1, Pathway 8). As such, plasma membrane heme importers could also be sources of heme for these enzymes. One such transporter is Hrg1. The heme-responsive paralogs, *hrg-1* and *hrg-4*, were initially discovered as transmembrane domain-containing permeases upregulated in response to heme deficiency in *C. elegans* (40). HRG-4 is localized to the apical plasma membrane of the worm intestine and serves to import dietary heme into the animal (40, 41). HRG-1 localizes to lysosome-like vesicles in the intestine, and serves to mobilize heme stored in these compartments (40, 41). While *hrg-4* does not appear to have homologs in other species, homologs of *hrg-1*, also called solute carrier 48 A1 (SLC48A1) proteins, have been found in diverse organisms, including *Leishmania* spp., zebrafish, and mammals (40-43). Knockdown of *hrg1* in zebrafish leads to anemia, although the genetic etiology for the anemia phenotype is not known. Transport of heme by *hrg-1* and *hrg-4* has been demonstrated directly using electrophysiological currents in *Xenopus* oocytes, and indirectly using heme-dependent growth of *C. elegans* and *Saccharomyces cerevisiae* or uptake of heme analogs as indicators of heme import.

Mammalian Hrg1 has been shown to be expressed widely, with the highest expression in the brain, heart, kidney, and muscle, and with some expression in the placenta and intestine (40). Hrg1 has been linked to a possible role in cancer

progression, as its interaction with V-type ATPases is associated with changes in endocytic trafficking, extracellular acidification, altered glucose metabolism, and matrix metalloprotease activity (44, 45). Depletion of Hrg1 in MCF7 cells resulted in decreased invasiveness and migration capabilities in these cells. Hrg1 has also been found to be a target of nuclear factor (erythroid-derived 2)-like 2 (Nrf2), the antioxidant response transcription factor (46). In independent studies, human Hrg1 colocalized with Lamp1 in lysosomes, and Hrg1 is found on the erythrophagolysosome in macrophages during red blood cell recycling (43, 47). Hrg1 has been shown to mediate export of hemoglobin-derived heme from this compartment in macrophages.

Heme Requirements in the Secretory Pathway

A variety of hemoproteins function in multiple components of the secretory pathway (Table 1). Lysosomal, peroxisomal, plasma membrane-targeted and secreted hemoproteins are folded and processed within the ER and Golgi, and thus the cell must have a means of transferring heme from the mitochondria into various subcellular membrane-bound compartments. These hemoproteins include prostaglandin synthases (COX1 and COX2) in the ER, myeloperoxidase in lysosome-like azurophil granules, eosinophil peroxidase in eosinophil granules, catalase in peroxisomes, the plasma membrane proteins thyroperoxidase and ferric reductase, as well as numerous secreted proteins such as lactoperoxidase, fungal ligninase and chloroperoxidase, *C. elegans hrg-3*, *Drosophila* peroxidase, RHBP (*Rhodnius* heme-binding protein) in the blood-feeding insect *Rhodnius prolixus*.

Almost nothing is known with regards to how these proteins obtain their heme cofactors. Given that the secretory and endocytic pathways are somewhat contiguous, with protein and lipid components being shuttled from location to another, it is feasible that heme need only be transported across a single membrane into the lumen of one such compartment, and from there can be mobilized to its intended destination by carrier proteins (Figure 1, Pathways 3-7) (48). For example, heme exiting the mitochondria may be transported into the ER, and from there be inserted into its target hemoprotein during protein folding, following which the holoprotein can then traffic to its target organelle. It is also possible that one or many heme chaperones exist in the secretory pathway for delivery of heme to hemoproteins in their destination compartments. The fact that no mechanism for targeting heme to the secretory pathway has been discovered hints that multiple mechanisms exist and can compensate for loss of a single such constituent.

In contrast to the majority of hemoproteins in the secretory pathway, the maturation process of myeloperoxidase (MPO) has been well-characterized. MPO is a microbicidal protein generated by myeloid cells; its ability to chlorinate substrates enables it to generate hypochlorous acid from hydrogen peroxide [Reviewed in (49)]. This hemoprotein is extensively processed as it moves through the ER and Golgi; a single 80 kDa apo-proMPO peptide is converted to a glycosylated, heme-containing protein consisting of a 59 kDa heavy subunit and a 15.5 kDa light subunit that is targeted for secretion in its pro-form or for storage in azurophil granules as a mature protein (Reviewed in (50)). Early studies showed that disruption of the Golgi stacks with brefeldin A treatment resulted in MPO that is able to acquire heme but was

improperly processed and remained in the pro-form (51). Moreover, treatment of cells with succinyl acetone to inhibit heme synthesis also resulted in MPO that was improperly processed, while the processing and trafficking of other lysosomal proteins remained unchanged. The authors concluded that that insertion of heme occurred in the ER, and that heme insertion was required for further processing, and that cleavage of MPO into its mature heavy and light subunits occurred in a post-ER compartment. Further support for these conclusions was provided by mutants, such as the R569W MPO mutant which is unable to acquire heme and remains trapped in an apo-form in the ER (a result suggesting that heme insertion is necessary for ER exit), and the Y173C MPO mutant, which does acquire heme but is unable to exit the ER (suggesting that heme insertion is mediated within the ER) (52, 53). The aberrant processing of these mutant forms of MPO is especially informative, as these results lack the confounding effects of brefeldin A treatment.

Heme Delivery to the Secretory Pathway

Theoretically, there are a number of ways heme could enter the lumen of the secretory pathway. Heme released from the mitochondria could pass through the cytosol to be actively transported across the membrane of any subcellular compartment, (although no such transporter has been identified) (Figure 1, Pathway 5). Heme imported into the cytosol could be moved into the secretory pathway in this manner as well. Heme entering the cell through an endocytic process (i.e. heme bound to hemopexin internalized via the low-density lipoprotein receptor-related protein (LRP)/CD91) could be trafficking to such compartments, with the possible participation of a chaperone to sequester and guide heme to its destination (Figure 1,

Pathway 7). One appealing possibility is that nascent heme synthesized in the mitochondria could be shielded by vesicles entering the secretory pathway through direct contacts between the ER and mitochondrial membranes (Figure 1, Pathways 3 & 4).

Contacts between the ER and mitochondrial outer membranes were observed over 40 years ago (54, 55). Jean Vance coined the term mitochondria-associated membrane (MAM) when she identified a functional relationship between these organelles to exchange phospholipids (56). With better subcellular fractionation techniques, and the advent of fluorescent imaging, especially the recent development of superresolution imaging, dynamic microdomains where mitochondrial membranes are tethered to ER membranes have been observed. These include the ER-mitochondrion encounter structure (ERMES) in yeast and the previously mentioned MAMs, found in plants and animals (57, 58). These structures are involved in facilitating the transport of ionic calcium into the mitochondria, regulation of autophagy and apoptosis, and, most relevant to this review, the trafficking of lipids (59). The transport of phosphatidylserine from the ER to mitochondria has been demonstrated and it is hypothesized that other lipids are mobilized between these two organelles in a similar manner. Interestingly, two independent proteomic analyses of MAMs have detected the presence of coproporphyrinogen III oxidase, ferrochelatase, heme binding protein 1, and heme oxygenase 2 (60, 61). It is intriguing to postulate that these ER-mitochondria connections could serve as an axis for heme transport (Figure 1, Pathway 3).

Another possible mechanism for the trafficking of heme from the mitochondria to other organelles is the use of mitochondrial-derived vesicles (MDVs), which have been shown to traffic to both peroxisomes and lysosomes (Figure 1, Pathway 4) (62, 63). Initially, 70-100 nm vesicles were shown to deliver specific mitochondrial cargo proteins to peroxisomes. Other vesicles were later observed carrying cargo to lysosomes in response to increases in cellular oxidative stress (64, 65). As the processes of heme synthesis, mitochondrial respiration, and responding to oxidative stress are innately coupled by their shared metabolic pathways and mitochondrial location in the cell, it is possible to speculate that heme may be mobilized to these organelles via this mechanism.

Heme Trafficking During Physiological Processes

Heme Mobilization During Erythrophagocytosis

Much like the birth of red blood cells (RBCs), which differentiate from hematopoietic progenitors in the presence of nurse macrophages, the final moments of an RBC are spent in the care of a macrophage. Human RBCs have a lifespan of about 120 days, after which they become senescent and are recycled by macrophages of the reticuloendothelial system (RES) found in the spleen and liver [Reviewed in (66)]. This process - phagocytosis of RBCs and the breakdown of billions of molecules of hemoglobin - is termed erythrophagocytosis (EP) (Figure 1.2). EP is essential, as the bulk of iron required for the synthesis of new hemoglobin (~25 mg/day) derives from the recycling of RBCs (67). By contrast, only about 1 mg per day of dietary iron contributes to erythropoiesis. Heme oxygenase 1 (Hmox1) plays a

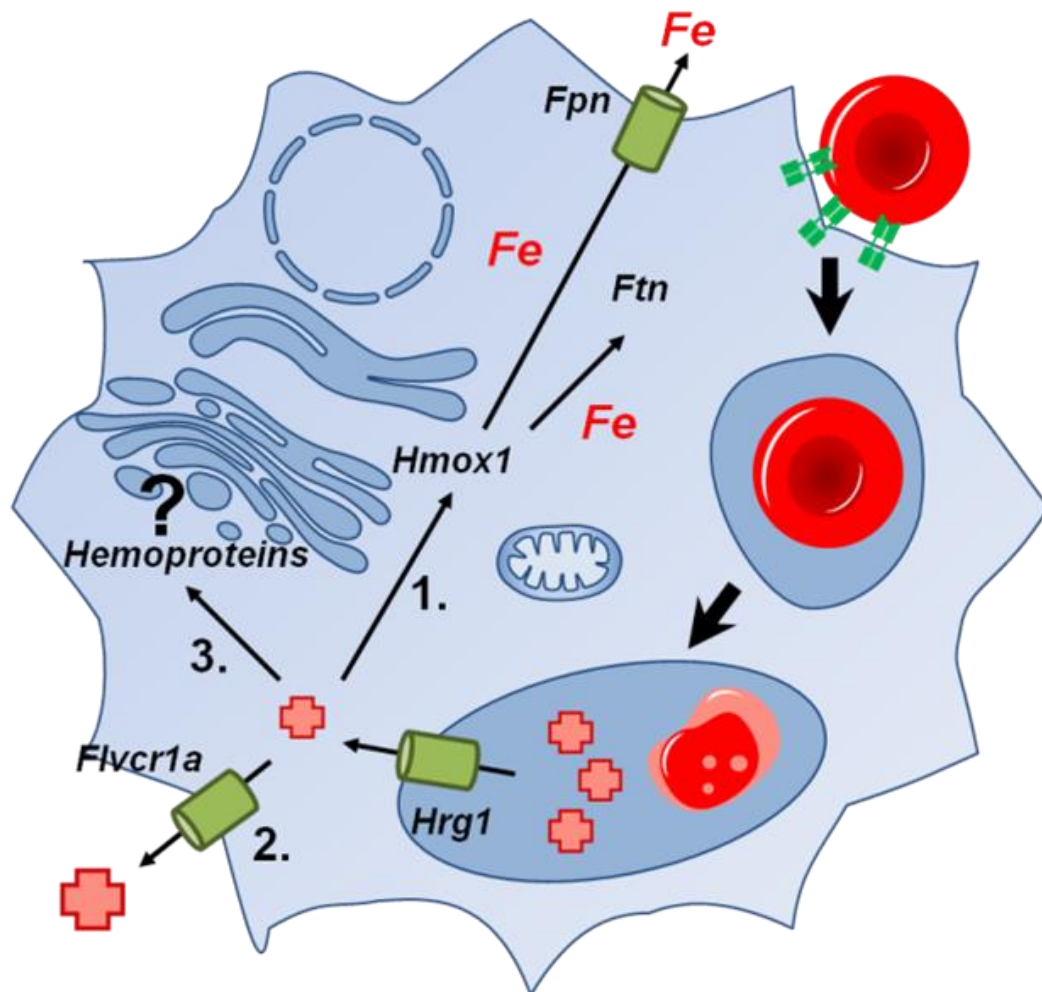


Figure 1.2: Heme transport pathways during erythrophagocytosis.

Pathways for iron and heme recycling during erythrophagocytosis. Unknown pathways are indicated with a (?). Hrg1 imports heme into the cytoplasm from the erythrophagolysosome. A portion of heme is (1) degraded by Hmox1 and iron released is either stored in ferritin (Ftn) or exported by ferroportin (Fpn). (2) Some heme may be exported via a plasma membrane heme transporter such as Flvcr1a, or (3) used by the cell for incorporation into hemoproteins.

vital role in this process, freeing iron from its protoporphyrin ring, and enabling the release of this iron for reuse. *Hmox1*^{-/-} mice suffer from anemia, reduced serum iron, and accumulation of iron in the spleen and liver, as the ability to recycle heme-iron in these mutants is almost completely crippled (68). *In vitro* experiments showed that *Hmox1*^{-/-} macrophages die when fed RBCs, and that splenic and liver macrophages are absent in *Hmox1*^{-/-} mice (69).

Heme extracted from RBCs was postulated by some to be degraded by Hmox1 inside the phagolysosome (70). Subsequently, the newly-released iron was either stored in ferritin (Ftn) or returned to the circulating pool of iron via the cellular iron exporter, ferroportin (Fpn). A major problem with this model is that Hmox1, while localizing to the ER via a C-terminal transmembrane segment, has been shown to be oriented with its active site facing the cytosol (71). Furthermore, the pH optimum for heme catabolism by Hmox1 is closer to physiological pH (pH 7.6) than lysosomal pH and maximal Hmox1 activity requires biliverdin reductase (72, 73). Studies have shown that heme oxygenases are not present on the phagolysosomal membrane, even though this membrane is partially derived from the ER (47). Thus Hmox1 likely does not have access to heme within the phagolysosomal compartment, suggesting that heme must exit this membrane compartment before degradation.

Hrg1, which has been shown to localize to endocytic compartments in mammalian cells, has recently been reported to transport heme across the phagolysosomal membrane (43). Hrg1 is expressed in RES macrophages and is upregulated at both the mRNA and protein level in the presence of heme and during EP. This was true in both an *ex vivo* model using bone-marrow derived macrophages

(BMDMs) treated with damaged RBCs, as well as in the livers of mice treated with heme, damaged RBCs, or the hemolysis agent phenylhydrazine (43). During EP, Hrg1 accumulates on the membrane of the phagolysosome, and when Hrg1 is depleted by siRNA, BMDMs are incapable of upregulating the machinery normally required to deal with the influx of heme and iron (including Hmox1, Ftn, Fpn, and Hrg1 itself) indicating a lack of heme export from the phagolysosome. Interestingly, a polymorphism of Hrg1 (P36L mutation) associated with anemia in four patients was shown to be defective in heme export in both a yeast model of heme transport, and during EP in BMDMs (43). These experiments used a heterologously expressed hemoprotein reporter, horseradish peroxidase (HRP), targeted to the Golgi to interrogate cellular heme availability – and showed that heme derived from recycled RBCs could be incorporated into an apohemoprotein by assaying HRP activity in BMDMs during EP. This opens the intriguing possibility that not all heme liberated during EP is degraded via Hmox1, and that a portion can be reused in the cell or exported by a transporter like Flvcr1a.

Heme Trafficking During Embryogenesis

It has long been known that metal homeostasis plays a vital role in embryonic and post-embryonic development (74). For example, mouse pups from iron- or copper-depleted dams experience developmental and neurological abnormalities whose severity is dependent on the timing and extent of the maternal deficiency. A number of metal transporters are embryonic lethal when targeted for gene knockout. There are two interconnected factors that need to be taken into account: a) maternal transfer of metals to developing embryos that lack an independent dietary source for

these nutrients; and b) metal transport within the embryo as pluripotent cells grow and differentiate into tissues.

The respective phenotypes of the *Flvcr1* and *Flvcr1a* knockout mice provide some insight into the role of heme transport during embryogenesis. As previously mentioned, Keel *et al* report that homozygous *Flvcr1* knockout pups (which lack both the mitochondrial and plasma membrane isoforms of *Flvcr1*) are found dead at either E7.5 or later at E14.5-E16.5 (35). The authors infer from this observation that *Flvcr1* is required for definitive erythropoiesis (which begins at ~E12) and not embryonic erythropoiesis. In support of this, they mention that yolk sac-derived erythroblasts do not express *Flvcr1* and appear normal in *Flvcr1*^{-/-} mice. If the cause of mortality in *Flvcr1*^{-/-} mice is defective heme export from the mitochondria, then we must wonder about the source of heme used for embryonic erythropoiesis. It may be that this heme is maternally-derived via one or more heme importers in the early embryo. However, it is known that homozygous ferrochelatase knockout embryos can be detected at the E3.5 preimplantation stage, but are reabsorbed and undetectable at E9-E10 - a phenotype also observed for uroporphyrinogen decarboxylase knockout animals [J. Phillips, personal communication and (75, 76)]. Although the ferrochelatase null phenotype should overlap with the *Flvcr1*^{-/-} phenotype, as both would cause heme deficiency in the cell, this is not the case. The greater severity of the ferrochelatase mutant hints that maternal heme cannot completely support embryonic development, and that a small portion of heme can exit the mitochondria in the *Flvcr1*^{-/-} mice in an *Flvcr1*-independent manner to sustain life for a few extra days.

Interestingly, deletion of the plasma membrane-localized Flvcr1a isoform also causes embryonic lethality (36). This lethality, due to hemorrhages, edema, and skeletal malformations, is observed later during development, usually between E14.5 and birth. Chiabrando *et al* speculate that many of these defects, also observed in mice with defects in endothelial integrity, are due to heme buildup within endothelial cells leading to widespread oxidative stress and hypoxic conditions in developing embryos. Interestingly, Flvcr1b is upregulated in these mice, presumably leading to increased cytoplasmic heme as evidenced by increased levels of Hmox1. Thus, plasma membrane heme export is an essential regulator of heme homeostasis during development.

While intercellular and intracellular heme transport are critical during embryogenesis, maternal transfer of heme to offspring may also play a critical role in embryonic development. This process has been demonstrated in *C. elegans*, where the small peptide HRG-3 serves as a chaperone for heme delivery to developing embryos and extraintestinal tissues (77). When the worm is heme deprived, expression of *hrg-3* in the intestine is upregulated >300-fold. HRG-3 is processed in the secretory pathway into a 45-amino acid chaperone which binds heme in a stoichiometry of 1:2 (heme:protein). Mature HRG-3 is secreted into the worm's circulation and taken up by extracellular tissues and developing oocytes. When *hrg-3* null worms are grown under heme limiting conditions, they show embryonic lethality and delayed growth, indicating a role for *hrg-3* in the distribution of heme from the intestine during early embryonic and later larval development (77).

ABC Transporters

ATP-binding cassette (ABC) transporters form one of the largest protein superfamilies and are found in all three domains of life. ABC transporters are active transporters that utilize ATP-derived energy to transport a diverse range of substrates across biological membranes. These substrates are often referred to as allocrites, in order to distinguish them from biochemical substrates, which unlike transport substrates, are enzymatically modified by the protein acting upon them (78) The human genome encodes 49 ABC transporters, divided into seven subfamilies, termed ABCA through ABCG, at least eighteen of which cause disease when mutated (79).

ABC transporters possess a basic architecture consisting of two transmembrane domains (TMDs) which form the transport channel, as well as two cytosolic nucleotide-binding domains (NBDs) which hydrolyze ATP. ABC transporters have been shown to transport assorted allocrites, including sugars, amino acids, peptides, vitamins, ions, hormones, as well as xenobiotics such as antimicrobial and chemotherapeutic agents. In eukaryotes, the vast majority of ABC transporters have been shown to function as effluxers (with the exceptions listed in Table 1.2) [Reviewed in (80)]. As such, these transporters are excellent candidates to serve as eukaryotic heme exporters.

ATP Hydrolysis by Nucleotide Binding Domains

ABC transporters, from bacteria to humans, are characterized by conserved motifs, including the LSGGQ signature, and Walker A and Walker B motifs (Figure 1.3A). These motifs function in the NBD to facilitate ATP hydrolysis, and are therefore highly conserved across all ABC transporters [Reviewed in (80, 81)]. Each

Table 1.2: List of Eukaryotic ABC Importers¹

Transporter	Substrate	Cellular Function	Reference
<i>Toxoplasma gondii</i> ABCG5	Cholesterol	Lipid Transport	(82)
Yeast Aus1, Pdr11 (ABCG1-like)	Cholesterols	Lipid Transport	(83)
Arabidopsis AtABCB14	Malate	Stomatal Movement	(84)
Arabidopsis AtPDR12/ABCG40	Abscisic Acid	Drought Tolerance	(85)
<i>Coptis japonica</i> CjMDR1	Berberine	Secondary Metabolite	(86)

¹ Adapted from (80)

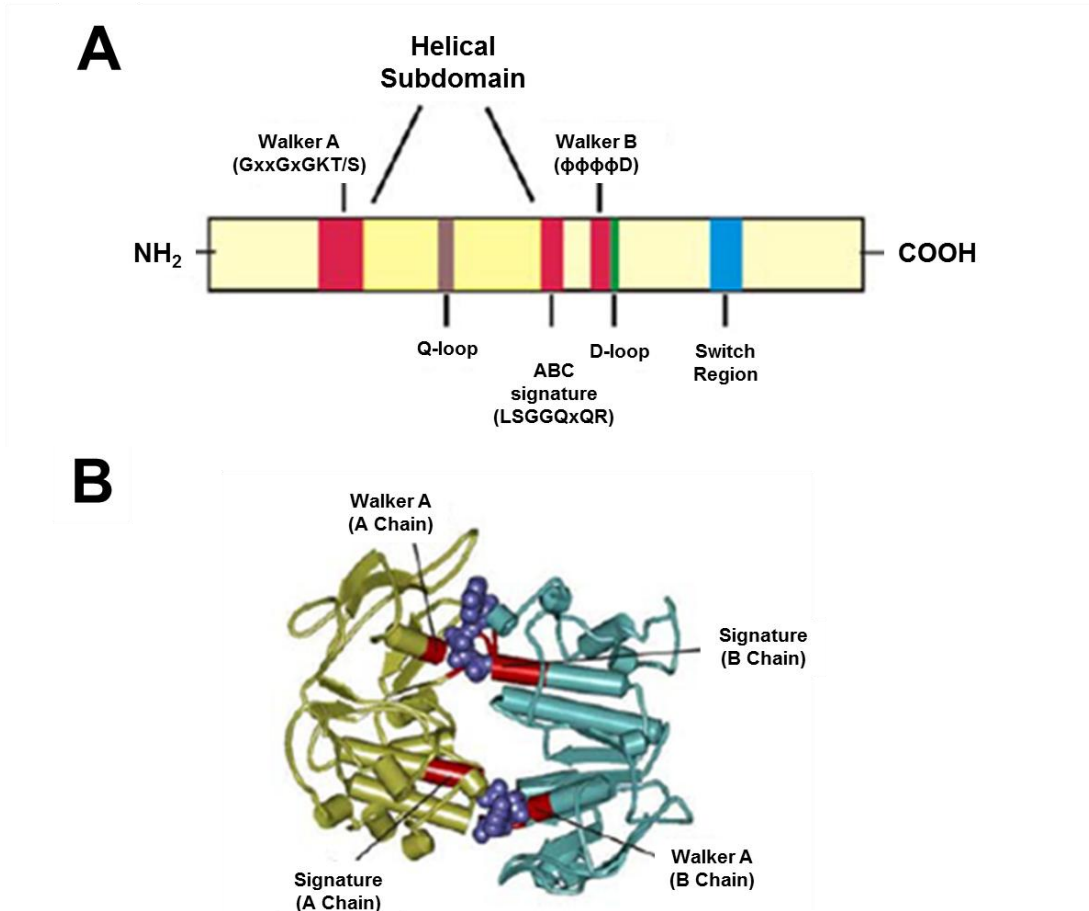


Figure 1.3: Conserved Motifs in Nucleotide Binding Domains.

(A) Cartoon representation of a nucleotide binding domain (NBD). Conserved sequences are in parenthesis, using the one letter code for amino acids (x, any residue, ϕ , hydrophobic residue.) Motifs involved in nucleotide binding are shown in red. (B) Structure of a NBD dimer [based on *Geobacillus stearothermophilus* ArtP, PDB code (2OUK)] indicating the location of the Walker A and signature motifs shown in (A). Two ATP molecules are shown in purple (space fill representation). One monomer, the A chain, is shown in yellow, and the other monomer, the B chain, is shown in blue. Image adapted from (80).

NBD has a bilobed structure, consisting of both a RecA-like subdomain (also known as the core subdomain), containing the Walker A/P loop and Walker B motifs (that contribute to nucleotide binding), and an alpha-helical subdomain, which contains the Q-loop and the signature LSSGQ sequence. The Q-loop senses the γ -phosphate, binds a divalent cation (usually Mg^{2+}), and attacks water. Like the Q-loop, the signature motif interacts with the γ -phosphate and is also involved in ATP hydrolysis.

The nucleotide binding domains adopt a head-to-tail conformation, where the Walker A motif of one NBD interacts with the signature motif of the second NBD, and the Walker A motif of the second NBD interact with the signature motif of the first NBD (Figure 1.3B). In this manner, two ATP hydrolysis sites are formed as the two halves of the dimer bind together, with two molecules of ATP sandwiched in the interface.

Mechanism of Transport

Transport by ABC transporters can be broken down into discrete stages: substrate recognition by the TMDs, ATP hydrolysis by the NBDs, and the conformational change which facilitates translocation. There are a number of models that seek to describe these steps. One early model, called the alternating access model, postulates that the transporter can adopt either an inward-facing or outward-facing conformation; these conformations have different affinities for the allocrite, setting up a gradient across the membrane. In this way, ATP hydrolysis fuels cycling through the two conformations, facilitating transport (87). The second model, called the processive clamp model, outlines six steps of transport. First, the protein exists in the inward-conformation, where nucleotides can be exchanged by the NBDs. Second,

substrate binds to the TMDs. Third, there is an ATP-dependent association of the NBDs, which occurs concomitantly with the fourth step, substrate release. Fifth, ATP is hydrolyzed by the NBDs, resulting in the final sixth step, dissociation of the two NBDs, returning the transporter to its original state (88, 89).

A number of subtleties must be added to these models. First, it is known that a single transporter can be stimulated to different degrees by different drugs (90, 91). Thus, it is unlikely that these transporters exist in one of two binary states, as a more complex signal is clearly capable of being transmitted from the TMDs to the NBDs. Second, certain transporters (e.g. P-glycoprotein/ABCB1) have been shown to exhibit basal ATPase activity in the absence of substrate, while other transporters (such as yeast Pdr5) only exhibit basal activity (i.e. are not stimulated by their substrates) (90, 92). Therefore, the presence of substrate, and the subsequent dimerization of the NBDs, is not required for ATP hydrolysis, and the dimerization of the NBDs does not guarantee an increase in ATPase activity. Interestingly, the ATP hydrolysis site in one NBD interface has degenerated in Pdr5, which partially explains how this transporter is only capable of basal activity. A similar asymmetry in the NBDs is found in the human ABC transporters CFTR/ABCC7 and TAP1 (93, 94). Third, mutational analysis has identified residues in the NBDs that alter the substrate selectivity of certain transporters (95, 96). Thus, at least for a number of ABC transporters, the NBDs do play some role in substrate selection. Last, a study of at least one bacterial ABC transporter, HorA, demonstrated that reconstitution of the protein in liposomes changed its function relative to the protein in its native membrane. While HorA ATPase activity was retained in the liposomes, transport function was lost (97). We

can conclude that, at least for certain transporters, the local environment plays a role in the communication between the TMDs and NBDs.

A feature of many ABC transporters is their ability to transport a wide array of allocrites. This can be demonstrated in P-glycoprotein (P-gp), where certain substrates only compete with Hoechst 33342 transport, and not rhodamine transport, and vice versa (91). Other drugs compete with both, indicating that various drugs occupy different binding sites in the transporter. Structural and biochemical analysis of multidrug transporters indicate that a large, hydrophobic drug-binding pocket exists, but can be divided into smaller sub-sites with varying affinities for different drugs (98, 99). A complete understanding of how these transporters recognize their substrates has yet to be elucidated.

ABC Transporter Structure

The first structure of a full ABC transporter was published by Kaspar Locher's group in 2006 (100). This group determined the 3 Å structure of *Staphylococcus aureus* Sav1866, a homolog of human ABCB1 (P-glycoprotein/MDR1) and TAP1 transporters. The full transporter is 120 Å long, 65 Å wide, and 55 Å deep in the outward facing, ATP-bound state. It consists of twelve alpha helices, which form the transmembrane domains and intracellular loops (ICLs) which extend ~25 Å away from the plasma membrane, and two symmetrical nucleotide binding domains in a head-to-tail arrangement (Figure 1.4A and B).

The two halves of the protein showed extensive interactions, with the two NBDs cooperatively forming two ATP-hydrolysis sites, and portions of the ICLs from each half of the transporter contain short alpha helices parallel to the membrane

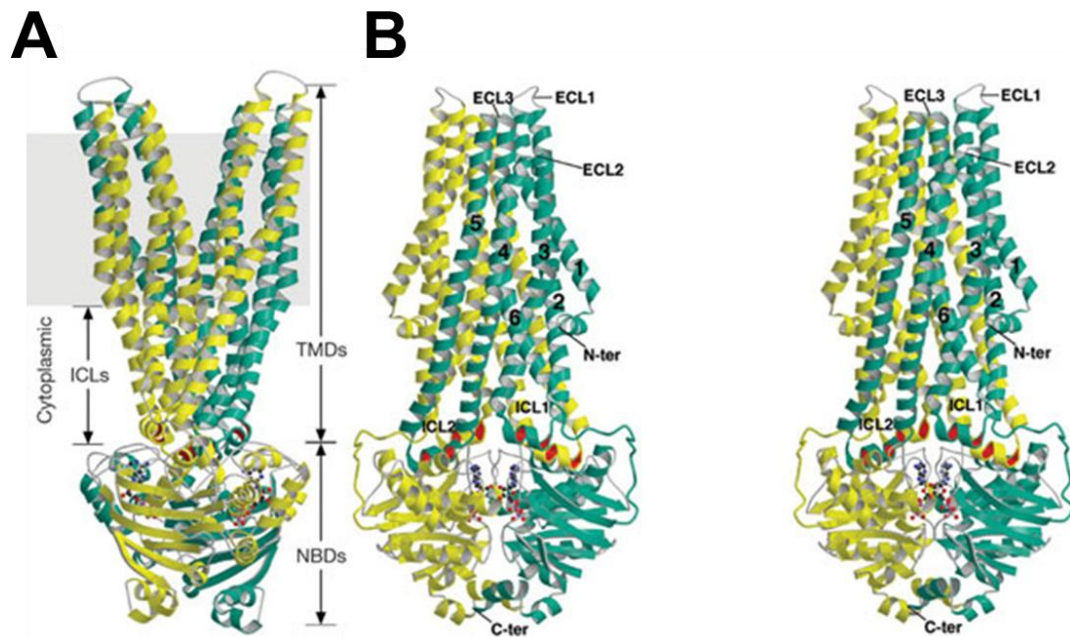


Figure 1.4: Sav1866 Structure.

(A) Structure of full length Sav1866 from *Staphylococcus aureus*, with each half (subunit) of the protein coloured yellow or turquoise. Bound ADP is shown in ball-and-stick representation. The view depicts the membrane-embedded “ears”; the grey box shows the probable location of the lipid bilayer. (B) Stereo view of the Sav1866 structure rotated 90° with respect to (A). The transmembrane helices of one subunit are numbered. Note that TMD1 is the only TMD that does not extend past the membrane. TMDs, transmembrane domains; NBDs, nucleotide-binding domains; ICL, intracellular loops; ECL, extracellular loops; N-ter, amino terminus; C-ter, carboxy terminus. Image is taken from (100).

plane. These helices, termed ‘coupling helices’, engage in domain swapping with the NBD of the other half of the transporter. For example, the ICL formed between transmembrane segments 4 and 5 from TMD1 interacts with NBD2 (Figure 1.3B). This interaction is thought to aid in transmitting conformational changes due to nucleotide binding from the NBDs to the TMDs. This is consistent with previous studies showing that these components interact and are required for optimal transport activity (101, 102). Interestingly, domain swapping of the coupling helices does not occur in the structure of ABC importers that have been solved thus far.

The translocation pathway in this structure does not connect to the cytoplasm; rather, it opens into the extracellular space. It is lined with polar and charged residues, which the authors conclude reflect a mechanism for the extrusion of hydrophobic allocrites. Additionally, residues from all transmembrane helices contribute to the surface of the pathway through the transporter, and no high-affinity binding sites are found in this channel.

Since the publication of the Sav1866 structure, a number of eukaryotic ABC transporter structures have been solved. The 3.8 Å structure of mouse p-glycoprotein (P-gp or ABCB1/MDR1) was published in 2009 (98). P-gp is of particular clinical interest in that it has unusually broad specificity, transporting chemically diverse compounds ranging from 330 to 4000 daltons. This structure was solved in the inward-facing conformation, with the two NBDs separated by 30 Å. However, the structure does reveal a large cavity open to both the cytoplasm and the inner leaflet of the membrane, allowing hydrophobic molecules found in the membrane direct access to the transport channel. The cavity is lined with mostly hydrophobic and aromatic

residues, to facilitate transport of hydrophobic allocrites. P-gp was also crystallized in the presence of two transport substrates, two cyclic peptides (QZ59-RRR and QZ59-SSS). P-gp can distinguish between these two stereoisomers, as they are shown to bind different residues. Indeed, upon comparing amino acids in contact with QZ59-RRR, QZ59-SSS, and another substrate, verapamil, the authors note that only two out of a total thirty three drug-binding residues are shared by all three allocrites.

Recently, the 3 Å structure of *C. elegans* P-gp (*pgp-1*) in the inward-facing conformation was published (103). Similar to mouse P-gp, the transport cavity is open to both the cytosol and the inner membrane leaflet. Given that worm P-gp shows 100- to 4,000-fold more allocrite-stimulated ATPase activity in the presence of membranes than in the presence of detergents, the authors conclude that indeed P-gp substrates are transported more efficiently directly from the membrane. Additionally, the authors show that the contact points between the intracellular loops and NBDs are similar to those in mouse P-gp; this is reflected in the high degree of sequence conservation (approaching 80% identity) between worm and mouse P-gp in these regions.

Multidrug Resistance Protein 5 (MRP5)

The focus of this work, MRP5, was discovered by three independent groups looking to identify novel ABC transporters (104-106). MRP5 transcripts were detected in all human tissues assayed, including the spleen and small intestine, with the highest expression in skeletal muscle and brain (105). MRP5 localizes to the basal membrane of syncytiotrophoblasts and fetal vessels of the placenta (107). In the blood-brain barrier, MRP5 is found in the apical membrane of capillary endothelial

cells (108). MRP5 localizes to intracellular structures in human bronchial epithelial cells (109).

Early on it was demonstrated that MRP5 is an organic anion transporter, capable of effluxing acidic, organic dyes and glutathione (GSH), as well as nucleotide monophosphate analogs (110). Soon afterward, it was demonstrated that MRP5 transported the cyclic nucleotides cGMP and cAMP with K_m values of 2.1 and 379 μM , respectively (111). The affinity of MRP5 for cAMP and cGMP appears to vary depending on the model system used (112). No resistance to cisplatin or doxorubicin was observed in MRP5-transfected cells (110, 113). In a review, Borst *et al* conclude that it is unlikely that MRP5 contributes substantially to drug resistance (114); however, it should be noted that *MRP5* is upregulated in certain cancer types (115-117). In the same review, published in 2006, the authors note that the function of MRP5 remained a mystery.

Summary

Heme is ubiquitously required by living organisms as a prosthetic group in proteins (118). Heme is synthesized in the mitochondrial matrix but must be trafficked to various subcellular compartments for incorporation into hemoproteins in the cytoplasm, ER/Golgi, lysosomes, and peroxisomes (119). However, unescorted movement of heme within a cell is inherently hazardous due to the reactivity of free heme. It follows that cells must have specific pathways for the directed movement of heme within and between cells and tissues but these intra- and intercellular pathways have remained poorly defined (118, 119).

We have exploited *Caenorhabditis elegans* as a genetic model organism because this roundworm is a heme auxotroph (120). *C. elegans* is dependent on both maternally-derived heme for embryonic development, as well as heme acquired from the diet during larval growth (120). How does intestinal heme, derived from the environment, get delivered to hemoproteins in extra-intestinal tissues? Are these intercellular heme transport pathways found in vertebrates? With this work, we show that a multidrug resistance protein, MRP-5/ABCC5, likely acts as a cellular heme exporter and is essential for viability in *C. elegans*. This conclusion is supported by our genetic studies in yeast, *C. elegans*, zebrafish, and mammalian cell culture models which ascribe a physiological role for a multidrug resistance protein in regulating systemic heme homeostasis in metazoans.

Chapter 2: Materials and Methods

Worm Methods

Worm Culture

Worms were maintained in axenic liquid mCeHR2 medium with continuous shaking or on nematode growth medium (NGM) plates seeded with OP50 or HT115(DE3) bacteria at 15°C or 20°C unless noted otherwise (121). NGM plates were 3 g/L NaCl, 2.5 g/L peptone, 20 g/L agar, 5 mg/L cholesterol, 0.1 M CaCl₂, 0.1 M MgSO₄, and 25 mM KH₂PO₄. Routine maintenance, synchronization, crosses, and observation of *C. elegans* were described by Epstein and Shakes (122).

Synchronization of Worms

Worms were collected from plates using M9 buffer (86 mM NaCl, 42 mM Na₂HPO₄, 22 mM KH₂PO₄, and 1 mM MgSO₄) and washed three times to remove bacteria. Worms from liquid mCeHR-2 medium were harvested by centrifugation at 800 x g for 5 minutes (121). The medium was aspirated and 0.1 M NaCl was added. The worms were allowed to settle on ice for 5 minutes. The supernatant was aspirated and gravid worms remaining were bleached using a 1.1% sodium hypochlorite and 0.55 M NaOH solution. After eggs were observed being released from adult worms, the mixture was centrifuged (800 x g, 1 minute) and washed twice with sterile water. Eggs were resuspended in M9 buffer and allowed to hatch overnight.

Worm Strains

Worms strains used in this study are listed in Appendix I. VC1599, WM118, NR222, and VP303 strains were obtained from the Caenorhabditis Genetics Center (CGC, USA). The deletion strain *mrp-5(ok2067)* was obtained by crossing the balanced strain VC1599 to wild-type N2 worms on plates seeded with OP50 grown in media supplemented with 500 μ M heme. F₂ progeny were analyzed by single worm PCR to identify homozygous mutants and wild-type brood mates. Genotyping primers for the *mrp-5(ok2067)* allele can be found in Appendix II. Homozygous *mrp-5* worms were outcrossed three times to N2 worms, and maintained on plates seeded with OP50 bacteria grown in LB broth supplemented with >200 μ M heme.

Gateway Cloning

The *mrp-5* transcriptional and translational reporter constructs were generated using Multisite Gateway recombination (Invitrogen). *C. elegans* promoters, ORFs, and 3' untranslated regions were amplified with sequence-specific Gateway attB primers. PCR products were recombined into donor plasmids, and then into expression plasmids, according to the manufacturer's instructions (Invitrogen).

Generation of Transgenic Worms

Reporter constructs, along with the *unc-119* rescue construct, were introduced by microparticle bombardment into *unc-119(ed-3)* worms using the PDS-1000 particle delivery system (Bio-Rad) (123). At least two transgenic worm lines were analyzed per construct.

Single Worm PCR

For single worm PCR, worms were lysed in lysis buffer (50 mM KCl, 10 mM Tris-HCl, 2.5 mM MgCl₂, 0.45% NP-40, 0.45% Tween-20, 0.01% gelatin, 1 mg/ml proteinase K) by incubation for 2 hours at -80°C, 1 hour at 65°C, and 30 min at 95°C. Worm lysates were added to PCR reactions with primers to detect wild-type and mutant alleles. Genotyping primers for *mrp-5(ok2067)* are listed in Appendix II.

RNA Extraction, cDNA Synthesis, and Quantitative Real Time PCR

Synchronized worms were grown at varying heme concentrations (1.5-20 µM heme) for two generations and then harvested at the late L4 stage. Worms were washed in M9 buffer, lysed using Lysing Matrix C beads (MP Biomedicals) in a FastPrep-24 Beadbeater (MP Biomedicals). Total RNA was isolated with the TRIzol reagent (Invitrogen), purified by chloroform extraction, and DNase-treated with TURBO DNase (Life Technologies). RNA quality was monitored using gel electrophoresis and by measuring the absorbance at 260 nm and 280 nm using a spectrophotometer (Shimadzu).

After resuspension in Tris buffer (pH 8.0), 2 µg of total RNA was used to synthesize cDNA using oligo(dT) primers and the SuperScript III First-Strand Synthesis System (Invitrogen), according to manufacturer's instructions. Quantitative real-time PCR (qRT-PCR) was performed in triplicate using SYBR green as the detection dye in an iCycler iQ Multi-Colour Real-Time PCR Detection System (Bio-Rad). Gene specific primers were used as in (40) and are listed in Appendix II.

RNA Interference

RNAi experiments were performed by feeding the worms bacteria expressing double-stranded RNA (dsRNA) complimentary to the gene of interest. For RNAi feeding, the clones for *mrp-2*, *mrp-4*, *mrp-5*, *mrp-6*, and the *C. elegans* FLVCR homologs were taken from the Ahringer library (124). The clone for *mrp-8* was taken from the Vidal library (125). The clones for *hrg-1* and *hrg-4* were generated previously as in (40). The clones for *mrp-1*, *mrp-3*, *mrp-7*, and the *mrp-5* 3' UTR were generated by cloning portions of their transcripts into the L4440 plasmid (Fire Vector Kit, Addgene) which were then transformed into the RNase III-deficient bacteria, HT115(DE3). Bacterial cultures were grown and then spotted onto NGM plates containing 50 µg/mL carbenicillin, 12 µg/mL tetracycline, and 2 mM isopropyl-β-D-thiogalactopyranoside (IPTG). L1 larvae were placed on RNAi plates and incubated at 15°C or 20°C. Phenotypes were investigated as necessary after at least 72 hours.

Heme Analog Assays

Zinc mesoporphyrin, and gallium protoporphyrin IX were purchased from Frontier Scientific, Inc (Logan, UT). Heme analog solutions were prepared as 10 mM stock by dissolving in 0.3 M NH₄OH and pH-adjusted to 8.0 by addition of HCl. To assess uptake of ZnMP, synchronized L1 worms were grown on NGM plates seeded with OP50 or RNAi bacteria until they reached L4 stage. Worms were washed off plates and rinsed three times in M9 buffer to remove bacteria. Worms were incubated in mCeHR2 medium with 60 µM ZnMP for 3 hours, rinsed to remove excess ZnMP, and imaged as described previously (40). Briefly, worms were paralyzed with 10 mM

levamisole and imaged using a Leica DMIRE2 epifluorescence/DIC microscope. Images were obtained using a Retiga 1300 cooled mono 12-bit camera and quantified using SimplePCI software (Compix Inc).

To assess toxicity of GaPPIX, synchronized L1 worms were grown on NGM plates seeded with OP50 or RNAi bacteria until they reached L4 stage. Worms were washed off plates and added to NGM plates containing various concentrations of GaPPIX and seeded with OP50 or RNAi bacteria. After 48 hours, worms were scored as dead if they were unresponsive to a physical stimulus.

Quantification of Fluorescence using COPAS BioSort

Worms were grown from the L1 larval stage to the early adult stage on RNAi plates. Worms for each condition were analyzed for time of flight (length) and extinction (optical density) using a COPAS BioSort (Union Biometrica, Holliston, MA) with gating parameters for mixed worm populations as in Chen et al (77). The settings for measuring GFP intensity in IQ6011 ($P_{\text{hrg-1}}::\text{GFP}$) were gain = 2.5 and PMT voltage = 400 and in IQ8031 ($P_{\text{hrg-3}}::\text{GFP}$) were gain = 2.5 and PMT voltage = 600. The settings for measuring YFP intensity in IQ8122 ($P_{\text{hrg-2}}::\text{HRG-2-YFP}$) were gain = 2.5 and PMT voltage = 600.

Growth Assays

To assay embryonic lethality, worms were grown to gravid stage on NGM plates seeded with OP50 bacteria. (Wild-type N2 worms were grown on OP50 bacteria with no added heme, while *mrp-5(ok2067)* worms were grown on OP50 with >200 μM added heme.) Synchronized L1 larvae were placed on NGM plate

containing IPTG, tetracycline, and carbenicillin that were seeded with vector control or RNAi bacteria with or without added heme, and allowed to reach young adult stage. Adult worms were moved to fresh plates, allowed to lay eggs for 24 hours, and then removed. Hatched L1 worms and eggs were counted 24 hours after removal of adults; eggs that did not hatch after 24 hours were considered dead.

To assay larval development, wild-type N2 and *mrp-5(ok2067)* worms were grown to gravid stage on NGM plates seeded with OP50 bacteria grown in LB broth with the addition of >200 μ M heme. Synchronized L1 larvae were seeded onto NGM plates seeded with OP50 bacteria grown with or without 200 μ M added heme. Worms were incubated and DIC images were obtained when wild-type N2 worms reached gravid stage (4 days).

Yeast Methods

Strains and Growth

S. cerevisiae strains used in this study contained the *hem1* Δ mutation in the W303 and YPH499 strains and have been described previously (41, 126, 127). Cells were maintained at 30°C in yeast peptone dextrose (YPD) media supplemented with 250 μ M δ -aminolevulinic acid (ALA) unless otherwise noted (Frontier Scientific). The *hem1* Δ *fre1* Δ *fre2* Δ *PGK1-FRE1* strain was maintained on synthetic complete (SC) plates (-Trp) containing 2% w/v glucose supplemented with 250 μ M ALA.

Cloning and Transformation

To generate yeast expression plasmids, a yeast codon-optimized and flag-tagged ORF of CeMRP-5 was synthesized (Genscript), amplified with primers

containing BamHI and XbaI sites, digested, and ligated into the pYES-DEST52 vector (Invitrogen) digested with the same enzymes. Human MRP5 (Genbank #U83661) was amplified with primers containing BglII and SpeI sites (with and without a C-terminal HA tag), digested, and ligated into pYES-DEST52 digested with the compatible cohesive enzymes, BamHI and XbaI. The Pug1p ORF in pYES-DEST52 was a gift from Caroline Philpott (National Institutes of Health).

Growth Assays

The liquid and dilution spot assays were performed as described previously (41, 126, 127). Plasmids containing potential heme transporters were transformed into *hem1Δ* yeast using the lithium method (128) and selected on 2% w/v glucose SC (-Ura) plates supplemented with 250 μM ALA. Ten colonies were streaked onto 2% w/v raffinose SC (-Ura) plates supplemented with 250 μM ALA for 48 hrs. Cells were grown in 2% w/v raffinose SC (-Ura) liquid medium without heme or ALA for at least 12 hours to deplete endogenous heme. For the liquid growth assay, cells were then diluted to OD₆₀₀ of 0.05 in 96-well plate format, and grown in a humidity chamber at 30°C for 24 hours. OD₆₀₀ was measured using a Synergy HT microplate reader (Biotek). For the dilution spot assay, cells were diluted to OD₆₀₀ of 0.2, serially diluted, and spotted in 10 μl aliquots onto 2% w/v raffinose SC (-Ura) plates supplemented with varying amounts of heme or ALA and 0.4% w/v galactose to induce gene expression from the GAL1 promoter. Plates were incubated for 3 days before imaging. To assay aerobic growth exclusively, yeast were induced with 2% galactose in the of ALA, and then spotted onto plates containing indicated heme or ALA concentrations as well as 2% glycerol and 2% lactate as a carbon source.

β -Galactosidase Assay

Plasmids were co-transformed into the *hem1 Δ* strain with the reporter plasmid pRS314m-CYC1-LacZ. Transformants were selected on 2% w/v glucose SC (-Ura -Trp) plates supplemented with 250 μ M ALA. Cells were heme-depleted by growth in 2% w/v raffinose SC (-Ura -Trp) liquid medium with no added ALA for 12 hours. Cells were then resuspended to an OD₆₀₀ of 0.1 in 2% w/v raffinose SC (-Ura -Trp) liquid medium supplemented with varying concentrations of heme or ALA and 0.4% w/v galactose for gene induction and cultured overnight. Cells were washed in washing buffer (2% BSA, 0.1% Tween-20 in 2X PBS), lysed, and assayed for β -galactosidase activity as described elsewhere (129). Protein concentrations for each lysate were measured and β -galactosidase activity was normalized to total protein.

Ferric Reductase Assay

Plasmids were transformed into the *hem1 Δ fre1 Δ fre2 Δ PGK1-FRE1* strain as above and selected using 2% w/v glucose SC (-Ura -Trp) plates supplemented with 250 μ M ALA. Cells were restreaked on 2% w/v raffinose SC (-Ura -Trp) plates supplemented with 250 μ M ALA for 2 days. Cells were heme depleted by growth in 2% w/v raffinose SC (-Ura -Trp) liquid media with no added ALA for at least 12 hours. Cells were resuspended in 2% w/v raffinose SC (-Ura -Trp) liquid medium supplemented with 0.4% w/v galactose, 0.1 mM Na₂S, and varying concentrations of heme or ALA and grown overnight. Cells were washed repeatedly in washing buffer, then in reaction buffer (5% glucose, 0.05 M sodium citrate buffer, pH 6.5) and resuspended in reaction buffer. The OD of the suspended cells was measured, equal volume assay buffer (2 mM bathophenanthroline disulfonate, 2 mM FeCl₃ in reaction

buffer) was added (T=0 min), and cells were incubated at 30°C until a red color developed. OD₅₃₅ and OD₆₁₀ were measured and ferric reductase activity (nm/10⁶ cells/min) was determined.

Immunofluorescence

Transformed yeast were grown in 2% w/v raffinose SC (-Ura) liquid medium supplemented with 0.4% galactose and 250 μM ALA, and fixed with 4% formaldehyde for 1 hour at room temperature. Cells were washed twice with phosphate buffered saline (PBS) and resuspended in 1.2 M sorbitol with 1 mM dithiothreitol and treated with 30 μg zymolase at 30°C for 30 minutes. The resulting spheroplasts were washed twice with sorbitol buffer. Spheroplasts were added to poly-L-lysine-coated 8-well slides, incubated with anti-Flag or anti-HA antibody, and then Alexa-488 conjugated secondary antibody. Each sample was covered in ProLong Antifade solution (Invitrogen) and a coverslip and allowed to dry before analysis by confocal microscopy.

Mammalian Methods

Mouse Strains and Care

All animal experiments were approved by the University of Maryland Institutional Animal Care and Use Committee. FVB/NJ mice were purchased from Jackson Laboratories (Bar Harbor, ME). *Mrp5* mutant mice were a gift from Dr. Piet Borst (Netherlands Cancer Institute). Mouse pups and cell lines were genotyped for *Mrp5* using primers adapted from (130), which are listed in Appendix II.

Generation of Immortalized Fibroblasts

To generate mouse embryonic fibroblasts (MEFs), E12.5 embryos were isolated, and cultured as described (131). Immortalized *Mrp5*^{+/+}, *Mrp5*^{+/-}, and *Mrp5*^{-/-} cell lines were generated by retroviral infection of MEFs with conditioned media from Ψ2-U195 cells producing the SV40 large T antigen as in (132). SV40 large T antigen expression was confirmed in MEFs by Western blot and cell lines were genotyped using the *Mrp5* primers listed in Appendix II.

Mammalian Cell Culture

Mammalian cells were cultured at 37°C in a humidified incubator with 5% CO₂. MDCKII cells and MEFs were grown in Dulbecco's modified Eagle medium (DMEM) supplemented with 10% FBS and 1% penicillin/streptomycin/glutamine for cell culture studies. MDCKII cells expressing human MRP5 were a gift from Piet Borst (Netherlands Cancer Institute).

Isolation and culture of bone marrow from the femurs of C57BL/6 mice was carried out as described elsewhere (133). Differentiation of bone marrow monocytes was carried out in differentiation medium including L-929 cell-conditioned media (LCM) as a source of granulocyte/macrophage colony-stimulating factor (134). Differentiation media is RPMI 1640 (Invitrogen) supplemented with 30% LCM, 20% heat-inactivated fetal bovine serum (FBS, Atlanta Biologicals), 100 U/ml penicillin, 100 mg/ml streptomycin, and 2 mM L-glutamine (Invitrogen). L-929 cells were purchased from the American Type Culture Collection (ATCC). For production of LCM, L-929 cells were grown in the presence of RPMI 1640 supplemented with 10% heat-inactivated FBS, 100 U/ml penicillin, 100 mg/ml streptomycin, and 2 mM L-

glutamine for 30 days. Media was collected by sterile filtration and stored at -20°C . In all experiments, BMDMs were cultured in the presence of heme-depleted serum (HD) media as untreated control. HD media was prepared similarly to differentiation media with the exception of substituting 20% heme-depleted FBS for FBS. Heme depletion was achieved by treating FBS with ascorbic acid for $\sim 7-8$ hr, followed by dialysis against PBS and filter sterilization. The depletion of heme from the serum was monitored by measurement of the optical absorbance at 405 nm. Depletion was considered successful when the absorbance of serum was reduced at least 50% following ascorbic acid treatment (135).

DNA Cloning

The human MRP5 ORF cut with BglII and SpeI was cloned into pcDNA3.1(+)-zeo and pEGFP-N1 cut with BamHI and XbaI for mammalian expression. Plasmids were transfected into MDCKII cells and MEFs using Lipofectamine transfection reagent (Invitrogen).

Immunofluorescence

For MRP5 staining, cells were fixed in acetone, blocked in 5% BSA in 1X PBS, incubated with the primary antibody (anti-MRP5, 1:40 in blocking solution), secondary antibody (Alexa-conjugated anti-rat, 1:3000 in blocking solution), subjected to DAPI staining, and mounted using Prolong Gold Antifade (Invitrogen). Immunofluorescence staining was performed as in (136). Images were taken using an LSM710 confocal microscope (Zeiss) The MRP5 antibody was a gift from Piet Borst (Netherlands Cancer Institute).

Immunoblotting

For detection of MRP5, cells were lysed in SDS lysis buffer (2% SDS, 1% Triton X-100, 1 mM EDTA, 62.5 mM Tris-Cl pH 7.5) with protease inhibitors (1 mM phenylmethylsulfonyl fluoride, 4 mM benzamidine, 2 µg/ml leupeptin, and 1 µg/ml pepstatin), and sonicated twice. Cells were centrifuged at 14,000 x g for 15 min at 4°C, and total protein concentration in the supernatants was measured using the Pierce BCA assay kit (Thermo Scientific). Unboiled samples were mixed with Laemmli sample buffer and 200 mM dithiothreitol (DTT), and 100 µg protein/lane were separated on 7% SDS-PAGE and transferred to a nitrocellulose membrane. The anti-MRP5 monoclonal antibody was used at a concentration of 1:200, goat anti-rat HRP-conjugated secondary was used at 1:30,000, and blots were developed in SuperWest Femto Chemiluminescent Substrate (Thermo Scientific).

Horseradish Peroxidase Assay

Mrp5^{+/+} and *Mrp5^{-/-}* MEFs were transfected with GolgiHRP expressed from the pShuttle-IRES-hrGFP-1 vector using the Lipofectamine transfection reagent (Invitrogen). The following day, cells were incubated in heme-depleted media (DMEM with 10% heme depleted FBS and 1% PSG) and 0.5 mM succinylacetone (SA). The following day, cells were switch to HD media + SA with the addition of 1.5 or 2 µM heme. Cells were harvested a day later and lysed in 1% Triton X-100, 1 mM EDTA, 62.5 mM Tris-Cl pH 7.5, with protease inhibitors (1 mM phenylmethylsulfonyl fluoride, 4 mM benzamidine, 2 µg/ml leupeptin, and 1 µg/ml pepstatin). Total protein concentration for each sample was measured using the BioRad Protein Assay Dye Reagent Concentrate solution. Peroxidase activity for

each sample was measured as in (43). Each sample was normalized to the peroxidase activity in a corresponding empty vector control, as well as to total protein levels.

Preparation of Red Blood Cells and *In Vitro* Erythrophagocytosis

Preparation of red blood cells (RBCs) and *in vitro* erythrophagocytosis (EP) was performed as in (43). Human blood was collected by finger prick using heparinized blood gas capillaries (Ram Scientific Inc.) and then opsonized. Blood was centrifuged at 800 rpm for 5 minutes and the serum was discarded. Plasma was washed with PBS three times. RBCs were incubated at 1:500 dilution with rabbit anti-human RBC antibody (Cappel) at room temperature with gentle rocking for 1 hour. After incubation, RBCs were washed 3 times in PBS to remove excess unbound antibody. RBCs were counted and could be stored at 4°C for up to 4 days. Opsonization of carboxy-modified latex beads (CML beads) was carried out as follows: CML beads were incubated with bovine serum albumin (BSA, 1mg/ml in PBS) at 37°C for 1 hour. This was followed by centrifugation at 14,000 x g for 1 hour and a wash in PBS. The beads were centrifuged again at 14,000xg, and the PBS wash was discarded. The BSA-coated beads were then incubated in the presence of a mouse anti-BSA antibody (Sigma, 10 µg/ml) at 37°C for 1 hour, followed by 3 washed in PBS.

EP was performed in the presence of HD media. Opsonized RBCs or latex beads were added to cultured BMDMs at the indicated RBC:BMDM ratio. Phagocytosis was allowed to occur for 60 min at 37°C, 5% CO₂. Following EP, BMDMs were washed once with PBS, and incubated with hypotonic solution (140 mM NH₄Cl, 17 mM Tris-HCl pH 7.6) for 5 min to allow lysis of any remaining

extracellular RBCs. Following 2 additional washes with PBS, BMDMs were cultured with HD media for the indicated periods of time.

RNA Isolation, cDNA Synthesis and Quantitative RT-PCR

RNA was isolated from BMDMs using the Nucleospin RNA II kit (Macherey Nagel). First strand cDNA was synthesized from 2 μg total RNA using the SuperScript III First-Strand Synthesis System (Invitrogen) and oligo(dT) primers. For qRT-PCR, primers used are listed in Appendix II. Real-time quantification of transcripts was performed in an iCycler iQ Real-Time PCR detection system (Bio-Rad). Total reaction volume was 15 μl with 0.12U/ml Taq DNA polymerase, 40nM fluorescein (Invitrogen), 10 pmol of forward and reverse primer, and SYBR Green I Nucleic Acid Gel Stain (Invitrogen). Dissociation curve analysis and gel electrophoresis were used to monitor the quality of PCR products. In each experiments, biological samples were run in triplicates, and quantitative analysis for each sample was run in duplicate (n=6 per experiment). For each gene, results were normalized to the CT value of mGapdh. Relative fold changes in gene expression were assessed using the $\Delta\Delta\text{CT}$ method. Changes in gene expression were assessed relative to control samples of BMDM grown in HD media and harvested at each experimental time point.

General Procedures

Preparation of Hemin Chloride

For all experiments, heme was added in the form of hemin chloride (Frontier Scientific, Logan, UT). Hemin chloride was prepared 10 mM stock by dissolving in 0.3 M NH₄OH. The pH of the solution was adjusted to 8.0 by addition of HCl.

Microscopy

GFP, YFP, and ZnMP fluorescence in worms, yeast, or mammalian cells was imaged using a DMIRE2 epifluorescence microscope (Leica) connected to a Retiga 1300 cooled mono 12-bit camera or using a laser scanning confocal microscope (LSM710) (Zeiss).

Bioinformatics and Statistics

ClustalW and MEGA5 were used to generate a phylogenetic tree for the full length sequences of all human, mouse, zebrafish, and *C. elegans* MRP/ABCC proteins (137, 138). Membrane protein topologies were generated using TMHMM and drawn using TOPO2 (139, 140). All data are presented as mean \pm the standard error of the mean. Statistical significance was determined using one-way or two-way ANOVA with Bonferroni post-tests (as indicated in figure legends) in GraphPad Prism, version 5.00 (GraphPad Software, Inc).

Chapter 3: Delineating the role of *mrp-5* in *C. elegans* heme homeostasis

*My days are in the yellow leaf;
The flowers and fruits of Love are gone;
The worm, the canker, and the grief
Are mine alone!*

Lord Byron
“On This Day I Complete My Thirty-Sixth Year”

Summary

Hemes are metalloporphyrins used by nearly all organisms as protein cofactors for energy production, binding and sensing gases, and as an electron donor or acceptor for various redox reactions. While heme biosynthesis has been well-characterized, the pathways for transporting heme between cells and within a cell remain poorly understood. *C. elegans* serves as a unique animal model for uncovering these pathways, as it is unable to synthesize its own heme. As a heme auxotroph, *C. elegans* is dependent on both maternally-derived heme for embryonic development, as well as heme acquired from the diet during larval growth (120). Heme is imported into the cytosol of the worm intestine via the conserved heme permease, HRG-1 and its paralog HRG-4 (40). The intercellular heme-trafficking protein, HRG-3, is secreted from the intestine and carries heme to developing embryos (77). HRG-2 is an extra-intestinal, heme-binding membrane protein that facilitates heme utilization in the worm hypodermis (141). Given that *hrg-3* is only expressed under heme-limiting

conditions, we postulated the existence an alternate mechanism for heme export from the intestine.

We previously identified *mrp-5* as one of several regulators of heme homeostasis in *C. elegans* via an RNAi screen (142). Here we show that this candidate gene, a conserved ABC transporter, is transcriptionally heme responsive and regulates GFP expression in the heme sensor worm strain (IQ6011). RNAi depletion of *mrp-5* results in embryonic lethality in the F₁ generation, and deletion of *mrp-5* results in larval growth arrest. Both these phenotypes can be rescued by the addition of excess heme to the diet. Regulation of *mrp-5* is different than previously studied heme transporters in *C. elegans*, as it is expressed across a wide spectrum of heme concentrations. In the intestine, MRP-5 is found in basolateral sorting vesicles and on the basolateral plasma membrane. Knockdown of *mrp-5* additionally results in the accumulation of a fluorescent heme analog in the worm intestine and upregulates extra-intestinal heme deprivation signals. While *mrp-5* is expressed in multiple tissues, we show that loss of *mrp-5* specifically from the intestine leads to altered heme homeostasis in the worm and the associated embryonic lethality. Taken together, these data indicate that *mrp-5* is the intestinal heme effluxer in *C. elegans*.

Results

Identification of *mrp-5* as a regulator of heme homeostasis in *C. elegans*

Our previous studies implicated HRG-3 in the directed trafficking of heme to extra-intestinal tissues, including embryos (Figure 3.1). However, *hrg-3* mutant embryos are viable unless subjected to severe maternal heme limitations *in utero* (77).

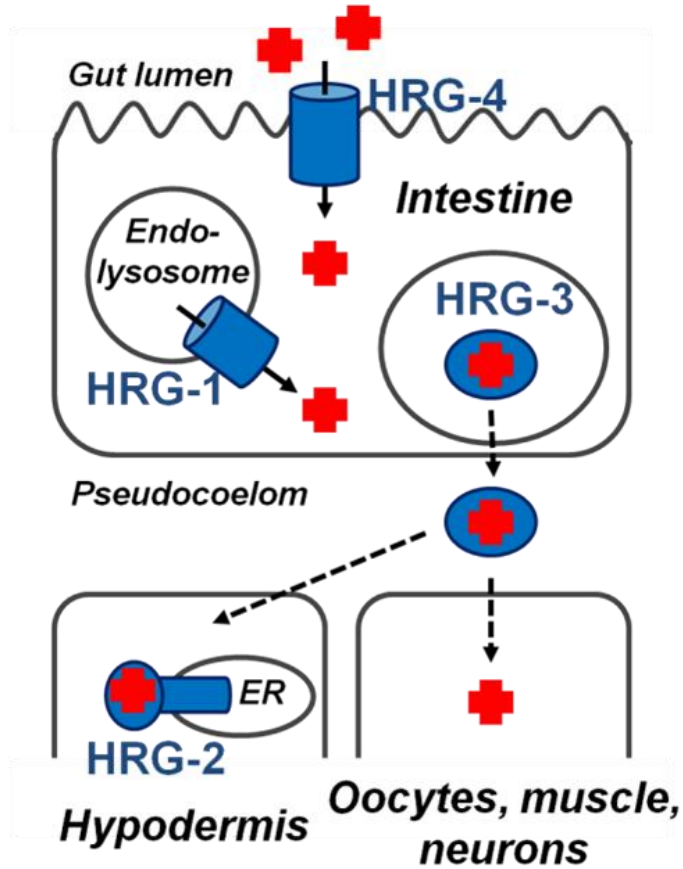


Figure 3.1: Current model of heme homeostasis in *C. elegans*.

The heme permeases HRG-4, and HRG-1, which are localized to the apical plasma membrane and endolysosomal compartments, respectively, both import heme into the cytosol of intestinal cells. HRG-3 is secreted from the intestine for heme delivery to other tissues, and HRG-2 is a resident ER protein involved in heme utilization within the hypodermis.

In fact, when worms are grown in the presence of $>6 \mu\text{M}$ heme, *hrg-3* mRNA is undetectable (77). Thus, HRG-3 serves as an inducible mechanism for redirecting heme stores only under heme-limiting conditions. These results would also predict that, in the absence of HRG-3, an alternate pathway exist in *C. elegans*.

We postulated that membrane-bound heme transporters would be suitable candidates for regulating systemic heme homeostasis in the worm, and consequently impact the regulation of other heme-responsive genes. By individually depleting 288 heme-responsive genes, which included 41 genes encoding transmembrane domain-containing proteins, we uncovered *mrp-5*² (WormBase accession number F14F4.5) as a potent regulator of the *C. elegans* transgenic heme sensor strain, IQ6011. The IQ6011 strain expresses GFP in the intestine from the heme-responsive *hrg-1* promoter; GFP levels in this strain are inversely correlated with heme levels in the worm (40, 143). As proof-of-principle, when the intestinal heme importer, *hrg-4*, is depleted in worms grown at low heme ($\leq 20 \mu\text{M}$), GFP is upregulated compared to vector control worms. Depletion of *mrp-5* in IQ6011 by RNAi also resulted in significantly greater GFP levels compared to control RNAi, indicating that loss of *mrp-5* results in the animal sensing less heme (Figure 3.2A and (142)). Importantly, this heme depletion signal could be rescued in a concentration-dependent manner by supplementation with dietary heme (Figure 3.2A). The increased GFP signal observed by knockdown of the intestinal heme importer, *hrg-4*, could be completely suppressed with $50 \mu\text{M}$ heme, while the *mrp-5* RNAi signal persisted even at $500 \mu\text{M}$, indicating

² Throughout this text, worm genes will be written in the format *mrp-5*, and worm proteins will be written as MRP-5. Zebrafish genes will be written *mrp5*, and zebrafish proteins written as Mrp5. Mouse genes will be written as *Mrp5*, and proteins as Mrp5, while human genes will be written in the format *MRP5* and human proteins as MRP5. When referring to a MRP5 proteins from all four species, I will use the format MRP5.

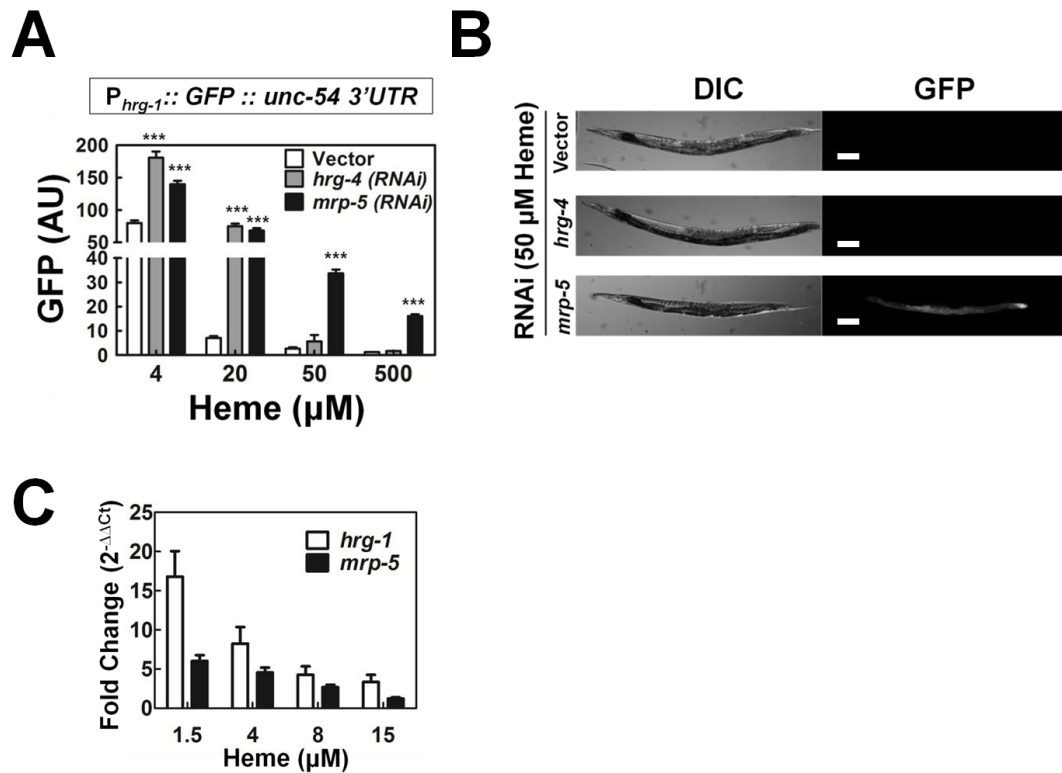


Figure 3.2: *mrp-5* is involved in heme homeostasis in *C. elegans*.

Loss of *mrp-5* results in a heme depletion signal that can be rescued by dietary heme.

(A) GFP fluorescence (60-120 worms per treatment) quantified using COPAS BioSort in IQ6011 ($P_{hrg-1}::GFP::unc-54\ 3'UTR$; *unc119(ed3)*; *unc-119* rescue fragment) exposed to vector, *hrg-4*, or *mrp-5* RNAi. *** $P < 0.001$ when compared to vector control under the same conditions (two-way ANOVA, Bonferroni post-test).

(B) Images of IQ6011 RNAi worms from (A) grown on RNAi bacteria supplemented with 50 µM heme. Scale bars, 50 µm. (C) Quantification of *hrg-1* and *mrp-5* mRNA by qRT-PCR. Relative fold changes were derived by normalizing the cycle threshold values to *gpd-2* and then to the control heme level of 20 µM using $\Delta\Delta CT$ methods.

Data are represented as the mean \pm SEM, $n = 3$.

a far more severe defect (Figure 3.2A and B). In addition, microarray analysis showed that *mrp-5* is itself a heme responsive gene as its mRNA increased over 3-fold under low heme conditions (142). This result was confirmed by qRT-PCR studies showing that the *mrp-5* transcript is upregulated about 5-fold in worms grown at 1.5 μ M heme compared to worms grown at 20 μ M heme (Figure 3.2C). Indeed, *in silico* analysis of the putative *mrp-5* promoter revealed the presence of a canonical 23-base pair heme response element, which we have previously shown is necessary and sufficient to mediate heme dependent regulation of *hrg-1* in the worm intestine (143).

Although the *C. elegans* genome contains eight *mrp* genes, *mrp-5* is the only *mrp* family member that significantly alters GFP expression in IQ6011 (Figure 3.3A), and is the sole *mrp* that is transcriptionally responsive to heme (142). An analysis of phenotypes associated with deletion of the eight *mrp* genes revealed that *mrp-5* is the sole *mrp* that is lethal when deleted. As Flvcr1 has been shown to be a heme exporter in mammals, we asked whether putative homologs of this transporter regulated heme homeostasis in *C. elegans* (34, 35, 144). Systematically depleting each of the five Flvcr1 worm homologs had no significant effect on GFP levels in the heme sensor worm (Figure 3.3B)

MRP-5 is essential for embryonic development and larval growth

In worms, *mrp-5* (*multidrug resistance protein 5*) encodes an ABC transporter of the MRP/ABCC family. The *mrp-5* open reading frame is encoded on the reverse strand of the X chromosome (Figure 3.4A). The gene contains 20 exons, is transcribed as a 8066 nucleotide transcript, with 4284 nucleotides of coding sequence that are translated into a 1427 amino acid polypeptide. *C. elegans* MRP-5 is predicted

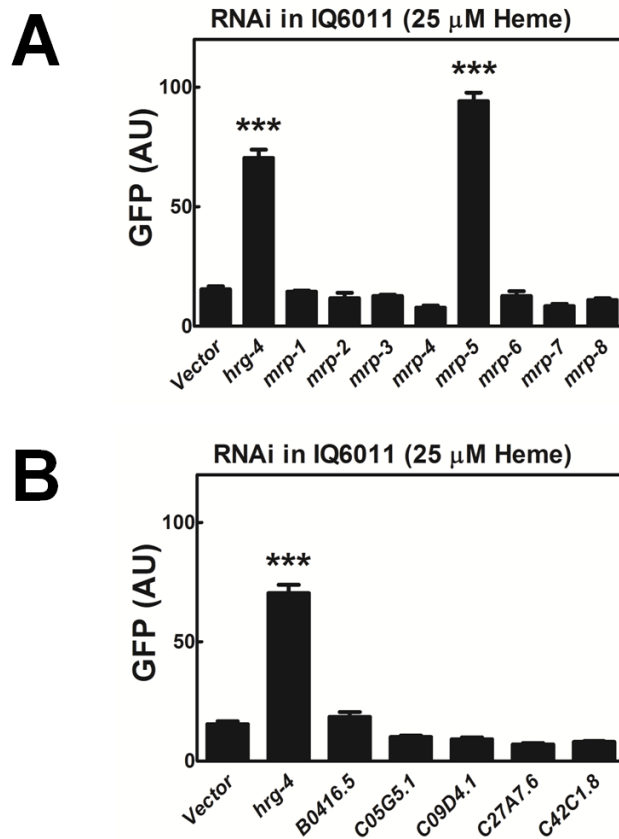


Figure 3.3: Loss of *mrp-5*, and no other *mrp*, results in a heme depletion signal in the heme sensor strain, IQ6011.

(A) GFP fluorescence (60-120 worms per treatment) quantified from the *hrg-1* transcriptional fusion line (IQ6011) exposed to vector, or RNAi against an *mrp* gene at 25 μ M heme. GFP was quantified using COPAS BioSort. ***P<0.001 when compared to vector control under the same conditions (one-way ANOVA, Bonferroni post-test). (B) RNAi of FLVCR1 homologs in *C. elegans* does not activate a heme depletion signal in IQ6011. GFP fluorescence in IQ6011 was measured as in Figures 1B and 1C. ***P<0.001 when compared to vector control under the same conditions (one-way ANOVA, Bonferroni post-test).

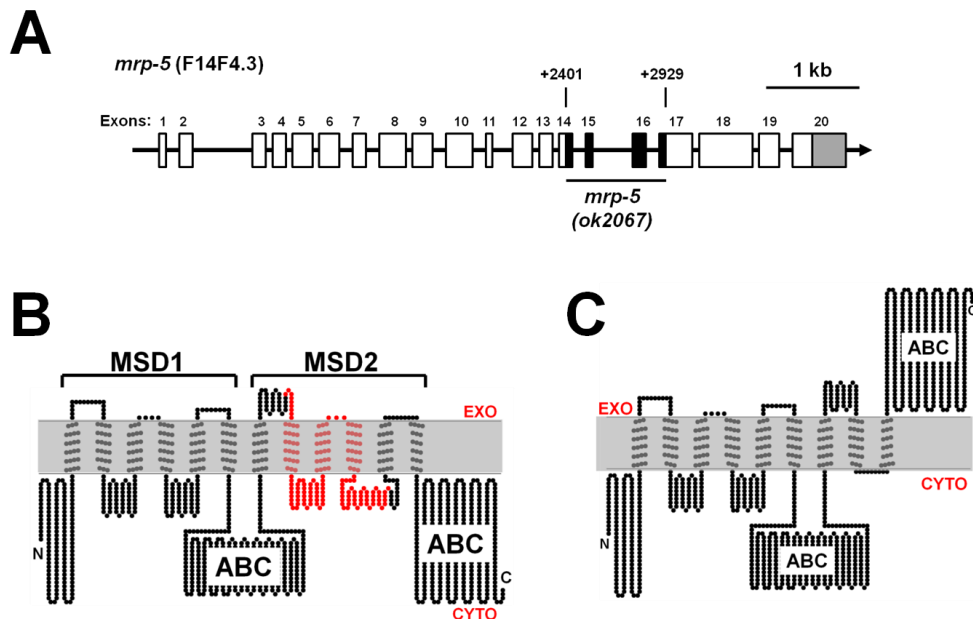


Figure 3.4: Gene structure and protein topology of *mrp-5*.

(A) Detailed exonic structure of *mrp-5*, including the *ok2067* deletion. Boxes indicate exons, with open boxes showing protein coding regions, and shaded boxes indicating untranslated regions. The region deleted in *ok2067* is shown in black, with the start and end positions of the mutation in the spliced transcript indicated above the deleted region. (B) MRP-5 membrane topology showing an N-terminal membrane spanning domain (MSD1) consisting of six TMDs, followed by a cytosolic ATP binding cassette (ABC) domain, a second MSD (MSD2) and a second ABC domain. Residues deleted in the *ok2067* mutant are shown in red. (C) Schematic of mutant MRP-5 protein produced from *mrp-5(ok2067)* deletion allele. The deletion removes three transmembrane domains, causing the second ATP-binding cassette (ABC) domain to be located on the extracellular side of the membrane.

to include two membrane spanning domains (MSDs), each containing six transmembrane helices, and two intracellular ATP binding cassette (ABC) domains (Figure 3.4B) (145). Worms were analyzed for growth and developmental phenotypes after RNAi depletion of *mrp-5*. When synchronized larvae (P₀) were fed *mrp-5* RNAi bacteria, they showed no major developmental defects and were able to reach adult gravid stage and lay eggs. However, 80% of the F₁ eggs laid by P₀ worms failed to hatch, and the small number that did hatch arrested as L1 larvae (Figure 3.5A). This striking embryonic lethal phenotype could be rescued by supplementation of the bacterial food with exogenous heme; 95% of F₁ progeny hatched and became adults in the presence of 500 μM heme. Together, these results indicate that *mrp-5* is required for embryonic development in *C. elegans*.

The strain VC1599 contains a deletion in *mrp-5* (*ok2067*) spanning exons 14 through 17 (Figure 3.4A and Figure 3.5A, top panel), but is genetically balanced by a marked chromosomal translocation as *mrp-5* mutant worms are embryonic lethal (146). The *mrp-5* (*ok2067*) deletion removes 176 amino acids, including three transmembrane helices. Consequently, the predicted topology of the mutant protein contains only nine transmembrane helices, resulting in a dysfunctional protein with the second ABC domain located on the exoplasmic side (Figure 3.4C). Although RT-PCR and sequencing analysis reveals the presence of *mrp-5* mRNA in mutant worms, depletion of *mrp-5* by RNAi in the *mrp-5(ok2067)* mutants does not enhance or result in additional phenotypes suggesting that *mrp-5(ok2067)* is likely a null mutation (Appendix III, A and B).

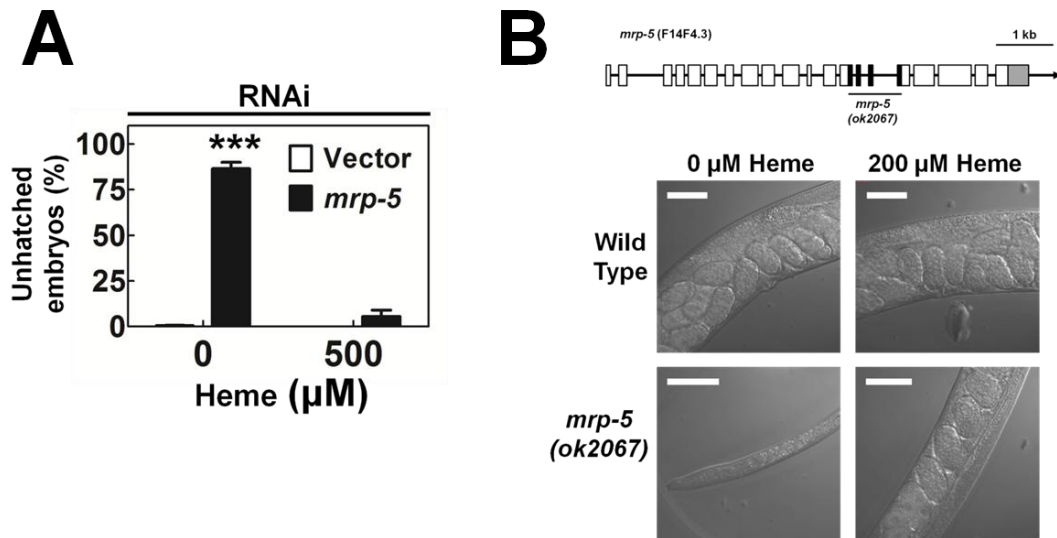


Figure 3.5: Loss of *mrp-5* results in embryonic lethality and larval arrest.

(A) Dead progeny of vector control or *mrp-5*(RNAi) worms. *** $P < 0.001$ when compared to vector control worms under identical conditions, $n=3$ (two-way ANOVA, Bonferroni post-test). (B) TOP: The *C. elegans mrp-5* gene contains 20 exons across 7 kb of the X chromosome. *mrp-5* mutants harbor a 1.2 kb deletion (*ok2067*) spanning exons 14 through 17. BOTTOM: Wild-type and *mrp-5* null brood mates were grown to gravid adult stage at 200 μ M heme. Their F_1 progeny were placed as synchronized L1 larvae on plates seeded with OP50 bacteria with or without 200 μ M added heme. Representative images of F_1 worms 4 days post-hatching are shown. Scale bar, 20 μ M.

We tested whether supplementary heme could rescue the embryonic lethality of *mrp-5* mutants and found that when VC1599 worms were crossed to wild-type N2 worms to eliminate the balancer, viable F2 homozygous *mrp-5* mutant worms were obtained and easily propagated - but only when worms were grown on food supplemented with >200 μ M heme. When grown on plates containing bacteria with no added heme, *mrp-5(ok2067)* homozygous mutant larva arrested at mid-larval stages, indicating that *mrp-5* is required not just maternally, but also during larval development (Figure 3.5B, lower panel). We performed a growth curve to assess the amount of heme required to rescue the *mrp-5(ok2067)* mutant. Synchronized wild-type and mutant worms (P_0) were placed as L1 larvae on plates seeded with bacteria grown in the presence of increasing concentrations of heme and hatching of their F_1 progeny was counted. Some rescue was observed in worms grown at 50 μ M, and full rescue was observed at 200 μ M heme (Figure 3.6A). Brood size was counted in N2 worms, *mrp-5(ok2067)* worms, and their wild-type brood mates under identical conditions. While *mrp-5(ok2067)* worms grown from the L1 stage at low heme did not reach adulthood and did not have progeny, the brood size of *mrp-5(ok2067)* worms grown in the presence of 200 μ M heme was not significantly different than that of N2 or wild-type broodmare worms (Figure 3.6B).

To determine if the rescue of *mrp-5* lethality by dietary heme was due to the presence of redundant mechanisms for heme transport, we depleted FLVCR homologs in the *mrp-5(ok2067)* background. Only one, B0416.5, showed a significantly enhanced phenotype in the *mrp-5* mutant worms when depleted (Appendix III, C); however, this effect could not be rescued in a dose-dependent

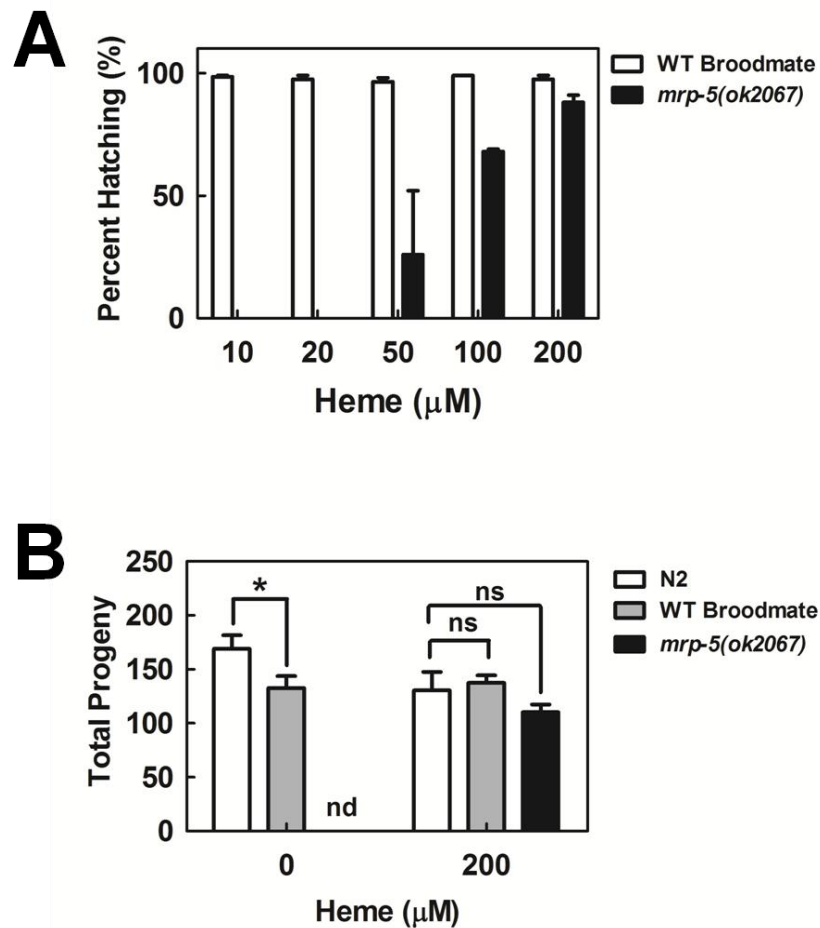


Figure 3.6: Heme-dependent rescue of the *mrp-5(ok2067)* mutant.

(A) Percent hatching in the progeny of *mrp-5(ok2067)* worms and wild-type brood mates grown on plates from L1 to gravid stage at indicated heme concentrations, n = 2. (B) Total progeny of *mrp-5(ok2067)* worms and wild-type brood mates grown on plates from L1 to gravid stage at indicated heme concentrations; nd, not detected, ns, not significant. *P<0.05 when compared to N2 worms under identical conditions, n=5 (two-way ANOVA, Bonferroni post-test).

manner by exogenous heme and is likely unrelated to heme export from the intestine.

***C. elegans* development requires intestinal MRP-5**

To determine the tissue-specific expression of *mrp-5*, a transcriptional reporter was generated using the putative promoter region of *mrp-5* (3 kb upstream of the ATG start codon) fused to a GFP reporter. $P_{mrp-5}::GFP$ was expressed at all developmental stages, with low levels in the hypodermis and in some neurons, and was consistently highly expressed in the intestine and pharynx (Figure 3.7A), confirming published intestinal and pharyngeal *in silico* gene expression analysis (147, 148). The expression pattern of *mrp-5* was identical whether the transcriptional reporters was fused to the *mrp-5* 3' untranslated region (UTR) or the generic *unc-54* 3' UTR (data not shown). We analyzed the expression pattern of this transgene grown at varying heme concentrations. GFP expression was observed in worms grown at both 1.5 and 50 μ M heme, with no significant difference observed (Figure 3.7B). In fact, $P_{mrp-5}::GFP$ is expressed in the presence of >500 μ M heme (data not shown).

To delineate the subcellular localization of MRP-5, GFP was fused to the C-terminus of MRP-5 and expressed from the intestinal *vha-6* promoter (149). In the polarized worm intestinal cells, $P_{vha-6}::MRP-5::GFP$ localized to basolateral membranes (Figure 3.8A and B) and to intracellular membrane compartments, reminiscent of basolateral sorting vesicles (Figure 3.8C) (150). Similar localization was observed for $MRP-5::GFP$ expressed from the endogenous *mrp-5* promoter (not shown). We next determined if the transgene was capable of rescuing the embryonic lethal phenotype induced by *mrp-5* deficiency. RNAi directed against the 3' untranslated region (UTR) of *mrp-5* depleted endogenous *mrp-5*, resulting in an

Figure 3.7: *mrp-5* is expressed in multiple tissues in *C. elegans*.

(A) GFP expression in IQ5051 ($P_{mrp-5}::GFP::unc-54$ 3'UTR; *unc-119(ed3)*; *unc-119* rescue fragment) as determined using confocal microscopy. *mrp-5* is expressed in the hypodermis and some neurons, and at higher levels in the pharynx and intestine. P, pharynx, I, intestine, H, hypodermis, E, embryo. Scale bars, 20 μ M. (B) *mrp-5* expression at different concentrations of heme. IQ5051 worms with the $P_{mrp-5}::GFP::unc-54$ 3'UTR construct were grown on plates seeded with bacteria grown in 1.5 μ M or 50 μ M heme for one generation. GFP signal was examined as a direct reporter for the activity of the *mrp-5* promoter. Representative images of adult worms are shown. Scale bars, 100 μ m.

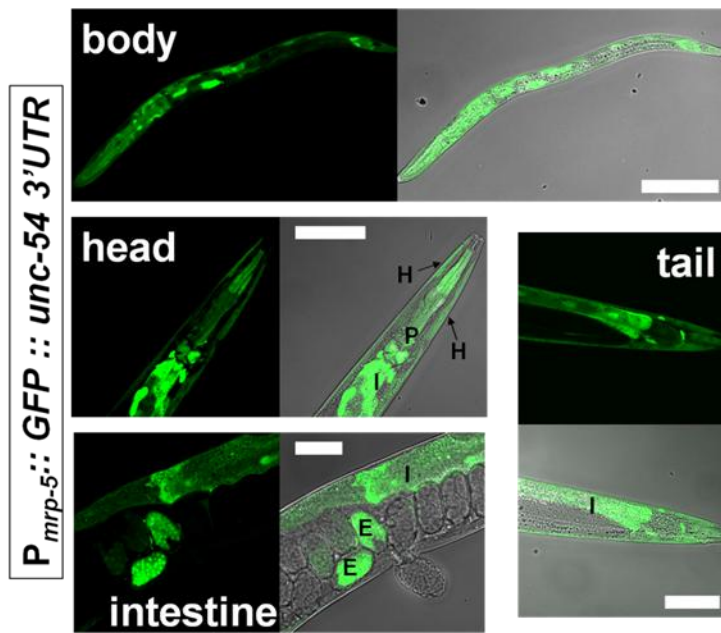
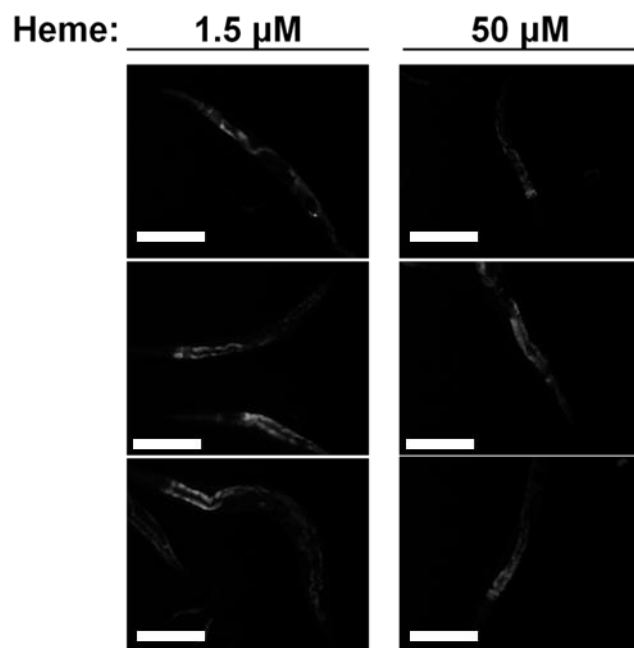
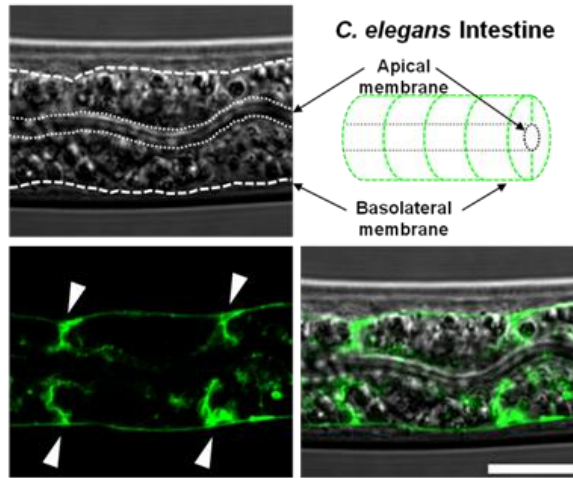
A**B**

Figure 3.8: MRP-5 localizes to the basolateral membrane of the intestine.

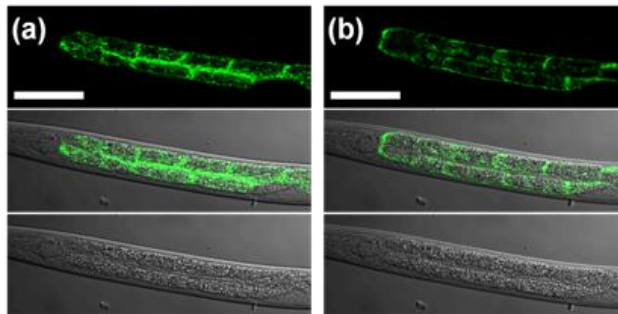
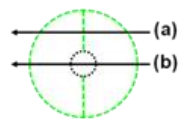
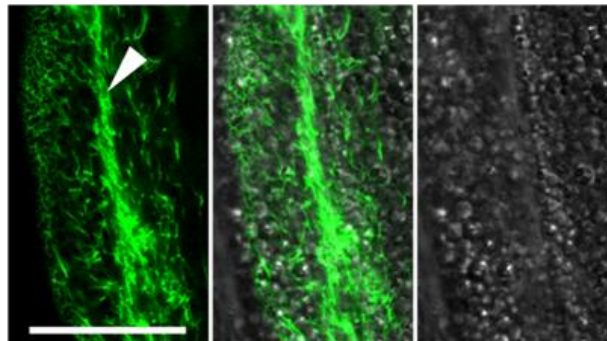
(A) Transgenic IQ5351 worms ($P_{vha-6}::MRP-5::GFP::unc-54$ 3'UTR; $unc-119(ed3)$; $unc-119$ rescue fragment) expressing an *mrp-5* translational reporter were imaged by confocal microscopy. Dotted lines indicate apical membrane, dashed lines indicate basolateral membrane, and arrowheads indicate lateral membranes between adjacent intestinal cells. Scale bar, 50 μ M. (B) Images of a worm expressing the *MRP-5::GFP* translational fusion protein. Images were taken at two different planes along the dorsal-ventral axis. Localization of *MRP-5::GFP* to lateral membranes of adjacent intestinal cells can be seen in (a), while localization of *MRP-5::GFP* to the basolateral membranes and not the apical membrane surrounding the intestinal lumen can be seen in (b). The anterior of the animal is to the left. Scale bar, 50 μ M. (C) Magnified image of *MRP-5::GFP* localization to basolateral sorting vesicles. Image is taken in the same plane as (a) in Figure 3.8B. Arrowhead indicates lateral membranes of adjacent intestinal cells. Scale bar, 20 μ M.

A

$P_{vha-6}:: MRP-5-GFP :: unc-54$ 3'UTR

**B**

Cross Section of Intestine

**C**

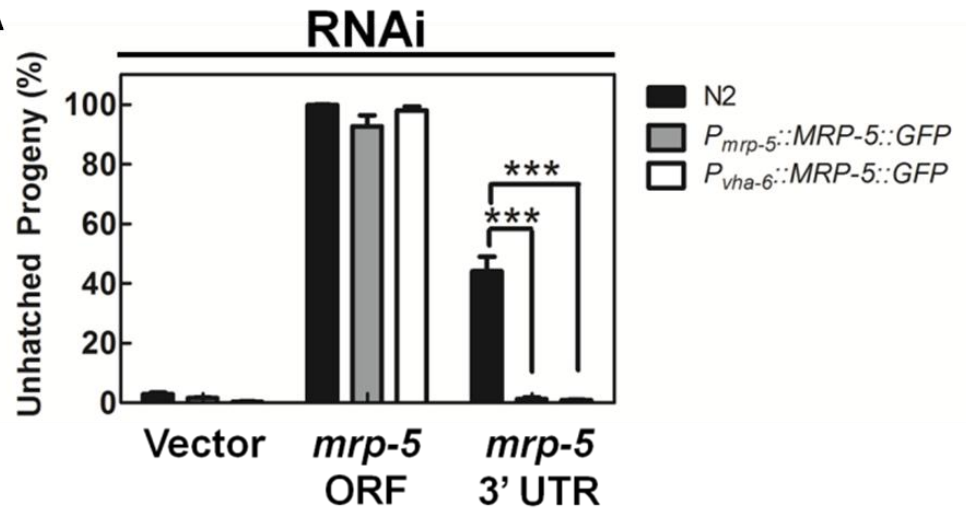
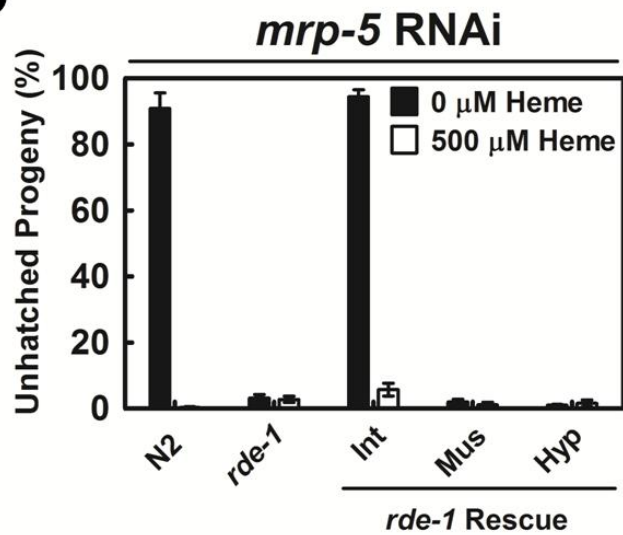
embryonic lethality phenotype (Figure 3.9A), whereas the *MRP-5::GFP* transgene, which is expressed with the generic *unc-54* 3' UTR, was left intact, as confirmed visually by GFP fluorescence (not shown). RNAi against the *mrp-5* 3' UTR in lines expressing *MRP-5::GFP* resulted in no embryonic lethality in *MRP-5::GFP* transgenic worms, indicating that *MRP-5::GFP* is a functional protein that can rescue the *mrp-5* RNAi phenotype (Figure 3.9A).

As MRP-5 is expressed in multiple tissues, it is conceivable that *mrp-5* depletion in any or all of the tissues may contribute to the embryonic lethal phenotype of *mrp-5* mutant worms. To address the contribution of each tissue to the *mrp-5* phenotype, we utilized tissue-specific RNAi worm strains. Worms carrying the *rde-1* mutation are resistant to RNAi; ectopic expression of *rde-1* from a tissue-specific promoter in the *rde-1* mutant background results in RNAi only in that tissue (151). We depleted *mrp-5* in the VP303 (*rde-1* rescue from the intestinal *nhx-2* promoter), WM118 (*rde-1* rescue from the muscle *myo-3* promoter), and NR222 (*rde-1* rescue from the hypodermal *lin-26* promoter) transgenic worm lines. Depletion of *mrp-5* in the intestine fully recapitulated the F₁ embryonic lethality of whole animal RNAi, while depletion of *mrp-5* either in the hypodermis or muscle had no effect on F₁ viability (Figure 3.9B). The lethality caused by RNAi in the VP303 strain could be rescued by supplementation with 500 μM heme in the diet. Thus, the lethality of *mrp-5* mutants can be attributed to loss of functional MRP-5 specifically in the intestine, even though *mrp-5* is expressed in extra-intestinal tissues. This is further supported by the fact that the *MRP-5::GFP* transgene expressed exclusively in the intestine

Figure 3.9: Loss of *mrp-5* specifically in the intestine causes embryonic lethality.

(A) Intestinal RNAi of *mrp-5* recapitulates the embryonic lethality of whole animal *mrp-5* RNAi. Wild type N2 worms and the tissue specific RNAi strains were grown on RNAi plates with no added heme. Int, intestinal RNAi, Mus, muscle RNAi, Hyp, hypodermal RNAi, n=2. See the text and Appendix I for further strain information.

(B) The *MRP-5::GFP* fusion gene can rescue the embryonic lethality of *mrp-5* RNAi. RNAi targeting the *mrp-5* ORF causes embryonic lethality in both wild type N2 and transgenic worms. RNAi against the *mrp-5* 3' UTR results in a less severe embryonic lethal phenotype in N2 worms, but this lethality is significantly rescued by expression of the *MRP-5::GFP* transgene from either the *mrp-5* or the intestinal *vha-6* promoter. ***P<0.001 when compared to wild type N2 worms under identical conditions, n=3 (two-way ANOVA, Bonferroni post-test).

A**B**

(*P_{vha-6}::MRP-GFP*) is capable of rescuing the hatching phenotype associated with depletion of endogenous *mrp-5* (Figure 3.9A).

MRP-5 is an intestinal heme exporter

As MRP-5 is a member of the ABCC/MRP transporter family, members of which function as exporters of lipophilic and organic compounds (114, 152), we examined whether MRP-5 was involved in heme transport in *C. elegans*. In order to do this, we examined the response of *mrp-5(RNAi)* worms to various heme analogs. We have previously shown that worms in which *mrp-5* was RNAi depleted are resistant to the toxic heme analog, gallium protoporphyrin IX (GaPPIX), indicating that heme analogs entered the intestine but were poorly accessible to extra-intestinal cells (142). Additionally, worms in which *mrp-5* had been depleted showed significantly greater accumulation of zinc mesoporphyrin IX (ZnMP), a fluorescent heme analog, in the intestine compared to control worms (Figure 3.10A and B). Notably, VC1599 worms, which are heterozygous for *mrp-5*, exhibited haploinsufficiency phenotypes. They not only accumulated ZnMP in the intestine, but were also resistant to GaPPIX (Figure 3.11A and B).

To evaluate the heme status in an extra-intestinal tissue when *mrp-5* is depleted, we utilized *P_{hrg-2}::HRG-2::YFP* transgenic worms. The *hrg-2* promoter is active only in the hypodermis and *P_{hrg-2}::HRG-2::YFP* is induced in the hypodermis when heme levels are limiting in that tissue (141). Depletion of *mrp-5* resulted in a striking increase in *HRG-2::YFP* levels and its expression was not fully suppressed until worms were fed 500 μ M heme (Figure 3.12A and B). By contrast, worms in which *hrg-4*, the intestinal heme importer, was depleted did not upregulate

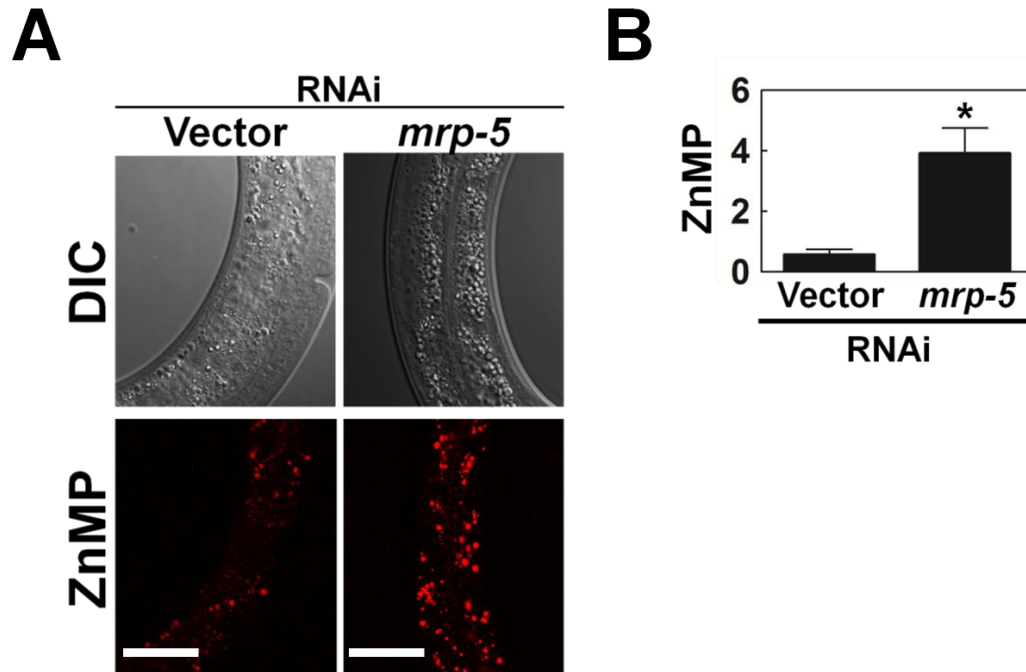


Figure 3.10 Loss of *mrp-5* leads to intestinal accumulation of a heme analog.

Zinc mesoporphyrin (ZnMP) staining in worms fed vector control or *mrp-5*(RNAi) bacteria. **(A)** Worms were exposed to RNAi from L1 to L4 larval stages, pulsed with 60 μ M ZnMP for 3 hr, and imaged using confocal microscopy. Scale bars, 20 μ m. **(B)** Quantification of ZnMP staining (mean \pm SEM of 10 worms) in worms from (A). * $P < 0.05$ when compared to control worms (one-way ANOVA, Bonferroni post-test).

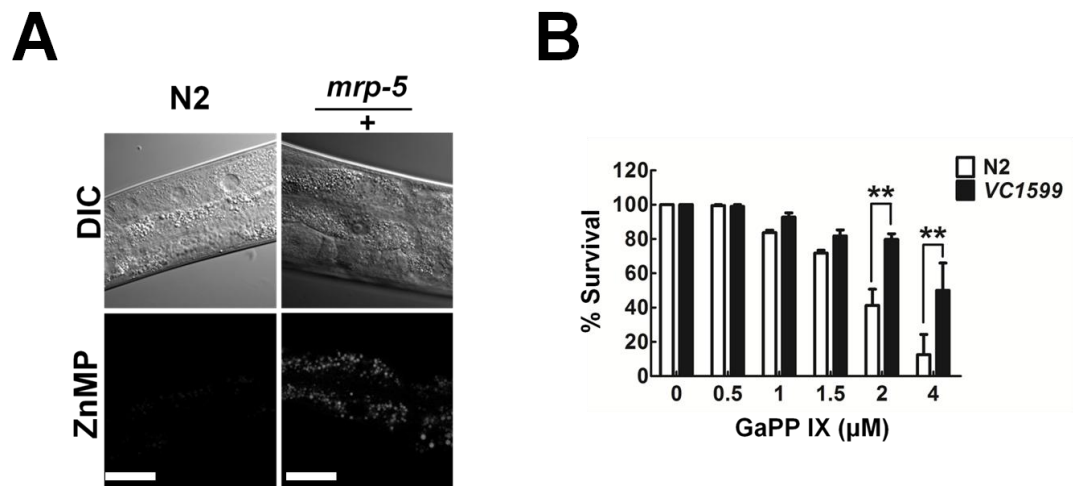


Figure 3.11: VC1599 (*mrp-5/+*) worms exhibit haploinsufficiency phenotypes.

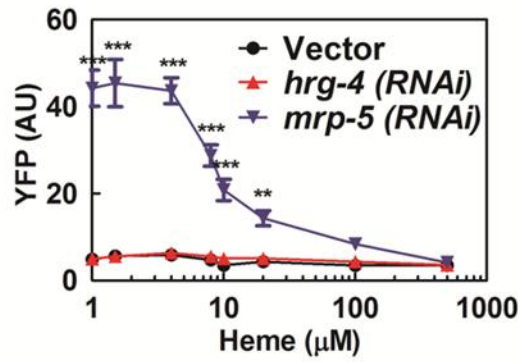
(A) ZnMP staining in N2 control or VC1599 (*mrp-5/+*) worms. Worms were exposed to RNAi from L1 to L4 stage, pulsed with 60 μM ZnMP for 3 hr, and imaged on an inverted microscope. Representative images of intestinal granules containing ZnMP in control and mutant worms are shown. Scale bars, 20 μm (B) Resistance to a toxic heme analog, gallium protoporphyrin IX (GaPPIX), was measured in wild-type N2 and VC1599 (*mrp-5/+*) worms. Resistance was assessed after L4 worms were exposed to varying concentrations of GaPPIX for 48 hours. Worms were considered dead when unresponsive to a physical stimulus. Each data point represents the mean ± SEM of three separate experiments and is depicted as percentage of survival compared to control plates with no GaPPIX. **P<0.01 when compared to wild-type worms on identical plates.

Figure 3.12: Loss of *mrp-5* results in an extraintestinal heme depletion signal.

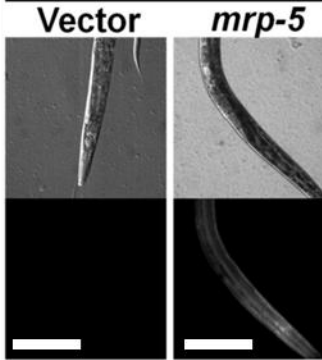
(A) LEFT: YFP fluorescence (60-100 worms per treatment) quantified using COPAS BioSort in the *hrg-2* translational fusion line, IQ8122 ($P_{hrg-2}::HRG-2::YFP::hrg-2$ 3' UTR, *unc-119(ed3)*; *unc-119* rescue fragment) exposed to vector, *hrg-4*, or *mrp-5* RNAi at varying heme concentrations. ***P<0.001, **P<0.01 when compared to vector control worms (two-way ANOVA, Bonferroni post-test). RIGHT: Representative images of worms grown at 1 μ M heme from left panel. Scale bars, 100 μ m. (B) Expression of GFP in IQ6011 L1 larvae. P₀ worms were grown in liquid at the indicated heme concentrations, and their synchronized progeny were placed as L1 worms on vector or *mrp-5* RNAi plates. These worms were grown to gravid stage, and GFP fluorescence was analyzed in their progeny (F₂) at the L1 stage. Scale bars, 20 μ m.

A

$P_{hrg-2}::HRG-2-YFP::hrg-2\ 3'UTR$



RNAi (1 μM Heme)

**B**

IQ6011

RNAi

F₂

vector

mrp-5

0 μM

200 μM

0 μM

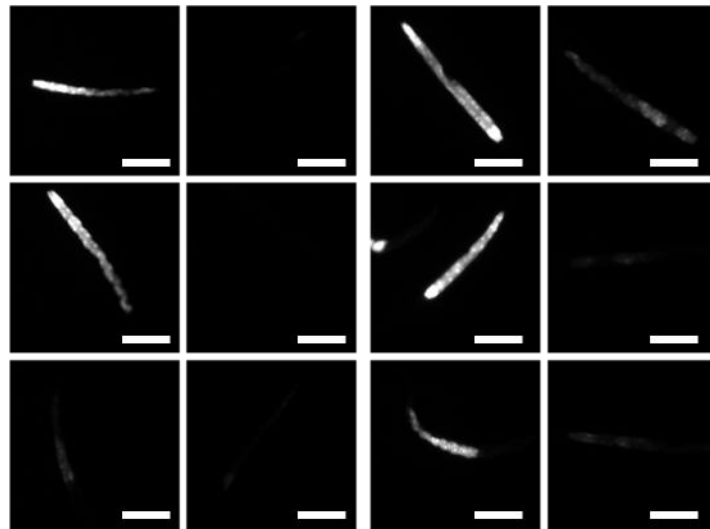
200 μM

2 μM

P₀

10 μM

500 μM



P_{hrg-2}::HRG-2::YFP, indicating that loss of this particular transporter does not result in limiting heme levels in the hypodermis (Figure 3.12A, left panel).

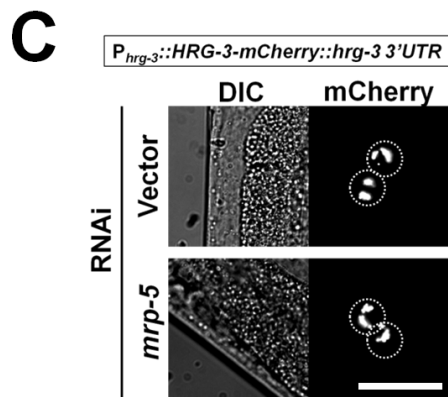
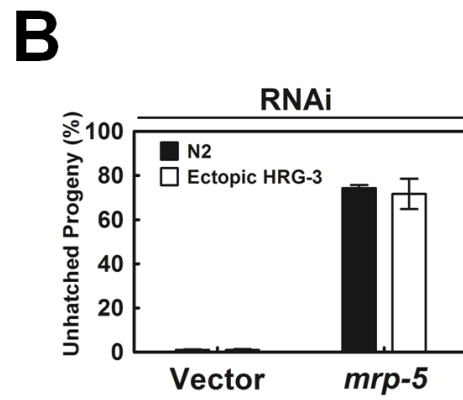
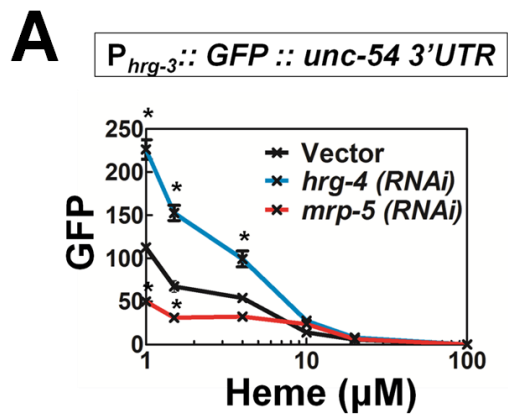
As heme levels in *C. elegans* embryos and newly hatched larvae are intrinsically linked to maternal heme status, we analyzed GFP levels in the progeny of IQ6011 worms. These larvae are predicted to behave like extra-intestinal tissues and upregulate depletion signals when heme is limiting. IQ6011 worms (P₀) were grown in liquid media at the indicated heme concentrations, and their synchronized progeny were placed as L1 worms on vector or *mrp-5* RNAi plates. These worms were grown to gravid stage, and GFP fluorescence was analyzed in their progeny (F₂) at the L1 stage. Regardless of the heme concentration at which the P₀ or F₁ worms were grown, F₂ worms that were the progeny of *mrp5(RNAi)* worms showed increased GFP compared to vector control worms (Figure 3.12B). These results, taken with the embryonic lethality associated with *mrp5* RNAi, indicate that worms lacking *mrp-5* are unable to deliver adequate heme to extra-intestinal targets – namely developing embryos. Taken together, these results provide strong evidence that MRP-5 is the major intestinal heme exporter.

HRG-3 overexpression cannot rescue MRP-5 loss-of-function phenotypes

We next determined whether MRP-5 deficiency phenotypes could be overcome by expressing HRG-3, the intercellular heme delivery protein, from the intestine. Notably, loss of *mrp-5* in a wild-type background suppresses *hrg-3* expression (Figure 3.13A). Thus, it is not surprising that *hrg-3* is unable to rescue heme delivery to extra-intestinal tissues in the absence of *mrp-5*. We next determined if expression of *hrg-3* from a constitutively active promoter would be able to rescue

Figure 3.13: Ectopic expression of *hrg-3* cannot rescue *mrp-5*-associated lethality.

(A) GFP fluorescence (60-100 worms per treatment) quantified using COPAS BioSort in the *hrg-3* transcriptional fusion line, IQ8031 ($P_{hrg-3}::GFP::hrg-3$ 3' UTR, *unc-119(ed3)*; *unc-119* rescue fragment) exposed to vector, *hrg-4*, or *mrp-5* RNAi at varying heme concentrations. * $P < 0.05$ when compared to vector control worms (two-way ANOVA, Bonferroni post-test). (B) Ectopic expression of *hrg-3* does not rescue the embryonic lethality of whole animal *mrp-5* RNAi. Experiment was performed using wild-type N2 worms and worms ectopically expressing HRG-3 and GFP separated by the SL2 intercistronic sequence (*hrg-3(tm2468)*; $P_{vha-6}::HRG-3::ICS::GFP$, *unc-119(ed3)*; *unc-119* rescue fragment) grown on RNAi plates with no added heme. (C) RNAi depletion of *mrp-5* does not inhibit the secretion of *hrg-3* from the intestine. Transgenic worms containing the $P_{hrg-3}::HRG-3::mCherry$ translational fusion were fed vector control or *mrp-5* RNAi bacteria from L1 to L4 stages. HRG-3::mCherry in extraintestinal cells (coelomocytes) was imaged on an inverted microscope. Dotted circles indicate location of coelomocytes. Scale bars, 10 μm .



mrp-5 lethality. Ectopic expression of *hrg-3* from the intestinal *vha-6* promoter was unable to rescue the embryonic lethality of *mrp-5* RNAi (Figure 3.13B). This was not due to impaired secretion of HRG-3 from the intestine, as *HRG-3::mCherry* still accumulated in the extraintestinal coelomocytes when *mrp-5* was depleted by RNAi (Figure 3.13C).

Discussion

The nematode *C. elegans* is unable to synthesize heme and is therefore dependent on a network of heme sensing, trafficking, and transport molecules to import environmental heme into the intestine and then export this heme to different tissues and subcellular compartments. We have previously shown that a network of heme importers regulates heme entry into the intestine, and that a heme chaperone delivers this essential nutrient to extra-intestinal tissues under heme-limiting conditions (40, 41, 77). However, a constitutive mechanism for heme export from the intestine remained elusive.

In the current study, we show that MRP-5 plays an essential role in *C. elegans* heme homeostasis. Our conclusions about MRP-5 function are supported by the following findings: 1) targeted *mrp-5* deficiency in the intestine causes embryonic lethality; 2) MRP-5 primarily localizes to the basolateral plasma membrane and MRP-5 deficiency results in ZnMP accumulation in the worm intestine; 3) *mrp-5* is expressed during all developmental stages, and over a wide range of heme concentrations; 4) loss of *mrp-5* activates a number of heme deficiency signals in the worm. Altogether, these results suggest that MRP-5 is the intestinal heme exporter in *C. elegans*.

In our model (Figure 3.14), HRG-4 imports heme into the intestinal cytosol, where it can be exported to extra-intestinal targets or stored in endocytic vesicles. HRG-1 mobilizes heme from these storage vesicles when necessary. Presumably, cytosolic heme in the intestine is available for export by MRP-5, either directly into the pseudocoelom or into secretory vesicles, or both. HRG-3 is secreted from the intestine to escort heme to other tissues, and possibly acquires its heme from MRP-5. Mechanisms for heme uptake by other tissues remain unknown.

It is useful to compare the transcriptional regulation and phenotypes of *mrp-5* with that of the other *hrgs*. While *hrg-1*, *hrg-4*, and *hrg-3* are only upregulated at <20 μ M heme, an *mrp-5* transcriptional reporter is expressed even when worms are grown at >500 μ M heme. While *hrg-1*, *hrg-4*, and *hrg-3* are upregulated 20- to 400-fold in response to low heme, *mrp-5* is upregulated 3- to 5-fold maximally. We can infer that only small changes in the regulation of *mrp-5* are required to adjust to major changes in available dietary heme. This is also apparent from the haploinsufficiency phenotypes in the VC1599 (*mrp-5/+*) strain, demonstrating that relatively minor changes in *mrp-5* expression result in observable physiological consequences in the worm. Additionally, loss of *hrg-1*, *hrg-4*, or *hrg-3* individually results in no apparent phenotypes until worms are nutritionally deprived of heme. By contrast, loss of *mrp-5* results in crippling embryonic lethality and larval arrest that can only be rescued with very high concentrations of heme. Thus, while *hrg-1*, *hrg-4*, and *hrg-3* cooperate to form an emergency response to heme starvation, *mrp-5* functions as a part of the basal heme transport machinery. While redundancy exists among the paralogs of *hrg1*-type permeases in *C. elegans*, the severe *mrp-5* loss of function phenotype

MRP-5 Export in *C. elegans*

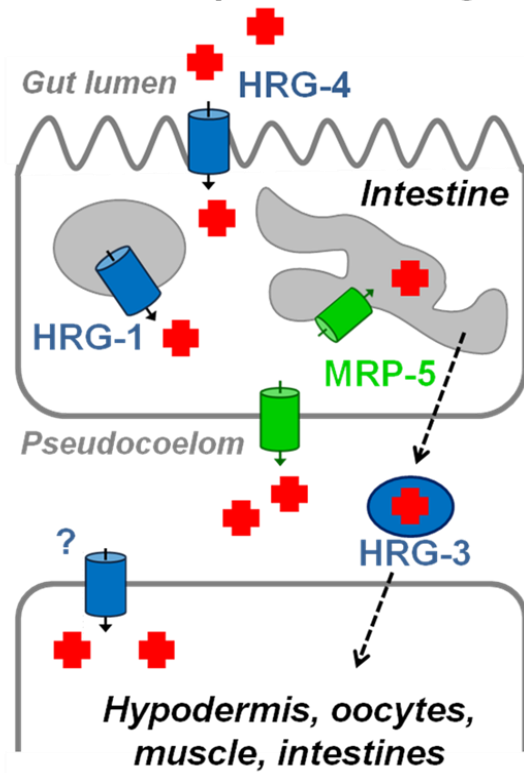


Figure 3.14: Proposed model of heme transport pathways in *C. elegans*.

In *C. elegans*, *mrp-5* is expressed at all developmental stages, mainly in the intestine. After heme is imported into the cytosol of intestinal cells, MRP-5, which localizes to the basolateral membrane, can export heme to extra-intestinal tissues. As MRP-5 also localizes to basolateral sorting vesicles, it may also be responsible for delivery of heme to HRG-3, and other hemoproteins in the secretory pathway. Heme uptake mechanisms for extra-intestinal tissues remain unknown.

indicates that there are likely no alternate mechanisms for heme efflux from the intestine.

Interestingly, loss of *mrp-5* expression negatively regulates an *hrg-3* promoter-driven transcriptional reporter. One explanation for this observation is that the *hrg-3* promoter is regulated exclusively by heme located within the intestinal compartment. According to our model, depletion of *mrp-5* would result in heme accumulation in the intestine, repressing *hrg-3* expression. This also explains why loss of *mrp-5* is lethal despite the presence of HRG-3-mediated heme export from the intestine. Another, not mutually exclusive, explanation is that MRP-5 is responsible for delivering heme to apoHRG-3 as it progresses through the secretory pathway. In the absence of MRP-5, HRG-3 is unable to acquire heme and deliver it to other tissues. In support of this hypothesis, we showed that even constitutive overexpression of HRG-3 was unable to rescue the embryonic lethality associated with *mrp-5* RNAi.

An unanticipated consequence of MRP-5 deficiency in worms is the apparent uncoupling of heme levels in the intestine and heme levels in extra-intestinal tissues. In the absence of an intestinal heme exporter, it would be expected that heme will accumulate in the intestine and extra-intestinal tissues will be heme-deprived, as seen when *mrp-5* is depleted in the *HRG-2::YFP* reporter strain. However, depletion of *mrp-5* also results in robust expression of the *P_{hrg-1}::GFP* intestinal heme reporter, and this occurs when heme is accumulating within the intestine, a condition when such transporters are not normally expressed. If the *hrg-1* promoter was solely regulated by intestinal heme levels, we would expect intestinal GFP to be suppressed.

It is possible that *mrp-5* depletion causes compartmentalization of accumulated heme in the intestine such that this heme can no longer be detected by the *hrg-1* promoter. However, another plausible interpretation of this paradox is that intestinal heme levels are integrated with and regulated by heme-dependent signals from extra-intestinal tissues. That low extra-intestinal heme levels can activate a depletion signal within a heme-loaded intestine implies the existence of a network for communicating heme status between extra-intestinal tissues and their sole source of heme, the intestine. It is plausible that cellular heme levels in *C. elegans* are not solely regulated by internal heme content, but also by distally located proteins which signal systemic heme requirements to an inter-tissue heme trafficking network.

A number of questions remain. First, it is unlikely that cytotoxic heme is floating freely in the cellular milieu of the intestine. Is there an intestinal chaperone responsible for sequestering and ferrying heme in these cells? Does this chaperone interact with the heme importers, HRG-1 and HRG-4, or the heme exporter, MRP-5, or both? We predict that this protein will be constitutively expressed, like *mrp-5*, as it is required for basal heme trafficking; however we cannot rule out the existence of multiple chaperones, as observed for copper trafficking - each directing a specific pathway (153), some of which may be regulated by heme levels.

Second, MRP-5 is found in recycling vesicles targeted to the basolateral membrane. Is MRP-5 responsible for transporting heme from the cytosol into the intestinal secretory pathway, possibly for insertion into heme-binding proteins located in subcellular organelles? As previously mentioned, HRG-3 expression cannot rescue *mrp-5(RNAi)*-associated lethality. This could be because this pathway is incapable of

delivering sufficient heme to developing embryos, but we alternatively hypothesize that heme-loading into HRG-3 may require MRP-5. An alternative explanation could be that RNAi of *mrp-5* somehow downregulates the currently unknown receptor for HRG-3 in worm embryos.

Third, how are high concentrations of dietary heme able to rescue lethality associated with loss of *mrp-5*? We showed that depletion of FLVCR homologs in *mrp-5(ok2067)* worms does not result in a stronger phenotype, indicating that these proteins are not the alternate low-affinity heme exporters delivering heme to extra-intestinal tissues in the absence of MRP-5. It is worth noting, however, that this experiment does not rule out the presence of other low-affinity transporters that can compensate for the loss of *mrp-5*, or the possibility that at such high dietary concentrations, heme, which can intercalate into membrane lipids, is traversing the membrane without the assistance of a transporter.

Last, evidence from this study indicates that MRP-5 is found in tissues outside the intestine – namely the pharynx. It is possible that MRP-5 protects these tissues from the buildup of toxic heme, or perhaps plays a role in targeting heme to a specific subcellular compartment, such as the ER or Golgi apparatus? Further subcellular localization studies and analysis of tissue-specific knockdown mutants will be critical to answering this question.

Chapter 4: Conserved Heme Transport by Metazoan MRP5 Proteins

*Who goes there? Hankering, gross, mystical, nude,
How is it I extract strength from the beef I eat?*

Walt Whitman
“Song of Myself”

Summary

While *C. elegans* is a heme auxotroph, and thus necessarily relies on elaborate heme trafficking mechanisms, it has been assumed that organisms capable of synthesizing heme do not similarly mobilize heme. However, there is evidence for conserved heme transport pathways. We have previously showed that while *C. elegans* and human HRG1 only share about 20% sequence identity, they both bind and transport heme (41). Furthermore, depletion of zebrafish *hrg1* using morpholino knockdown results in severe anemia and morphological defects that can be rescued by co-injection with *C. elegans hrg-1* (40). To determine if heme transport by MRP-5 is conserved in other species, we took advantage of a heme synthesis-deficient yeast strain. The *hem1Δ* strain lacks δ-aminolevulinic acid (ALA) synthase; as yeast do not possess a robust plasma membrane heme import system, the *hem1Δ* strain is incapable of growth in the absence of ALA or high levels of exogenous heme. We have previously shown that HRG permease homologs from multiple species can

rescue the growth of this strain in the presence of low heme, indicating that they are *bone fide* heme transporters.

Here we show that MRP5 proteins, which are conserved among metazoans, are broadly capable of transporting heme. Studies in zebrafish show that, similar to *hrg1*, loss of *mrp5* results in severe anemia. Expression of this heme effluxer decreases growth of *hem1Δ* yeast grown on either heme or ALA, indicating that both exogenous heme and endogenously synthesized heme are capable of being transported by MRP5. We additionally use heme reporter assays to determine that MRP5, which localizes to intracellular membranes, exports heme into the secretory pathway, and as such decreases cytosolic heme levels in these yeast. Our results imply that regulation of heme homeostasis by MRP5 is highly conserved among metazoans.

Results

MRP5 is conserved in metazoans

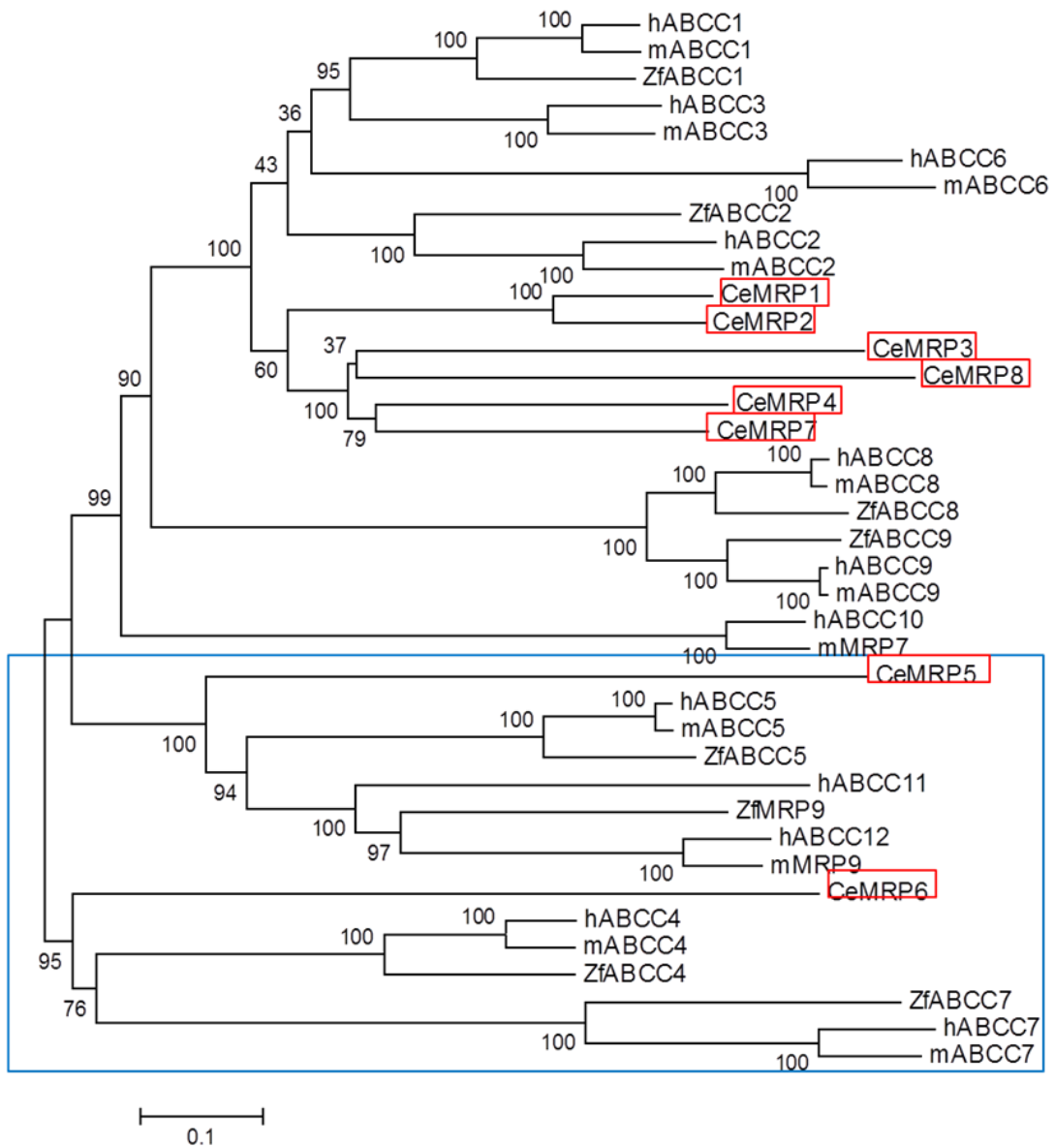
Vertebrate ABCC5/MRP5 is 39% identical to worm MRP-5 with similar overall membrane topology (Table 4.1). Within the ABCC/MRP family, the lack of an additional amino-terminal MSD (called MSD0) places ABCC5/MRP5 in a distinct group containing the ABCC4/MRP4, ABCC7 (CFTR), and ABCC12/MRP9 proteins (Figure 4.1, blue box) (154). Although *C. elegans* contains a single *mrp-5*, the gene has undergone a duplication event and two MRP5 paralogs are found in most vertebrates (Figure 4.1, red boxes). Interestingly, the human genome contains three paralogs; in addition to *ABCC5/MRP5* on chromosome 3, *ABCC11/MRP8* and

Table 4.1: Pairwise Alignment Scores (% Identity) of MRP5/ABCC5 Homologs

Species (Genbank Accession Number)	Human	Mouse	Rat	Chicken	<i>Xenopus</i>	Zebrafish	<i>C. elegans</i>
Human (NP_005679.2)							
Mouse (NP_038818.2)	95.1						
Rat (NP_446376.1)	94.8	97.8					
Chicken (XP_004943449.1)	89.1	87.2	87.3				
<i>Xenopus</i> (XP_004914448.1)	84.2	83.4	83.9	87.0			
Zebrafish (NP_001182542.1)	73.9	73.2	73.6	74.3	76.3		
<i>C. elegans</i> (NP_510479.1)	39.0	38.9	39.3	39.8	39.4	39.0	
Asian Rice (NP_001046583.1)	37.2	36.8	37.1	38.3	36.0	36.7	33.1

Figure 4.1: Phylogenetic analysis of MRP and ABCC proteins.

Phylogenetic tree of the MRP/ABCC family members in *C. elegans* (Ce), zebrafish (Zf), mice (m), and humans (h). Protein sequences were aligned using ClustalW and a phylogenetic tree was generated using the Neighbor-Joining method in MEGA5. The tree is drawn to scale, with branch lengths in the same units as those of the evolutionary distances used to infer the phylogenetic tree. The evolutionary distances are in the units of the number of amino acid substitutions per site. *C. elegans mrp* proteins are boxed in red, ABCC/MRP proteins lacking the N-terminal MSD0 domain are boxed in blue.



ABCC12/MRP9 are located in tandem on chromosome 16 (155). Orthologs of *ABCC11/MRP8* can be found in other eutherians, including primates, dogs, and cows, but are not found in rodent genomes. In all analyzed vertebrate species, the closest homolog of *C. elegans mrp-5* is the vertebrate *ABCC5/MRP5*.

Previous studies with HRG-1 have shown that even though zebrafish and worm HRG-1 are only ~20% identical, they both function as heme transporters (40). Because zebrafish embryos provide a vertebrate animal model to interrogate hematological changes as a function of aberrant heme homeostasis (156), we analyzed the expression and function of *mrp5/abcc5* in zebrafish. Whole mount *in situ* hybridization revealed that *mrp5/abcc5* is widely expressed throughout the embryo, with the greatest expression in the developing central nervous system (Appendix IV and Appendix V, A).

To knockdown *mrp5/abcc5*, we injected fish embryos with morpholinos (MO) specifically targeted against the ATG start codon of *mrp5/abcc5* (MO^{*mrp5*}) mRNA. Embryos injected with MO^{*mrp5*} showed severe anemia with very few *o*-dianisidine-positive red blood cells (RBCs) compared to embryos injected with control MO (Appendix V, B and E). MO^{*mrp5*} morphants also exhibited developmental malformations including body axis curvature defects and enlarged hearts. To quantify the severe anemia phenotype, we analyzed levels of globin-expressing RBCs in the morphant fish. Transgenic zebrafish expressing GFP from the globin locus control region (LCR-GFP) were injected with control and *mrp5* morpholinos, and morphant blood was analyzed two days post-fertilization for GFP expression. Fish injected with MO^{*mrp5*} showed significantly decreased GFP-positive RBCs compared to control MO

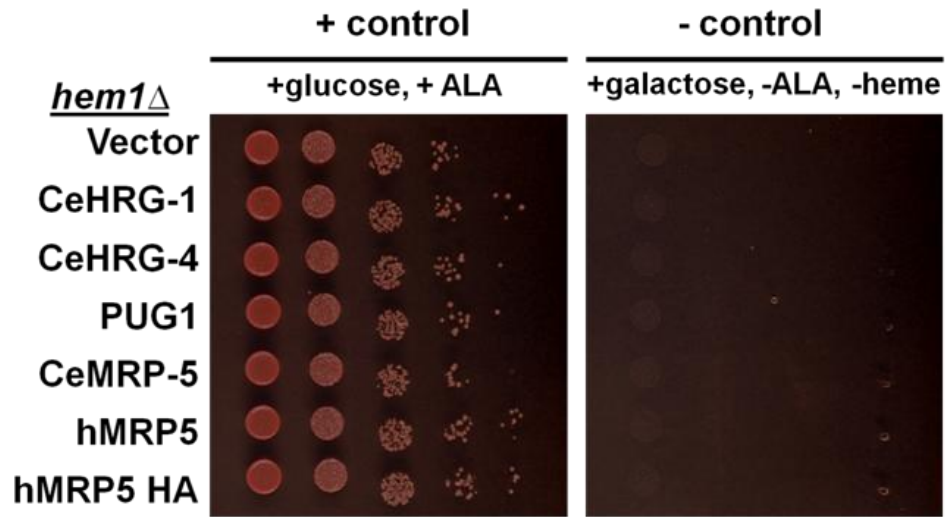
fish (Appendix V, C). Correspondingly, *gata1*, a transcription factor required for primitive erythropoiesis (157) was robustly expressed in wild-type and control MO embryos, but little or no *gata1* staining was observed in MO^{*mrp5*} morphants (Appendix V, D). The MO^{*mrp5*} anemia was indeed due to Mrp5/Abcc5 deficiency, as co-injecting zebrafish with cRNA encoding Mrp5/Abcc5 significantly corrected the anemia phenotype (Appendix V, E). Taken together, these data indicate that *mrp5* is critical for zebrafish erythropoiesis, and that MRP5 regulation of systemic heme homeostasis is likely conserved from worms to vertebrates.

MRP5 expression alters heme homeostasis in a heterologous system

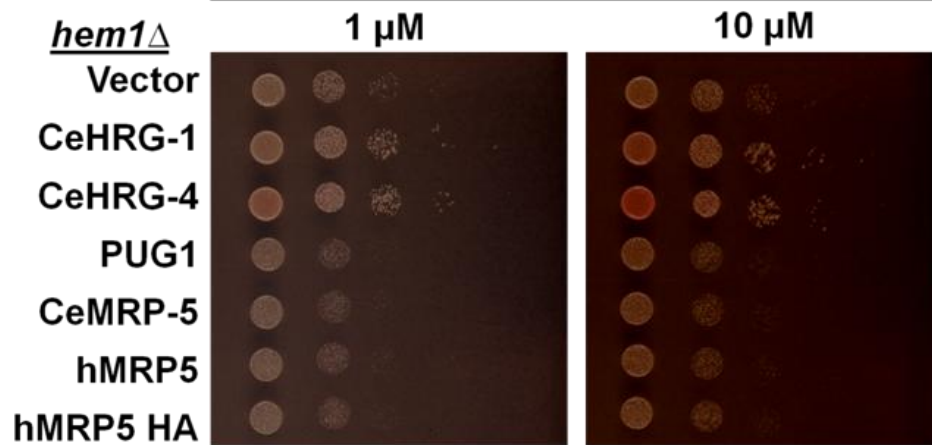
To determine whether MRP5 likely transports heme, we exploited previously established assays in yeast and mammalian cells. *Saccharomyces cerevisiae hem1Δ* mutants are unable to synthesize ALA, a precursor for heme synthesis, and grow poorly even in the presence of exogenous heme due to an inefficient heme uptake system (126, 158). This inadequate growth of *hem1Δ* can be greatly improved by either expression of a heme importer in the presence of heme or supplementation of ALA to the growth medium (41). When *hem1Δ* yeast express the *C. elegans* heme importers HRG-4 (CeHRG-4) or HRG-1 (CeHRG-1), their growth is increased compared to control yeast grown on heme-supplemented plates (Figure 4.2). When *hem1Δ* yeast express the yeast heme exporter, Pug1p (PUG1), their growth is reduced compared to control yeast on heme plates. Similarly, the growth of *hem1Δ* yeast expressing *C. elegans* MRP5 (CeMRP-5) or human MRP5 (both hMRP5 and C terminal tagged hMRP5 HA) is decreased, both in the presence of heme and in the presence of ALA (Figure 4.2). Additional studies revealed that expression of

Figure 4.2: Expression of MRP5 inhibits growth of a heme synthesis-deficient yeast strain.

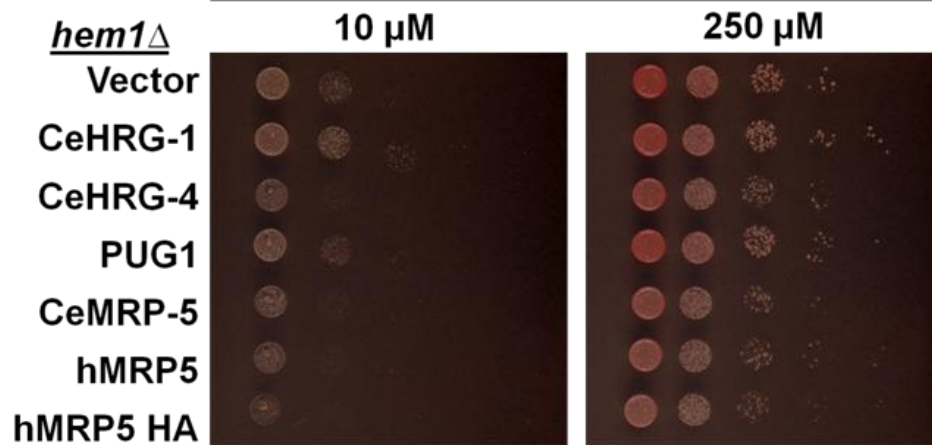
The *hem1Δ* yeast strain was transformed with indicated constructs and grown overnight in SC medium without ALA and spotted in serial dilutions on 2% raffinose SC (-Ura, +0.4% galactose) plates supplemented with indicated concentrations of ALA or hemin. Plates were incubated 3 days prior to imaging.



Heme



ALA



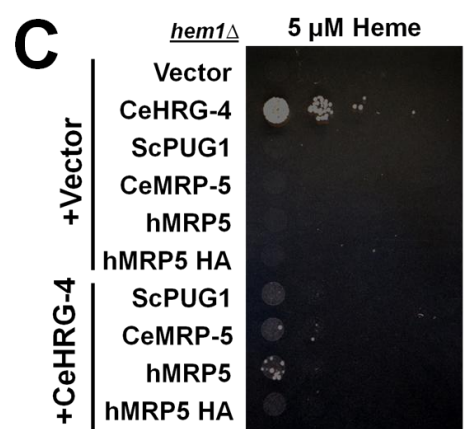
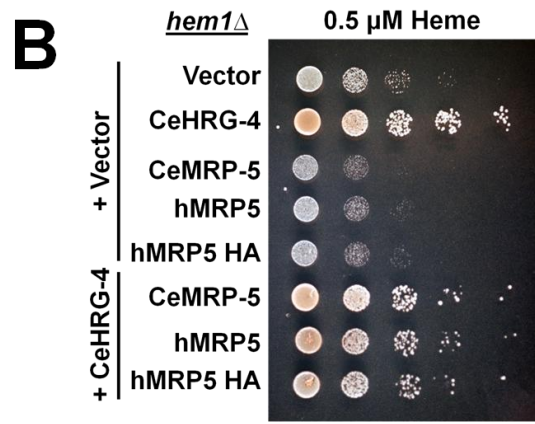
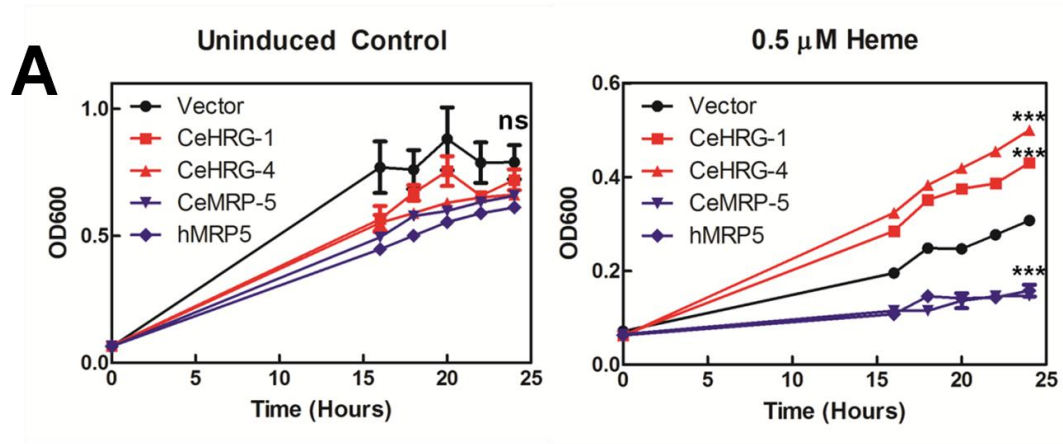
zebrafish Mrp5 inhibited growth of *hem1Δ* yeast on heme-containing plates as well (Appendix VI).

In order to quantify the ability of MRP5 to inhibit the growth of *hem1Δ* yeast, we grew yeast in the liquid culture and assayed yeast growth by measuring OD₆₀₀ over time. Uninduced yeast showed no significant difference in growth (Figure 4.3A, left panel). Upon induction with galactose, yeast expressing CeHRG-1 and CeHRG-4 show significantly improved growth in medium supplemented with 0.5 μM heme when compared to control yeast (Figure 4.3B) (41). However, yeast expressing *C. elegans* MRP-5 or human MRP5 showed significantly reduced growth. The reduced growth of yeast expressing CeMRP-5 or hMRP5 was not due to cell toxicity associated with overexpression of a large polytopic membrane protein, as growth was restored when cells were co-transformed with the heme importer CeHRG-4 (Figure 4.3B, bottom three rows).

Yeast are capable of using sugar-based carbon sources such as galactose or raffinose for a mixture of aerobic and anaerobic respiration (159). Thus under heme deprivation conditions, yeast growing in the presence of a sugar-based carbon source can alternatively derive energy via fermentation, which is less heme-dependent than aerobic respiration. To further exacerbate the MRP5-dependent growth phenotype in *hem1Δ* yeast, we grew yeast expressing these putative heme transporters in the presence of glycerol and lactate, which yeast can utilize exclusively for aerobic respiration. While yeast expressing CeHRG-4 grew in the spot growth assay, neither control yeast nor yeast expressing PUG1, CeMRP-5, or hMRP5 were capable of growth. Interestingly, when co-expressed with CeHRG-4, the phenotype of each of

Figure 4.3: Expression of MRP5 inhibits growth in a heme-dependent manner.

(A) The *hem1Δ* yeast strain was transformed with indicated vectors, grown for 12 hours in SC medium without added heme or ALA, and then grown in 2% raffinose SC (-Ura, +0.4% galactose) medium for 24 hours under the indicated conditions. Yeast growth was assessed by measuring OD₆₀₀. LEFT: Uninduced yeast (+0.4% glucose) which did not express the transgenes showed no difference in growth after 24 hours in the presence of 250 μM ALA. RIGHT: Induced yeast (+0.4% galactose) expressing heme importers HRG-1 and HRG-4 grow significantly better than control yeast. Yeast expressing MRP-5 grow significantly worse. ***P<0.001 compared to vector control after 24 hours, n=3 (two-way ANOVA, Bonferroni post-test). (B) The *hem1Δ* yeast strain was transformed with the indicated constructs, grown overnight without added heme or ALA and spotted in serial dilutions on 2% raffinose SC (-Ura, +0.4% galactose) plates supplemented with 0.5 μM heme. Plates were incubated at 30°C for 72 h before imaging. (C) The *hem1Δ* yeast strain was transformed, grown overnight without added heme or ALA and spotted in serial dilutions on SC (-Ura, glycerol, lactate) plates supplemented with 5 μM heme. Plates were incubated for 3 days prior to imaging.



the three heme exporters was dominant over that of the heme importer (Figure 4.3C). Taken together, these results indicate that MRP5 has a conserved ability to regulate cellular heme homeostasis.

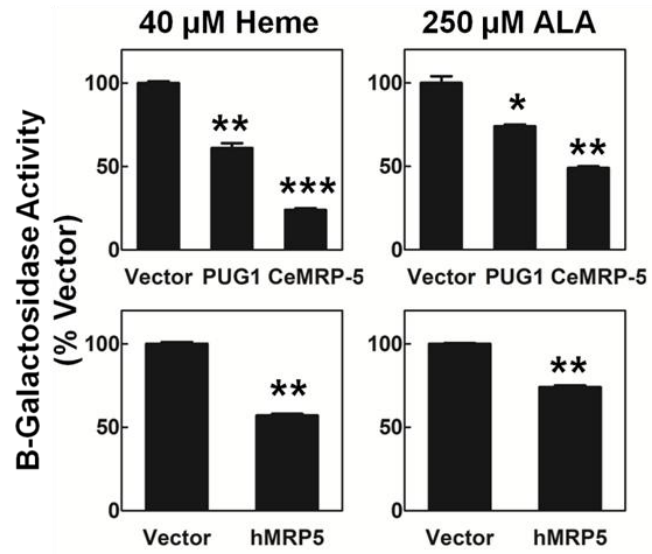
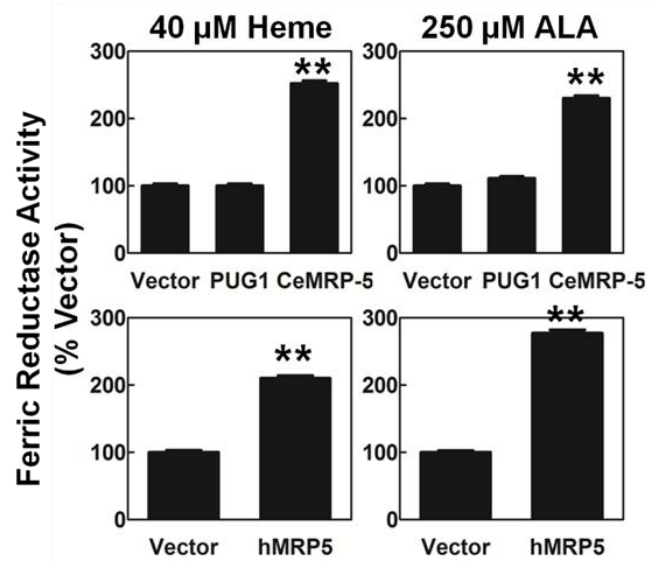
MRP5 is a conserved heme transporter

To assess whether MRP5 expression could alter intracellular heme levels in the yeast, we measured the activity of β -galactosidase derived from the *lacZ* reporter under control of the cytochrome c (*CYC1*) promoter. This promoter is activated by Hap1, a transcription factor positively regulated by cytosolic heme levels (160). Thus, in this assay, levels of β -galactosidase activity reflect the availability of heme in the cytosol to activate the *CYC1* promoter. As proof of principle, yeast expressing Pug1p, a yeast heme effluxer, show decreased β -galactosidase activity. Supporting the hypothesis that they are heme transporters, both CeMRP-5 and hMRP5 showed decreased β -galactosidase activity when assayed in this system (Figure 4.4A, left panels). This result was consistent with the poor growth phenotype in the spot assay. This result was also reproducible in yeast grown in the presence of ALA, indicating that expression of MRP5 can also affect availability of endogenously synthesized heme (Figure 4.4A, right panels). Interestingly, yeast expressing MRP5 showed lower β -galactosidase activity than cells expressing PUG1 (126).

To evaluate heme availability in the yeast secretory compartment, we measured the activity of a heme-dependent enzyme (ferric reductase) as an indicator of intracellular heme concentrations (126). In yeast, ferric reductase (Fre1p) acquires a heme cofactor needed for enzymatic activity in the secretory pathway before being trafficked to the plasma membrane (161). The ferric reductase assay is performed

Figure 4.4: Ectopic expression of MRP5 in yeast alters heme availability in the cytosol and the secretory pathway.

(A) Heme-dependent β -galactosidase activity. The *hem1* Δ yeast strain was transformed with pCYC1-LacZ, as well as empty vector, ScPUG1, CeMRP-5, or hMRP5 and grown with the indicated amount of heme or ALA. Cell lysates were then analyzed for β -galactosidase activity, normalized to vector. ***P<0.001, **P<0.01, *P<0.05 when compared to yeast expressing empty vector under identical conditions, n=2 (one-way ANOVA, Bonferroni post-test). **(B)** Heme-dependent ferric reductase activity. The *hem1* Δ *fre1* Δ *fre2* Δ *PGK1-FRE1* yeast strain was transformed with indicated vectors and grown with the indicated amount of heme or ALA. Ferric reductase activity from whole cells was analyzed. **P<0.01, *P<0.05 when compared to yeast expressing empty vector under identical conditions, n=2 (one-way ANOVA, Bonferroni post-test).

A**B**

in a *hem1Δfre1Δfre2ΔMET3-FRE1* yeast strain. In this strain, the endogenous genes for *FRE1* and *FRE2*, which are regulated by the presence of iron and copper, are deleted, and Fre1p is constitutively expressed from the MET3 promoter. Thus, in this strain, ferric reductase activity is indicative of heme availability in the secretory pathway. While Pug1p expression had minimal effect at these heme and ALA concentrations, yeast expressing CeMRP-5 or hMRP5 showed significantly greater ferric reductase activity in the presence of either heme or ALA, indicating greater heme availability in the secretory pathway (Figure 4.4B).

Although most MRP transporters expressed in yeast localize to the vacuolar membranes (162), indirect immunofluorescence microscopy localized CeMRP-5 and hMRP5 primarily to intracellular compartments that are distinct from the plasma membrane and the vacuole (Figure 4.5A and B). Taken together, these results indicate that when expressed in yeast, MRP5 proteins are capable of exporting heme from the cytosol into intracellular organelles for delivery to hemoproteins such as Fre1p.

Discussion

Genetic evidence indicated that *C. elegans* MRP-5 functions as a heme effluxer. As MRP5 is conserved in metazoans, we sought to determine if its ability to regulate heme homeostasis is conserved in other species. The current study showed that *mrp5* is widely expressed early during zebrafish development and that loss of *Mrp5* leads to severe anemia and developmental defects. We also sought to determine if *C. elegans* MRP-5 was capable of transporting heme, and if this ability was conserved in other MRP5 family members. Indeed, *C. elegans* MRP-5, zebrafish *Mrp5*, and human MRP5 all inhibit growth when expressed in *hem1Δ* yeast. We

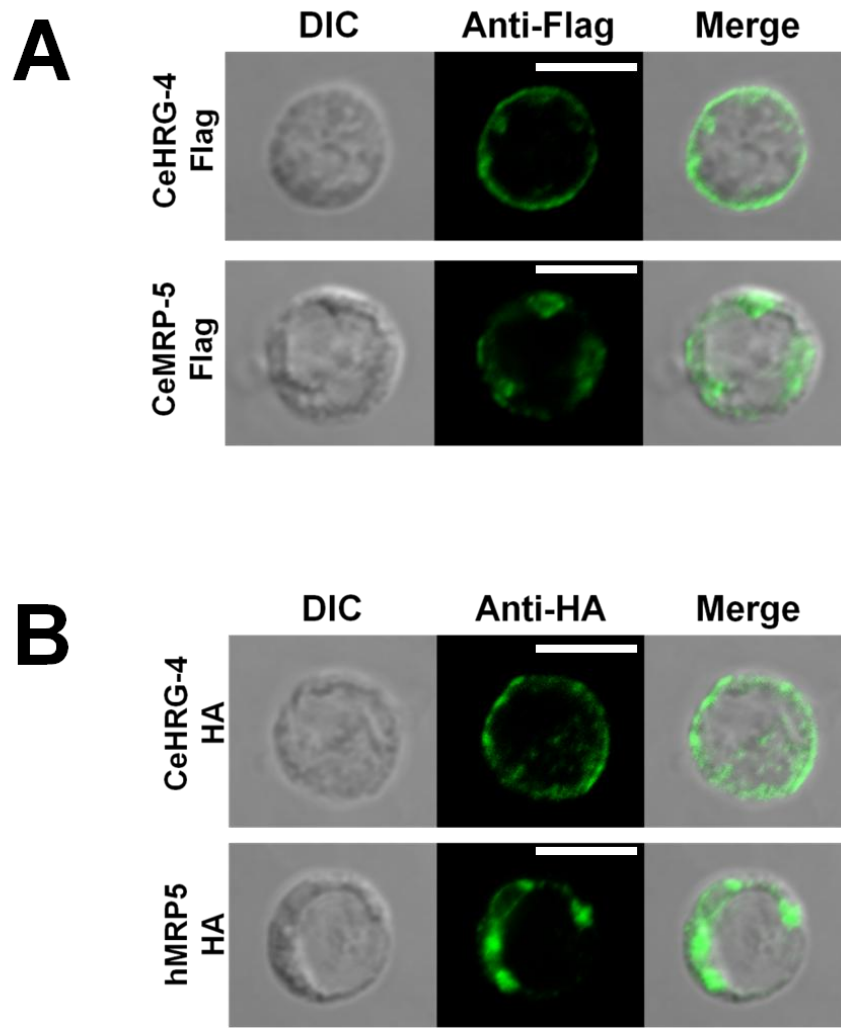


Figure 4.5: MRP5 localizes to intracellular membranes in yeast.

The *hem1Δ* yeast strain expressing (A) CeHRG-4-flag or CeMRP-5-flag or (B) CeHRG-4-HA or hMRP5-HA was subjected to indirect immunofluorescence microscopy using anti-flag or anti-HA antibodies and imaged by confocal microscopy. Scale bars, 5 μ m.

analyzed the effect of MRP5 expression on subcellular heme reporters in this yeast strain, and further showed that both *C. elegans* MRP-5 and human MRP5 reduce heme availability in the cytosol with a concomitant increase in heme availability in the secretory pathway. When expressed in yeast, both worm and human MRP5 localize to intracellular membranes which are distinct from the vacuole or plasma membrane. Taking these data together, we conclude that MRP5 proteins are capable of effluxing heme from the cytosol into the secretory pathway in yeast.

Results from our experiments in zebrafish indicate that MRP5 proteins play a conserved role in organismal heme homeostasis. Morpholino knockdown experiments show that zebrafish *mrp5* is required for the differentiation of the erythroid lineage and for development of normal morphology (Appendix V). The mechanism underlying these functions is still unclear; however, it is interesting that morpholino knockdown of *hrg1* in zebrafish results in comparable anemia and identical developmental phenotypes as *mrp5* knockdown (40). The similar *hrg1* and *mrp5* phenotypes suggest that intercellular transport of heme plays a critical role in early development and erythropoiesis in zebrafish.

We utilized a heme-synthesis deficient yeast strain to show that expression of worm, zebrafish, and human MRP5 proteins can alter heme homeostasis in a heterologous system (Figures 4.2 and 4.3). Though *C. elegans* MRP-5 and human MRP5 are only 39% identical, they have similar localization and phenotypes in *hem1Δ* yeast. This is again reminiscent of worm and human HRG1 proteins, which are only ~20% identical, yet are both able to import heme in these assays using conserved transport mechanisms (41). While the zebrafish ortholog was only tested in

the growth assay, we predict that it will show similar localization and phenotypes in the *CYCI-LacZ* and ferric reductase assays.

It can be argued that the growth assays are an indirect method of showing heme transport by MRP5 proteins, as expression of these proteins may be resulting in numerous physiological changes in the yeast. We have shown, however, that expression of MRP5 can alter two heme-specific reporters located in distinct compartments within the cell (Figure 4.4). It is difficult to imagine a mechanism whereby heme availability is concomitantly reduced in the cytosol and increased in the secretory pathway without invoking direct transport from the former to the latter.

It should be noted that, while expression of MRP5 significantly alters both heme reporters, the effect is somewhat mild. For example, in the presence of heme, expression of human MRP5 in *hem1Δ* yeast decreases β -galactosidase activity to 50% of vector and increase ferric reductase activity two-fold above vector (Figure 4.4A and B). Expression of *C. elegans* MRP-5 reduces β -galactosidase activity to half that of vector in the presence of ALA. It is possible, given that the MRP5 transporters are being expressed in a heterologous system, that they are missing critical partners involved in heme transport. One example of this is heme export by FLVCR1, which becomes one hundred times more efficient in the presence of hemopexin (163). Another example is the mitochondrial iron import complex comprised of mitoferrin and ABCB10. While mitoferrin alone can transport iron into the mitochondrial matrix, it requires binding to ABCB10 for increased stability and enhancement of iron transport (164).

We have additionally shown that the defect caused by MRP5 expression can be rescued by co-expression with the heme importer, *C. elegans* HRG-4 (Figure 4.3B and C). It is noteworthy that co-expression with HRG-4 does not fully recapitulate the growth of yeast expressing HRG-4 alone. This result suggests that, while HRG-4 is the strongest heme importer yet identified in these yeast assays (41), heme is exported by MRP5 proteins with enough affinity to mitigate the positive effects of HRG-4-mediated heme import.

Chapter 5: The Role of MRP5 in Mammalian Heme Homeostasis

*If e'er thy breast with freedom glowed,
And spurned a tyrant's chain,
Let not thy strong oppressive force
A free-born mouse detain!*

Anna Laetitia Barbauld
"The Mouse's Petition to Dr. Priestley"

Summary

We have previously shown that *mrp-5* is a heme exporter in *C. elegans* and that regulation of heme homeostasis is probably a conserved function for MRP5 proteins in metazoans. Here we show that although mice lacking *Mrp5* appear to be phenotypically normal, cell culture models show that *Mrp5* may play a role in mammalian heme transport. Similar to its localization in worms, human MRP5 localizes to the basolateral membrane in polarized MDCKII cells. In unpolarized cells, human MRP5 localizes to the plasma membrane as well as a number of endocytic compartments. Mouse embryonic fibroblasts (MEFs) lacking *Mrp5* show a reduced ability to deliver heme to a hemoprotein reporter targeted to the Golgi, indicating that *Mrp5* may play a role in delivering heme to the secretory pathway. Furthermore, *Mrp5*, which is expressed in bone marrow-derived macrophages (BMDMs), is upregulated in these cells during erythrophagocytosis (EP). In the absence of *Mrp5* expression, BMDMs are unable to upregulate the program of genes

required to respond to EP. These results indicate that MRP5 likely regulates heme homeostasis in mammals and possibly plays a role during recycling of senescent red blood cells.

Results

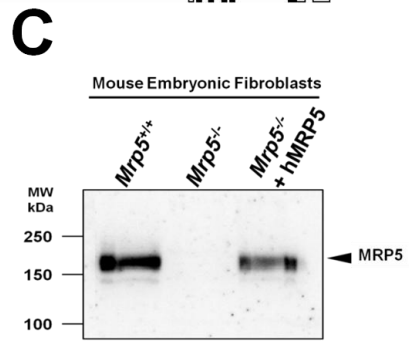
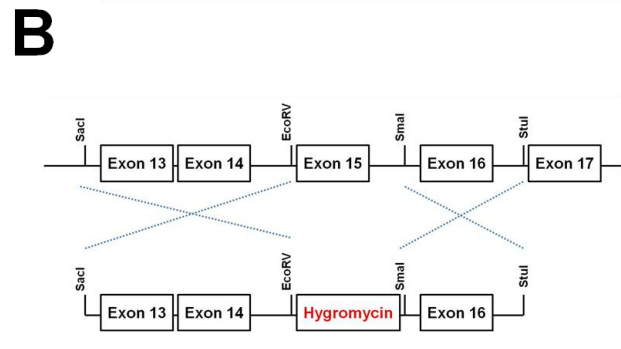
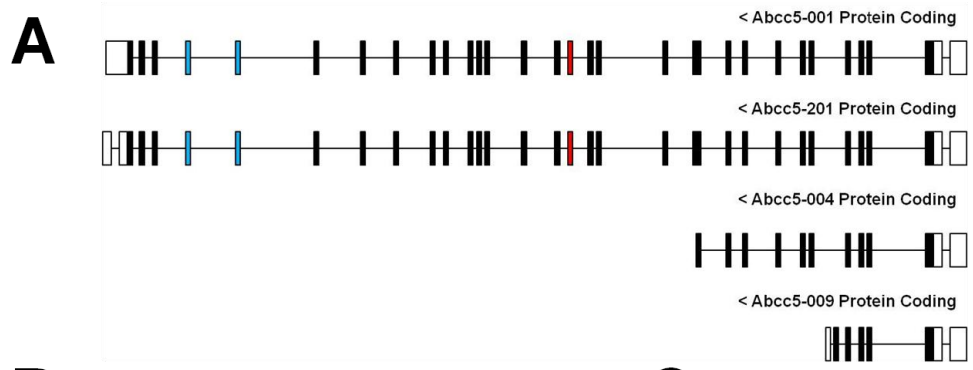
***Mrp5*^{-/-} mice do not have hematological defects**

According to the February 2014 release of the annotated mouse genome from Ensembl, there are four protein-coding splice isoforms of *Mrp5* (Figure 5.1A). The two longest transcripts encode identical 1436 amino acid full length *Mrp5* proteins, but differ in their 3' untranslated regions. The two shorter transcripts encode shorter proteins of 512 and 208 amino acids respectively. These two shorter proteins do not contain ABC domains, and are not predicted to be functional transporters. In mammals, MRP5 is expressed almost ubiquitously (113, 114, 165) but *Mrp5* knockout mice are viable with no overt phenotypes (130). To knock out *Mrp5*, de Wolf *et al* targeted exon 15 for replacement with a hygromycin resistance cassette in 129/Ola-derived E14 embryonic stem (ES) cells (Figure 5.1B) (130). F₁ offspring confirmed to have germline transmission of the mutant *Mrp5* allele were backcrossed into the FVB genetic background.

Analysis of hematological parameters in adult *Mrp5*^{+/+} and *Mrp5*^{-/-} mice fed chow diets [300 parts per million (ppm) iron] showed no difference between the two genotypes (Appendix VII, A). It is important to note that the FVB mouse strain inherently has high liver and spleen iron content and is therefore ill-suited for studies of systemic iron homeostasis (166). We therefore backcrossed the *Mrp5* mutant allele

Figure 5.1: Generation of *Mrp5*^{+/+} and *Mrp5*^{-/-} fibroblasts.

(A) In mice, *Mrp5* is encoded on the reverse strand of chromosome 16. Four alternatively spliced protein-coding variants of *Mrp5* are listed on Ensembl and are shown here. The two longest transcripts encode identical 1436 amino acid full length MRP5 proteins, but differ in their 3' untranslated regions. The two shorter transcripts encode shorter proteins of 512 and 208 amino respectively. These two shorter proteins do not contain ABC domains. Protein coding exons are shown in black and untranslated regions are shown in white. The red exon is exon 15 targeted for deletion; the exons detected by qRT-PCR are shown in blue. (B) Schematic showing targeting strategy used to delete *Mrp5*. Exon 15 was replaced with a hygromycin resistance cassette in mouse embryonic stem cells. (C) Immunoblot analysis of *Mrp5* expression in mouse embryonic fibroblasts (MEFs) generated from *Mrp5*^{+/+} and *Mrp5*^{-/-} mice. Membranes were probed with the monoclonal anti-MRP5 antibody, and then incubated with HRP-conjugated anti-rat secondary antibody. The MRP5 antibody specifically recognizes mouse *Mrp5*, as well as human MRP5 ectopically expressed in *Mrp5*^{-/-} MEFs.



into the C57BL/6 background five times before subjecting *Mrp5*^{+/+} and *Mrp5*^{-/-} mice to adequate and low iron diets to perturb heme and iron homeostasis. Mice were genotyped and weaned at day 19 postpartum and fed a diet of deionized water and food containing either 8 ppm iron (low iron) or 50 ppm iron (adequate iron). After eight weeks on the diet, hematological parameters were measured and compared between genotypes and diets. All mice fed the low iron diet developed severe anemia, as characterized by low hematocrit, low hemoglobin levels and leukocytosis. However, no significant difference was seen between *Mrp5*^{+/+} and *Mrp5*^{-/-} mice on either diet (Appendix VII, B). Additionally, when treated with phenylhydrazine, *Mrp5*^{-/-} mice did not show increased mortality or changes in blood and tissue iron levels compared to wild-type brood mates (Mark Fleming, Boston Children's Hospital, personal communication).

MRP5 regulates heme availability in the secretory pathway

To determine how loss of *Mrp5* affected heme homeostasis in a mammalian cell model, we generated mouse embryonic fibroblasts (MEFs) from *Mrp5*^{+/+} and *Mrp5*^{-/-} embryos. Probing MEF lysates with M₅I-10, a monoclonal antibody generated against the first 38 amino acids of the mouse *Mrp5*, revealed a band of the expected molecular weight by immunoblotting (Figure 5.1C) (167). The antibody recognized endogenous *Mrp5* in cell lysates from *Mrp5*^{+/+} mouse embryonic fibroblasts (MEFs), as well as human MRP5 ectopically expressed in *Mrp5*^{-/-} MEFs (Figure 5.1C, first and last lanes). In agreement with previous reports (110), human MRP5 colocalized with the basolateral membrane marker, Na⁺-taurochlorate co-transporting polypeptide (NTCP), and not with the apical membrane marker, syntaxin 3, in polarized MDCKII

cells (Figure 5.2). We attempted to generate a C-terminal GFP-tagged MRP5 fusion protein; however, this construct was mislocalized to the Golgi in polarized cells (Appendix VIII). Because of this, and as endogenous Mrp5 was difficult to stain with the monoclonal antibody, we instead performed localization studies using ectopically-expressed untagged human MRP5. In *Mrp5*^{+/+} MEFs, ectopically expressed human MRP5 was found to colocalize not only with the plasma membrane (WGA), but also partially with the Golgi (galactosyltransferase) and endosomal recycling organelles (Rab4- , Rab5- , Rab9- , and Rab11-positive vesicles) (Figure 5.3). Endogenous mouse MRP5 was found to be similarly localized in punctuate intracellular vesicles throughout the cytoplasm, with some protein on the cell periphery (Figure 5.4A).

To verify the yeast results, we transfected *Mrp5*^{+/+} and *Mrp5*^{-/-} MEFs with an engineered horseradish peroxidase (HRP) that was confined to the Golgi with a targeting sequence (43). Because holo-HRP requires heme as a cofactor, HRP activity reflects heme availability in the Golgi compartment (43). When heme-depleted MEFs expressing HRP were supplemented with heme in the growth medium, robust HRP activity was detected in *Mrp5*^{+/+} cells but not *Mrp5*^{-/-} cells; HRP activity was significantly suppressed by 65 to 80% in *Mrp5*^{-/-} cells (Figure 5.4B). Together, these results support a model in which mammalian MRP5 is a heme exporter that transports heme from the cytosol into the lumen of the secretory pathway, and possibly across the plasma membrane.

***Mrp5*^{-/-} macrophages have an altered response during erythrophagocytosis**

In order to determine if *Mrp5* plays a physiological role in mammalian heme homeostasis, we analyzed the localization, regulation, and function of *Mrp5* in

Figure 5.2: Localization of human MRP5 in polarized MDCKII cells.

MDCKII cells stably expressing human MRP5 were transfected with the basolateral marker NTCP-GFP or the apical marker Syntaxin3-GFP and grown to confluency on transwell filters. Polarization of the monolayer was determined after measuring a transient spike in trans-epithelial electrical resistance, which remained above baseline level. Cells were fixed and probed with monoclonal anti-MRP5, followed by Alexa 568-conjugated secondary antibody and imaged using confocal microscopy. A single confocal section (xy) is depicted along with composite stacks in side views (yz , xz).

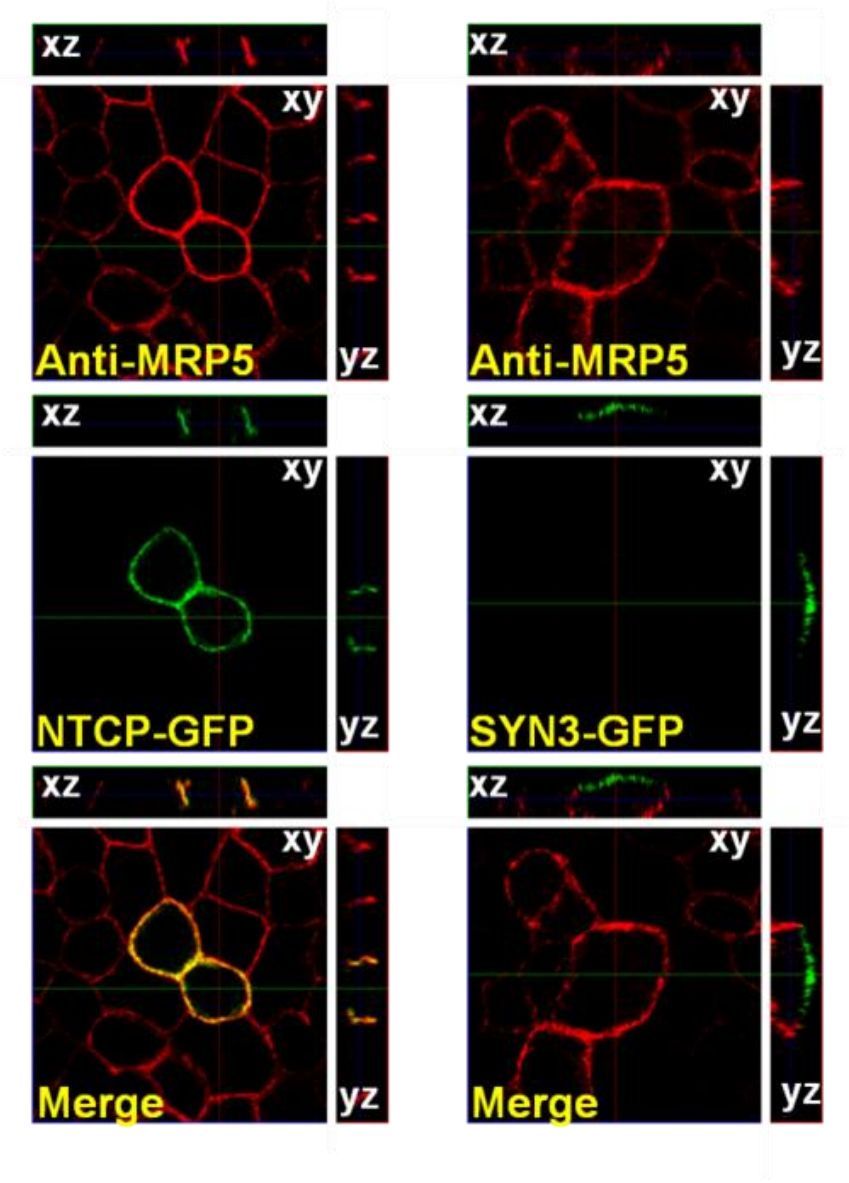


Figure 5.3: Localization of MRP5 in immortalized mouse embryonic fibroblasts.

Immunolocalization of human MRP5 overexpressed in MEFs by confocal microscopy. WGA is used as a plasma membrane (PM) marker, RFP-GalT as a trans-Golgi (TGN) marker, Rab4YFP marks early endosomes (EE) and the endocytic recycling compartment (ERC), Rab5YFP marks EEs, Rab9YFP marks late endosomes (LE) and the TGN, Rab11YFP marks the ERC and TGN. Scale bar, 20 μ M.

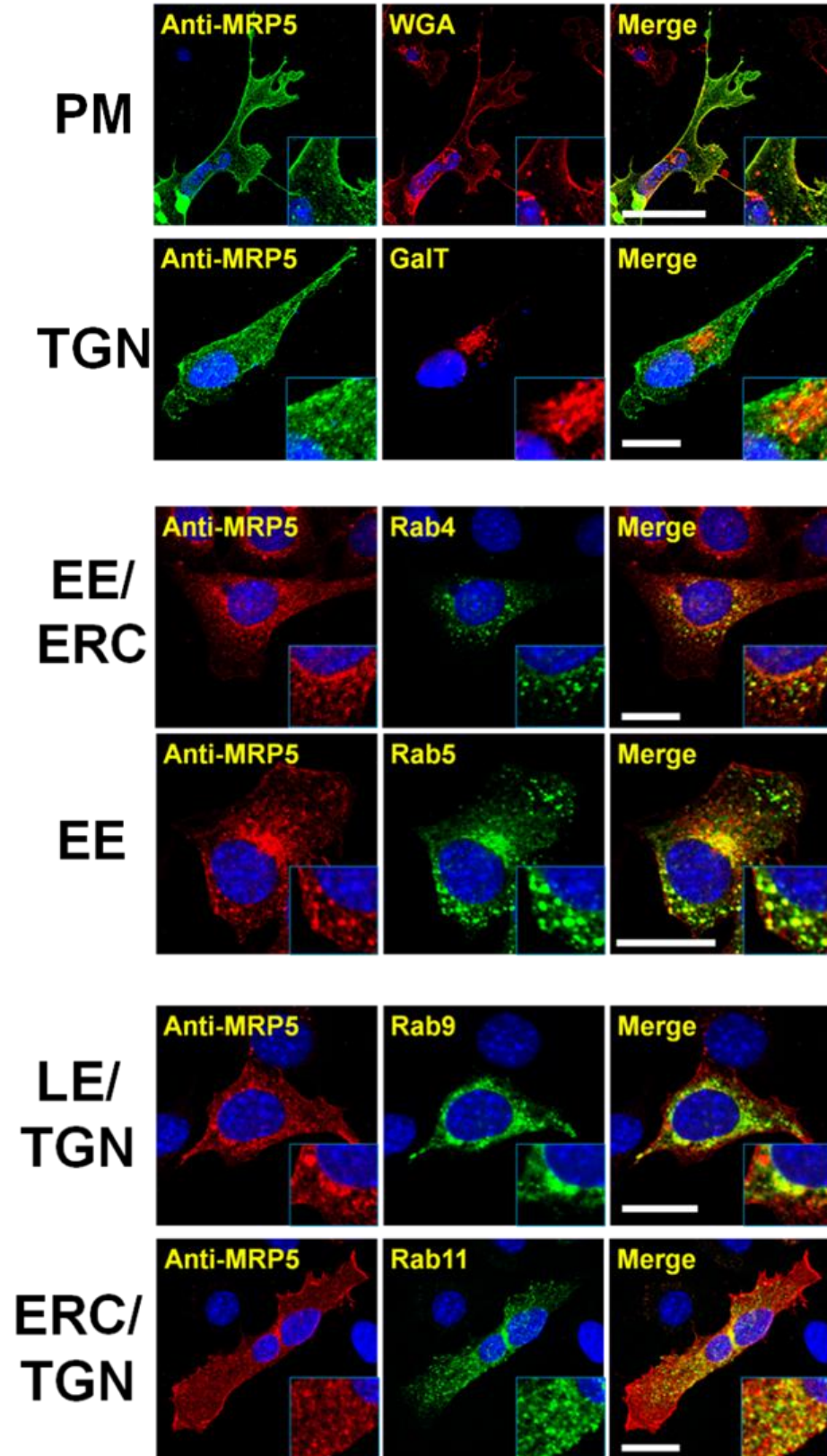
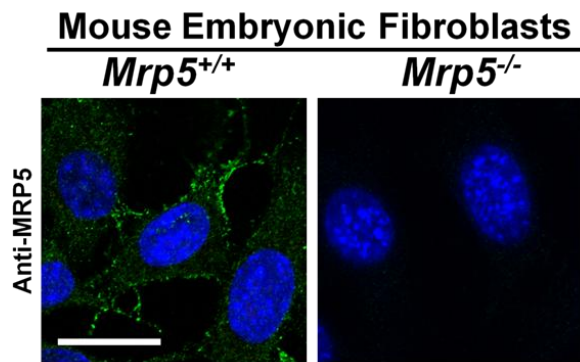
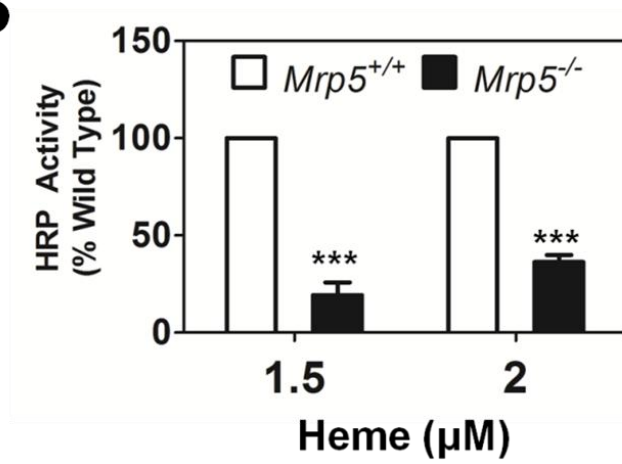


Figure 5.4: MRP5 localizes to the secretory pathway and alters heme levels in this compartment.

(A) Immunolocalization analysis of endogenous MRP5 expression in MEFs generated from *Mrp5*^{+/+} and *Mrp5*^{-/-} FVB mice. Cell lysates were resolved on SDS-PAGE and blotted to nitrocellulose membranes for probing with a monoclonal anti-MRP5 antibody. (B) Heme-dependent horseradish peroxidase activity in *Mrp5*^{+/+} or *Mrp5*^{-/-} MEFs. Cells were transfected with GolgiHRP and then grown for 24 hr in heme-depleted media plus succinyl acetone (HD+SA) for complete heme depletion. Indicated amounts of heme were added back and cells were incubated for a further 24 h. Cell lysates were harvested and analyzed for peroxidase activity, which was normalized to peroxidase activity from samples not expressing GolgiHRP and then to the protein concentration of each sample. ***P<0.001 for knockout MEFs when compared to wild type MEFs under identical conditions, n=3 (two-way ANOVA, Bonferroni post-test).

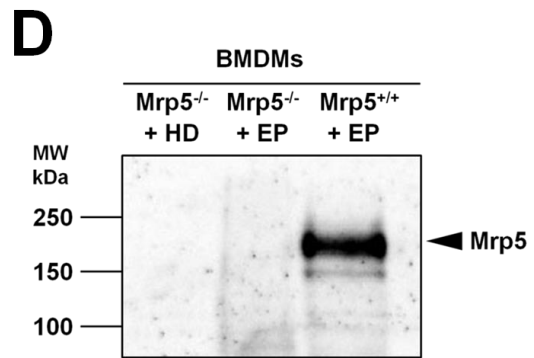
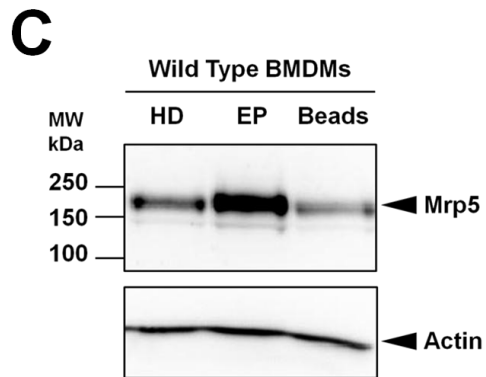
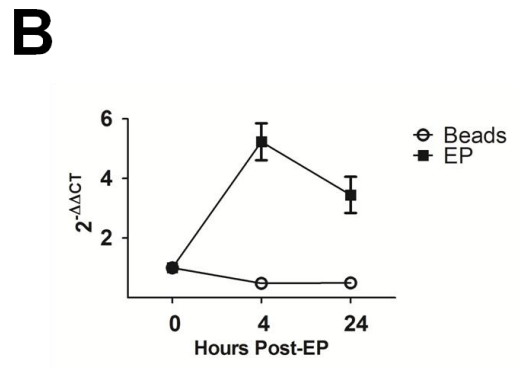
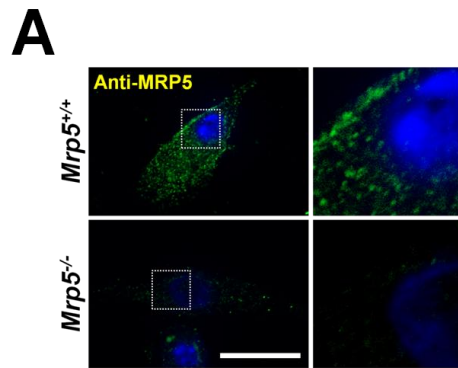
A**B**

macrophages (MΦs) of the reticuloendothelial system. MΦs play an essential role in heme-iron recycling from dying red blood cells, which are recognized, engulfed, and degraded by the MΦs in a process termed erythrophagocytosis (EP). EP is a physiological process with an enormous heme transport load, and a process which can be studied *ex vivo* by culturing mouse bone marrow-derived MΦs (BMDMs). Consistent with immunohistochemical analysis of MRP5 localization in MEFs, MRP5 was found in punctate intracellular vesicles with a small amount of plasma membrane staining in BMDMs (Figure 5.5A).

To determine if *Mrp5* gene expression was regulated during EP, BMDMs were fed damaged red blood cells, or latex beads as a negative control. Cells were harvested at subsequent time points, and RNA extracted from these samples was analyzed using quantitative RT-PCR. The *Mrp5* transcript was indeed upregulated 4 hours post-EP (Figure 5.5B); this effect was specific as it was not seen when the BMDMs were fed latex beads. Additionally, Western blot analysis showed that MRP5 protein levels were also upregulated under EP conditions (Figure 5.5C). Feeding BMDMs latex beads did not upregulate MRP5 protein levels, again demonstrating the specificity of the MRP5 upregulation (Figure 5.5C, last lane). We performed EP on *Mrp5*^{-/-} BMDMs and no increase in MRP5 signal was detected by Western blot, indicating that the increase in MRP5 protein levels was due to upregulation of endogenous MRP5, rather MRP5 derived from engulfed red blood cells (Figure 5.5D). While *Mrp5* is upregulated during EP in BMDMs, immunolocalization studies, however, showed that MRP5 does not localize to the phagolysosome in these cells (Figure 5.6).

Figure 5.5: MRP5 is upregulated during erythrophagocytosis in bone marrow-derived macrophages.

(A) Immunohistochemistry of endogenous MRP5 in mouse BMDMs. MRP5 staining was performed as in Figure 5.4A, using an Alexa 488-conjugated secondary antibody. Scale bar, 20 μ M. (B) qRT-PCR analysis of *Mrp5* transcriptional regulation during EP. Relative fold changes (mean \pm SEM, n=6) were determined by normalizing the C_T values to *Gapdh* and then to C_T values of control samples using the $\Delta\Delta C_T$ method. Control samples were grown in heme depleted media and harvested at time points identical to those of the BMDMs fed red blood cells (EP, 10:1 ratio of RBCs: BMDMs) or latex beads. (C) Western blot analysis of MRP5 expression in BMDMs grown in heme-depleted media (HD) or fed red blood cells (EP) or latex beads. Protein was harvested 24 hr after EP. Western blot was performed as in Figure 5.1C. Actin is shown as a loading control. (D) Western blot analysis of EP performed on BMDMs derived from *Mrp5*^{+/+} or *Mrp5*^{-/-} mice shows that MRP5 protein derived from phagocytosed erythrocytes is not detectable by immunoblotting.



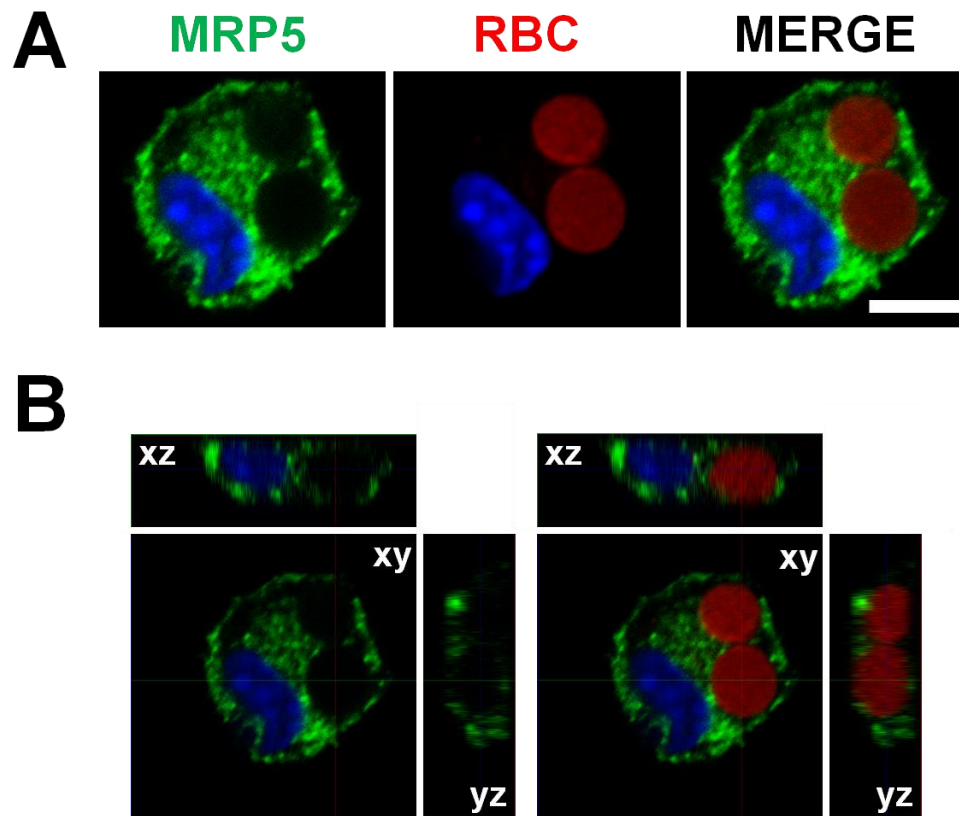


Figure 5.6: MRP5 does not localize to the phagolysosomal membrane during erythrophagocytosis in bone marrow-derived macrophages.

(A) Immunohistochemistry of ectopically expressed human MRP5 in mouse BMDMs. MRP5 staining was performed as in Figure 5.4A, using an Alexa 488-conjugated secondary antibody. The senescent red blood cells emit autofluorescence, as seen in the red channel. Scale bar, 5 μ M. (B) Confocal stack image of the cell in (A). A single confocal section (xy) is depicted along with composite stacks in side views (yz , xz).

To determine if loss of *Mrp5* alters the cellular response to EP, we analyzed BMDMs isolated from *Mrp5*^{+/+} and *Mrp5*^{-/-} mice over the course of EP. We measured levels of *Hmox1* (heme oxygenase 1) and *Hrg1* (heme responsive gene 1), which are both highly induced in BMDMs in response to EP (43). *Hrg1* is involved in heme export from the phagolysosome, and *Hmox1* is involved in degradation of a portion of that heme to release iron (43). When wild-type BMDMs were fed RBCs, both *Hmox1* and *Hrg1* were strongly induced at 12 hr post-EP. This post-EP induction was attenuated in *Mrp5*^{-/-} BMDMs, as upregulation of both *Hmox1* and *Hrg1* was significantly repressed in these cells (Figure 5.7A and B).

Discussion

Iron deficiency is the most common nutritional disorder in both developing and developed countries (168). According to a World Health Organization report in 2003, about 60-80% of the world's population may be iron-deficient (169). While intestinal absorption of iron is hindered by the acidic pH of the stomach and the presence of metal-chelating compounds found in many foods, dietary heme is a more readily absorbed source of nutrient iron (170). Furthermore, in order to meet cellular requirements for heme, while concurrently providing protection from heme-associated toxicity, cellular heme levels are regulated via transport and trafficking pathways. Thus heme transport pathways in mammals are important from both a nutritional and a cell biological perspective.

Using genetic analysis in *C. elegans* and biochemical assays in yeast, we identified a conserved family of transporters that regulate organismal heme homeostasis. To determine the function of mammalian MRP5, we performed a

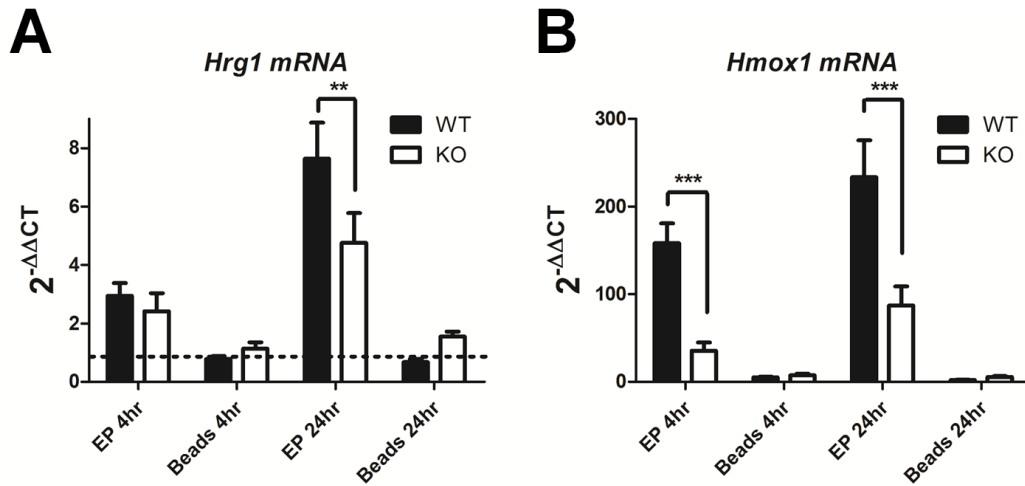


Figure 5.7: MRP5 is required for an appropriate cellular response to phagocytosed red blood cells during EP.

qRT-PCR analysis of EP-response genes in *Mrp5*^{+/+} and *Mrp5*^{-/-} BMDMs during EP. Upregulation of both (A) *Hrg1* and (B) *Hmox1* is attenuated in knockout cells compared to wild-type. Relative fold changes (mean ± SEM, n=6) were determined by normalizing the C_T values to *Gapdh* and then to C_T values of control samples using the ΔΔCT method. Control samples were grown in heme depleted media and harvested at time points identical to those of the BMDMs fed red blood cells (EP, 10:1 ratio of RBCs: BMDMs). BMDMs fed latex beads are shown as a negative control. ** P<0.01, *** P<0.001 compared to wild-type cells under identical conditions (two-way ANOVA, Bonferroni post-test).

number of experiments using both mice and cell culture models. While *Mrp5*^{-/-} mice have no apparent phenotype, we were able to uncover a number of defects in *Mrp5*^{-/-} cell types. In immortalized MEFs, Mrp5 localized to the plasma membrane and intracellular compartments, including endocytic recycling vesicles. Mirroring our results from assays in *hem1Δ* yeast, *Mrp5*^{-/-} MEFs have a decreased ability to deliver heme to a heme reporter localized to the Golgi apparatus. Additionally, BMDMs derived from *Mrp5*^{-/-} mice have a decreased ability to transcriptionally upregulate machinery necessary for erythrophagocytosis.

In worms, yeast, and mammalian cells, MRP5 localizes to both the plasma membrane and intracellular vesicles. The cell surface localization of MRP5 could be reconciled with the well-studied function of ABCC transporters to efflux substrates into the extracellular milieu, consistent with the expected role of exporting heme from the *C. elegans* intestine into the worm's circulatory system. However, MRP5 is also found in the secretory pathway as part of the endocytic recycling compartment. While we do not show that MRP5 has heme export activity by direct biochemical assays or that it can deliver heme to an endogenously-expressed mammalian hemoprotein, our genetic and cell biological results in yeast and MEFs support a model in which heme transported into the secretory pathway by MRP5 is incorporated into luminal hemoproteins (Figure 5.8).

Given the severe phenotypes associated with *mrp-5* deficiency in worms and zebrafish, why do *Mrp5* null mice not exhibit any overt hematological phenotypes? Clearly, worm and human MRP5 have similar phenotypes in yeast. One plausible explanation could be that, in mammals, FLVCR1 isoforms play a prominent role in

MRP5 Export in Vertebrates

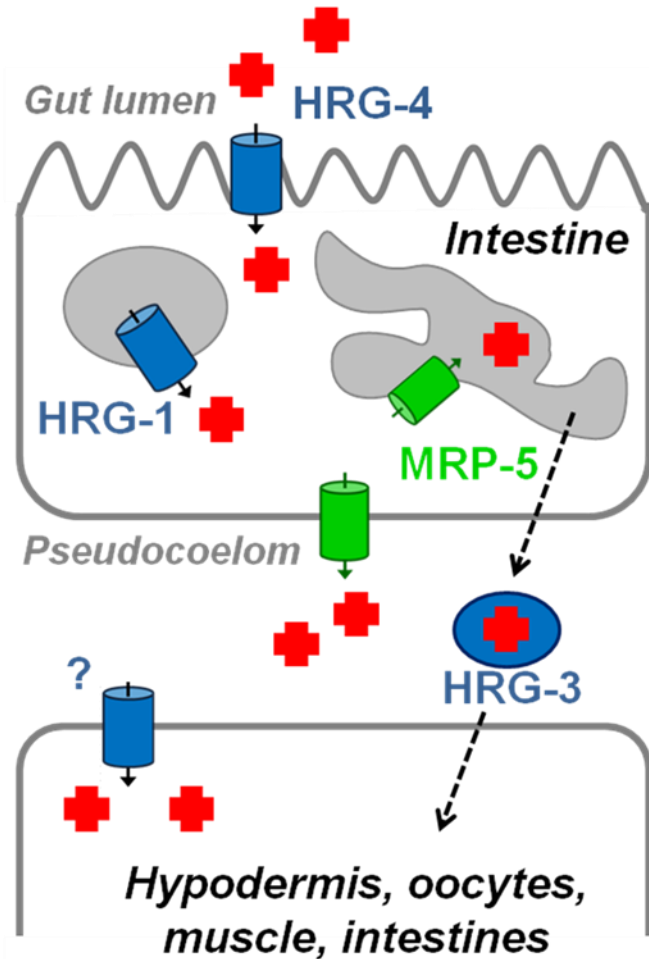


Figure 5.8: Proposed model for MRP5 function in mammalian cells.

Based on results from genetic, biochemical, and localization studies in yeast and cell culture models, MRP5 can localize to the plasma membrane for heme export as well as to the secretory pathway for heme delivery to luminal hemoproteins.

heme export, while MRP5 performs a more specialized role (35, 36, 171). It is notable that worms in which each of the five FLVCR homologs were depleted exhibited no heme-dependent phenotypes signifying that, at least in *C. elegans*, MRP-5 plays a definitive and essential role in heme homeostasis.

A second explanation is the influence of the FVB genetic background of the *Mrp5* mutant mouse (130). Inherently, the FVB strain has high liver and spleen iron content and therefore ill-suited for studies of systemic iron homeostasis. This is in contrast to the C57BL/6 strain which has a much lower liver and spleen iron content and, therefore, presents a mouse model that is more sensitive to perturbation in iron metabolism (166). For example, mutations in the iron transporter DMT1 are viable in certain mouse strains, but become lethal when backcrossed into the C57BL/6 background (Mark Fleming, Boston Children's Hospital, personal communication). While analysis of *Mrp5*^{+/+} and *Mrp5*^{-/-} mice was performed in mice that had been backcrossed to C57BL/6 five times, it is possible that residual background from the original FVB lineage is masking an iron-dependent phenotype.

Lastly, *in vivo* compensatory pathways may exist to overcome heme or iron metabolism defects in *Mrp5*^{-/-} mice. It is noteworthy that in humans and other placental mammals, *MRP5/ABCC5* has two recently described paralogs – *MRP8/ABCC11* and *MRP9/ABCC12*; mice and zebrafish genomes contain only *MRP9/ABCC12* (155, 172, 173). Although it has been reported that *MRP9/ABCC12* also localizes to the secretory pathway in unpolarized mammalian cells (174), the expression pattern and functions of *ABCC11* and *ABCC12* are largely unknown.

Our immunofluorescence studies indicated that, consistent with previous reports, MRP5 localizes to the plasma membrane and endocytic compartments in unpolarized cells. The endosomal trafficking of MRP5 could be mediated by an acidic-dileucine based sorting signal located in the cytoplasmic carboxy termini of vertebrate MRP-5 proteins (175). It is noteworthy that ATP7A, a copper-transporting P-type ATPase, pumps copper into the secretory compartment for metallation of essential cuproproteins in the Golgi, as well as export copper across the plasma membrane to regulate body copper stores (176). Conceivably, MRP5 may perform a similar dual function as a heme transporter.

The mechanism by which loss of *Mrp5* interferes with the erythrophagocytosis response in BMDMs remains unclear. Repression of *Hrg1* and *Hmox1* would seem to indicate that less heme is being transported into the cytosol of these cells; that is, that *Mrp5* is involved in the mobilization of heme from the phagolysosome. However, there are a number of reasons to indicate that this is not the case. First, localization studies have shown the *Mrp5* is not localized to the phagolysosomal membrane during EP. Second, with few exceptions, the vast majority of eukaryotic ABC transporters have been shown to be exporters. Every previous result in *C. elegans*, yeast, and MEFs has indicated that MRP5 proteins are indeed exporters, moving heme from cytosolic compartments to extracellular or luminal compartments. Transporting heme from the lumen of the phagolysosome into the cytosol would involve transport in the opposite direction.

One explanation for our results in BMDMs is that loss of *Mrp5* results in decreased phagocytosis in these cells. While this is a possibility, visual inspection of

the cells under a microscope does not reveal any obvious difference in the amount of senescent red cells taken up by *Mrp5*^{-/-} BMDMs. Another more provocative explanation is that macrophages sense and respond to the red cell-derived heme influx via the secretory pathway. Sterol response element binding protein (SREBP) is located in the secretory pathway but can signal cholesterol status to the nucleus via a cleaved transcription factor domain (177). It is possible that response proteins sense heme status in this same compartment and are part of the macrophage response during erythrophagocytosis. In the absence of a transporter such as *Mrp5* bringing heme into the secretory pathway, these responses are not sufficiently upregulated.

Chapter 6: Discussion

This tree has two million and seventy-five thousand leaves. Perhaps I missed a leaf or two but I do feel triumphant at having persisted in counting by hand branch by branch and marked down on paper with pencil each total. Adding them up was a pleasure I could understand; I did something on my own that was not dependent on others, and to count leaves is not less meaningful than to count the stars, as astronomers are always doing. They want the facts to be sure they have them all. It would help them to know whether the world is finite. I discovered one tree that is finite. I must try counting the hairs on my head, and you too. We could swap information.

David Ignatow
“Information”

Conclusions

For almost two decades, MRP5 has been studied as an exporter of cancer drugs, organic anions and nucleoside monophosphates, although none of these studies provided direct genetic evidence for a physiological role for MRP5 in growth and development (105, 110, 114). The goal of this project was to delineate the role that *mrp-5* plays in *C. elegans* heme homeostasis, and to determine if this protein is a conserved heme transporter. The major findings of these studies are outlined below.

- 1) Using microarray analysis and genetic screens, we identified *mrp-5* as a regulator of heme homeostasis and a putative heme transporter. MRP-5 is a membrane-bound ABC transporter that is upregulated in *C. elegans* during heme deficiency. Depletion of *mrp-5* causes upregulation of a heme deficiency signal in the IQ6011 heme sensor strain, and also protects worms

from toxicity associated with GaPPIX. These results indicated that *mrp-5* likely regulates heme entry into the worm.

2) Knockdown of seven *mrp* paralogs and five putative homologs of the heme exporter, *Flvcr1*, did not result in heme-dependent phenotypes in IQ6011. While any of these genes may play a more subtle role in regulating heme homeostasis in *C. elegans*, *mrp-5* appears to be the sole member of these genes that serves as a master regulator of heme entry into the worm. While *Flvcr1* clearly plays a role in mammalian heme homeostasis, as seen via the anemia and lethality of *Flvcr1*^{-/-} mice, it is apparent that *mrp-5* is the definitive heme homeostasis regulator in *C. elegans*.

3) Worms expressing *mrp-5* transcriptional and translational fusions revealed that *mrp-5* is expressed in multiple tissues, but that this protein is found mainly on the basolateral membrane of the intestine. Depletion of *mrp-5* specifically in the intestine results in F₁ lethality, and accumulation of ZnMP in the intestine, with a concomitant increase in extra-intestinal heme depletion signals. As most eukaryotic ABC transporters function as exporters, we concluded that *mrp-5* encodes an intestinal heme exporter. This conclusion is supported by biochemical assays in yeast, showing that *mrp-5* can modulate heme transport when expressed in a heterologous system.

4) Both RNAi-depletion and genetic deletion of *mrp-5* results in severe embryonic lethality and developmental arrest in *C. elegans*, indicating that an alternate pathway is unable to compensate for loss of heme export by *mrp-5*. As *mrp-5* is expressed at all worm stages, and, unlike *hrg-1*, *hrg-2*, *hrg-3* or

hrg-4, is not highly regulated by heme levels in the diet, we conclude that *mrp-5* is part of an essential, basal heme transport pathway. As *hrg-1* through *hrg-4* are not expressed at higher heme concentrations, and only exhibit mild heme-dependent phenotypes under severe heme limitation conditions, we conclude that these genes are part of an emergency network upregulated in response to heme starvation.

5) An HRG-3-dependent pathway for heme export from the intestine has already been delineated (77), but as previously noted, this pathway is unable to compensate for loss of *mrp-5*. While loss of *mrp-5* appears to downregulate *hrg-3* expression, this is not the reason for the inability of *hrg-3* to rescue *mrp-5(RNAi)*, as ectopic expression of *hrg-3* also failed to rescue the defect. It is possible that MRP-5 is required for heme delivery to HRG-3 during its maturation and exocytosis, as we showed that MRP5 delivers heme to the secretory pathway in assays in yeast and mammalian cell culture models.

6) Knockdown of *mrp-5* presumably results in heme buildup in the intestine, in parallel with depletion in extraintestinal tissues. This is reflected in the upregulation of the extraintestinal *hrg-2* promoter, and downregulation of the *hrg-3* promoter. Interestingly, the intestinal *hrg-1* promoter is upregulated by depletion of *mrp-5*. While it is possible that *mrp-5(RNAi)* partitions intestinal heme to compartment where it cannot be detected by the *hrg-1* promoter, a more intriguing possibility is that extraintestinal heme deprivation signals are capable of upregulating the *hrg-1* promoter. This would indicate an animal-wide communication system for coordinating the

release of stored intestinal heme in the event it was required by extraintestinal tissues.

7) Vertebrate MRP5 is 39% identical to *C. elegans* MRP-5 and zebrafish Mrp5 is ~74% identical to mammalian MRP5. Morpholino knockdown of *mrp5* resulted in severe anemia and developmental defects, which were specifically rescued by co-injection with zebrafish *mrp5*. Loss of the erythropoietic-specific transcription factor in *mrp5*^{MO} fish indicated that *mrp5* is required for differentiation of red blood cells. While the mechanism whereby loss of *mrp5* results in anemia remains unknown, these results indicate that MRP5 likely plays a role in regulating heme homeostasis. It is of note that knockdown of the heme importer *hrg1* results in similar defects in zebrafish – indicating that intra- and possibly inter- cellular heme transport is required for development and erythropoiesis.

8) Worm and human MRP5 localized to intracellular membranes when ectopically expressed in *Saccharomyces cerevisiae*. When expressed in a heme-synthesis deficient yeast strain, both proteins result in heme-dependent inhibition of growth, decreased heme availability in the cytoplasm and increased heme levels in the secretory pathway. We conclude that heme efflux by MRP5 transporters is likely conserved in metazoans.

9) Mice lacking *Mrp5* appear to be phenotypically normal. Even after being backcrossed five times into the iron-deficient C56BL/6 mouse strain, and even after induction of iron-deficiency anemia, their hematological parameters (which would reflect defects in iron or heme-iron homeostasis)

were indistinguishable from wild-type animals. Possible reasons for this include compensation by another heme transporter or the Mrp5 paralog, Mrp9/Abcc12; residual effects of the FVB genetic background; or that Mrp5 plays a more specialized role in heme homeostasis in mammals.

10) When ectopically expressed in unpolarized fibroblast cells, human MRP5 localizes to the plasma membrane and various endocytic and recycling vesicles. In polarized MDCKII cells, MRP5 localized to the basolateral membrane. Thus, in agreement with our previous studies of HRG1 and HRG4, MRP5 has a similar expression pattern in *C. elegans*, yeast, and mammalian cells.

11) In a cell culture model, loss of Mrp5 resulted in decreased activity of a genetically-encoded heme reporter localized to the Golgi apparatus. We conclude that Mrp5 may transport heme into the secretory compartment, a heme transport pathway that has yet to be elucidated.

12) Mrp5 is upregulated at the transcript and protein levels in bone marrow-derived macrophages undergoing erythrophagocytosis. Similar to its expression in fibroblasts, Mrp5 localizes to the plasma membrane and intracellular compartments in these cells; however, unlike Hrg1, Mrp5 is not enriched on the phagolysosomal membrane. Analysis of BMDMs lacking Mrp5 revealed that genes normally upregulated during EP are significantly attenuated. The mechanism behind this defect remains unknown, however it is unlikely that Mrp5 is involved in heme transport from the phagolysosome.

Future Directions

Structure/Function Analysis of MRP5 Proteins

A mechanistic understanding of how MRP5 proteins transport heme has yet to be elucidated. In general, the mechanisms of substrate binding by multidrug resistant ABC transporters remain poorly understood (178, 179). Many ABC proteins are able to transport a variety of drugs/substrates which have minimal structural similarities. It is unlikely that highly specific interactions between ABC transporter substrates and protein side chains exist for every single compound capable of being transported by this class of protein. We analyzed whether functional domains or motifs exist for heme binding in MRP-5. We found no regions of similarity between MRP5 and either HRG-1, HRG-4, PUG1, or even FLVCR. There are also no canonical heme binding motifs (CP, CxxCR, CxxCK, or CxxCM) in MRP5. Despite this, we have identified a number of possible heme-binding residues that are conserved in MRP5 proteins, but not in other ABCC family members. These include:

- tyrosines found in the second transmembrane segment (TM2) and nearby cytosolic loop (between TM2 and TM3) in human mouse, zebrafish, and worm MRP5 that are not conserved in any other worm or human ABCC/MRP protein
- tyrosine and cysteine residues in the cytosolic loop between TM4 and TM5 that are conserved in human, mouse, fish, and worm MRP5 and related proteins (ABCC11 and MRP9/ABCC12)
- a histidine in the cytosolic loop between TM10 and TM11 that is found in all MRP5 and related proteins in humans, mice, fish, and worms, but is a highly conserved arginine in all other human and worm ABCC/MRP proteins.

We propose to generate worm and human MRP5 proteins containing mutants in these residues and other conserved putative heme-binding residues. We will also generate mutants containing missense mutations in the conserved ABC transporter motifs (Walker A and signature motifs) in both the first and second NBDs of MRP5 as a positive control for abrogation of heme transport activity. Additionally, we found a single nucleotide polymorphism (SNP) in the human SNP database (dbSNP identification number: rs1053351) which is predicted to result in a premature stop codon before the second NBD (180, 181). We will test this mutation as well.

Similar to the structure/function analysis of HRG1 proteins, these mutants will first be tested in for modulation of growth and heme reporters in the *hem1Δ* yeast strain. We will also determine if expression of human MRP5 is capable of rescuing *mrp-5(ok2067)* worms. Any mutations found to affect heme transport by MRP5 in yeast will be further tested for their ability to rescue *mrp-5(ok2067)* in *C. elegans*.

MRP5 proteins from other species can be analyzed for heme transport in the various models used in this work. We can test MRP5 proteins from zebrafish or mouse for their ability to rescue *mrp-5(ok2067)*. While zebrafish Mrp5 has been shown to regulate growth of *hem1Δ* yeast, it is yet to be determined if it can modulate the activity of the *CYC1-LacZ* reporter gene or ferric reductase in the *hem1Δfre1Δfre2ΔMET3-FRE1* yeast strain. We can also test the ability of wild-type and mutant MRP5 from different species to rescue the loss of Golgi-HRP activity in an *Mrp5^{-/-}* background (although co-expression of proteins with the HRP construct in MEFs has proven to be challenging).

Interacting Partners and Other Heme Trafficking Mechanisms

The strong heme-dependent lethality phenotype of *mrp-5(ok2067)* worms makes them a powerful tool for uncovering additional mechanisms of heme transport in *C. elegans*. Simon Beardsley, a graduate student in our laboratory, has performed a mutagenic screen in this strain, looking for by-pass suppressor mutations that enable these worms to be propagated at low heme concentrations. He has identified over 30 mutants that suppress the lethality associated with *mrp-5(ok2067)* allele and is currently analyzing growth of these mutants in the presence of GaPPIX and localization of ingested ZnMP in these worms. Consistent with their restored ability to grow at low heme, preliminary analysis shows that all mutants suppress the *mrp-5(ok2067)*-associated rescue in the presence of GaPPIX. Interestingly, these suppressors appear to process ZnMP in different ways. For example, certain mutants show increased intestinal ZnMP compared to *mrp-5(ok2067)* worms, while others have intestinal ZnMP returned to wild-type levels. These results imply distinct mechanisms for rescue of the *mrp-5* deletion – either increased heme import to the intestine, or increased heme export from the intestine. It is likely that at least some of these mutations occur in genes involved in heme homeostasis. Given that MRP5 is conserved in metazoans, it is possible that mechanisms that rescue loss of *mrp-5* will be conserved as well.

Additionally, a number of members of our lab have performed immunoprecipitation experiments on proteins of interest (i.e. HRG1), followed by multidimensional protein identification technology (MudPIT) analysis in collaboration with Dr. James Wohlschlegel at UCLA (182, 183). In these

experiments, protein partners that are bound to the protein of interest are co-immunoprecipitated; mass spectrometry techniques are then used to identify interacting partners. This could be performed on MRP5 expressed in *C. elegans* or a mammalian system, and would act in parallel with the genetic screen to identify novel *in vivo* partners of MRP5.

Zebrafish Mutant Analysis

Jianbing Zhang, a graduate student in our laboratory has done extensive work characterizing phenotypes associated with morpholino knockdown of *mrp5* in zebrafish. He is currently using CRISPR technology to generate a null allele of *mrp5* in zebrafish. He has genotyped founder fish containing *mrp5* mutations, and intriguingly, offspring that are putatively *mrp5*-null appear unhealthy. Future work with the *mrp5* morpholino and mutant fish will determine the role that *mrp5* plays in maternal-fetal nutrient heme transfer, embryonic development, and differentiation of erythroid cells in these animals.

Heme Transport Assays

A major caveat of these studies is that we have not shown direct evidence of heme transport by MRP5. In most of biological models described in this work, MRP5 localizes to subcellular compartments. Changes in heme concentrations on a subcellular level are inherently difficult to demonstrate directly, as one would for a plasma membrane-localized transporter. One promising model is polarized MDCKII cells. First, in these cells, MRP5 traffics to the basolateral membrane, which thus lack the confounding effect of subcellular MRP5 localization. Second, unlike vesicular

transport assays, MRP5 would be present in its native milieu, including any interacting factors required for optimal transport. Directional transport of heme could be shown by adding radiolabelled heme to the media facing the apical surface of these cells, and showing differences in heme efflux from the basolateral membrane of cells overexpressing MRP5 or those treated with siRNA against MRP5. Dr. Tamika Samuel, a research assistant professor in our laboratory, is currently establishing assays to measure radiolabelled heme uptake in *Leishmania* and yeast. These assays could theoretically be modified to test heme efflux by MRP5.

Analysis of Mrp5 Knockout Mice

It was surprising to learn that *Mrp5*^{-/-} mice have no overt hematological defects, even when raised on an iron-depleted diet. We hypothesize that, unlike Flvcr1, Mrp5 might play a more specialized role regulating heme homeostasis in these animals. Analysis of *Mrp5*^{-/-} fibroblasts revealed defects in heme transport into the Golgi apparatus, as well as an altered cellular response to EP in bone marrow-derived macrophages, indicating, that at least in certain contexts, Mrp5 is required for normal heme trafficking.

Given the results of our yeast and Golgi-HRP assays, we identified hemoproteins found in the secretory pathway, whose activity could be modulated in the presence or absence of Mrp5. These include the prostaglandin-synthesizing cyclooxygenases (COX1 and COX2) and the neutrophil-specific antimicrobial protein, myeloperoxidase (MPO). We are currently collaborating with Dr. Sandeep Prabhu at The Pennsylvania State University to measure prostaglandin levels and MPO activity in wild-type and *Mrp5*^{-/-} mice. It is of note, that when deleted, neither

COX1 nor MPO has obvious phenotypes in mice (184, 185). COX2-deficient mice exhibit renal abnormalities and early mortality (185).

Significance

In most animals, heme is synthesized via a highly conserved eight-step pathway shared between the mitochondria and the cytosol (186). The pathway concludes in the mitochondrial matrix, where iron is catalytically inserted into a protoporphyrin IX ring to produce heme. Heme must be exported from the mitochondria for incorporation into hemoproteins located in various subcellular compartments (187). However, the process of trafficking unescorted heme to subcellular compartments exposes the cell to heme-associated toxicity. Thus heme levels within cells and within subcellular compartments must be highly regulated by a network of transporters and chaperones.

In this study, we show that *mrp-5* encodes an intestinal heme exporter that plays a vital role in maintaining heme homeostasis in the worm. Loss of maternal and larval *mrp-5* result in embryonic lethality and growth arrest, respectively, and both of these phenotypes can be rescued with dietary heme. Loss of *mrp-5* protects against lethality associated with ingestion of a toxic heme analog, and results in a number of heme deficiency signals that persist even as worms are fed greater than physiological amounts of heme. Data from functional yeast assays, combined with evidence that *mrp-5* is expressed in the intestine and localizes to the basolateral membrane, reveal that MRP-5 is poised to serve as a major valve for regulated release of heme from the intestine.

Additionally, we show that heme transport by MRP5 is conserved among metazoans. Knockdown of Mrp5 in zebrafish embryos results in developmental defects and decreased blood formation. Loss of Mrp5 in mammalian cells leads to decreased heme transport into the secretory pathway as measured by activity of a Golgi-targeted heme-dependent enzyme. Furthermore, macrophages from mice lacking Mrp5 are unable to activate a number of cellular responses when undergoing erythrophagocytosis. Altogether, our results implicate MRP-5 as a key heme transporter in *C. elegans*, and point to an evolutionarily conserved role for MRP-5 in regulating heme homeostasis.

We envisage that cellular heme levels in *C. elegans*, and plausibly vertebrates, are not solely regulated by internal heme content, but also by distally located proteins which signal systemic heme requirements to an inter-tissue heme trafficking network. This prediction is supported by our findings that depletion of either a heme exporter (*mrp-5*) or a heme importer (*hrg-1*) produces similar, overlapping phenotypes in worms and zebrafish *i.e.* that mobilization of heme in and out of tissues is as important as endogenous heme synthesis (40, 41, 43). Although both heme importers and exporters are obviously essential for survival of a heme auxotroph, these proteins also play an important role in vertebrates as demonstrated by developmental and blood defects in zebrafish.

The severity of phenotypes associated with loss of heme synthesis indicates that intracellular heme trafficking pathways are not the primary modes to support the heme requirements of animals. The generation of (a) tissue-specific heme synthesis knockout animals; (b) genetic chimeras using *in vivo* tissue-specific reporters; and (c)

new modalities of live imaging of heme using label-free microscopy at the tissue and subcellular level would be greatly beneficial in determining the capacity for inter- and intra-tissue heme transport. Ultimately, these pathways (including MRP5-mediated heme transport into the secretory pathway or across the plasma membrane) may be relevant under specific conditions of aberrant iron or RBC homeostasis, or during pathogenesis.

While heme transport pathways are of interest from a cell biological perspective, they are also of great interest to human health. Iron deficiency is the most common nutritional disorder in developing and developed countries (168). About 60-80% of the world's population may be iron deficient according to a World Health Organization report published in 2003 (169). Dietary heme is more readily absorbed than dietary iron, as a number of factors cause iron to be less bioavailable in the human gut (170). Knowledge of heme trafficking will aid in understanding and improving the efficiency of iron absorption and transport through the body. This understanding will additionally provide insight into role of heme in human disease, as many pathogens rely on host-derived iron for their virulence (188-190). Worm-specific heme transport pathways will be valuable targets for anthelmintics, because, like *C. elegans*, most parasitic nematodes do not synthesize heme but are dependent on host heme. These helminths, which are developing resistance to current drugs, present an enormous global threat to human health and agriculture and exacerbate global iron deficiency. Thus, characterization of worm and mammalian heme transporters will both illuminate heme transport pathways, and identify therapeutic targets to combat iron-deficiency anemia and helminthic infections.

Appendix I

Worm strains used in this study

Strain Name	Background	Transgene	Source
IQ5051	<i>unc-119 (ed3) III</i>	$P_{mrp-5}::GFP::unc-54$ 3' UTR; <i>unc-119 rescue</i>	This study
IQ5052	<i>unc-119 (ed3) III</i>	$P_{mrp-5}::GFP::mrp-5$ 3' UTR; <i>unc-119 rescue</i>	This study
IQ5151	<i>unc-119 (ed3) III</i>	$P_{mrp-5}::MRP-5-GFP::unc-54$ 3' UTR; <i>unc-119 rescue</i>	This study
IQ5351	<i>unc-119 (ed3) III</i>	$P_{vha-6}::MRP-5-GFP::unc-54$ 3' UTR; <i>unc-119 rescue</i>	This study
VC1599	<i>+/szT1[lon-2(e678)] I;</i> <i>mrp-5(ok2067)/szT1X.</i>	-	CGC
IQ5951	<i>mrp-5 (ok2067) X</i>	-	This study
IQ5051	<i>unc-119 (ed3) III</i>	$P_{mrp-5}::GFP::unc-54$ 3' UTR; <i>unc-119 rescue</i>	This study
IQ6011	N2	$P_{hrg-1}::GFP::unc-54$ 3' UTR; <i>rol-6 marker</i>	(40)
IQ8122	<i>unc-119 (ed3) III</i>	$P_{hrg-2}::HRG-2-YFP::hrg-2$ 3' UTR; <i>unc-119 rescue</i>	(141)
IQ8031	<i>unc-119 (ed3) III</i>	$P_{hrg-3}::GFP::hrg-3$ 3' UTR; <i>unc-119 rescue</i>	(77)
IQ8135	<i>unc-119 (ed3) III</i>	$P_{hrg-3}::HRG-3-mCherry::hrg-3$ 3' UTR; <i>unc-119 rescue</i>	(77)
IQ8136	<i>unc-119 (ed3) III</i>	$P_{hrg-3}::HRG-3:ICS:GFP::hrg-3$ 3' UTR; <i>unc-119 rescue</i>	(77)
VP303	<i>rde-1(ne213) V</i>	$P_{nhx-2}::rde-1$; <i>rol-6 marker</i>	CGC
WM118	<i>rde-1(ne300) V</i>	$P_{myo-3}::HA::RDE-1$; <i>rol-6</i> <i>marker</i>	CGC
NR222	<i>rde-1(ne219) V</i>	$P_{lin-26}::nls-gfp$; $P_{lin-26}::rde-1$; <i>rol-6 marker</i>	CGC

Appendix II

Oligonucleotide primers used in this study

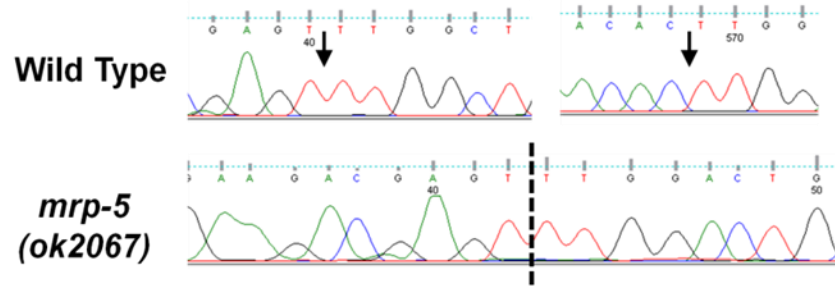
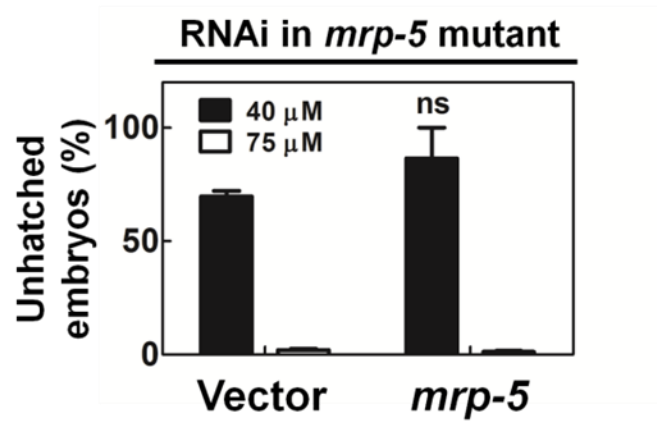
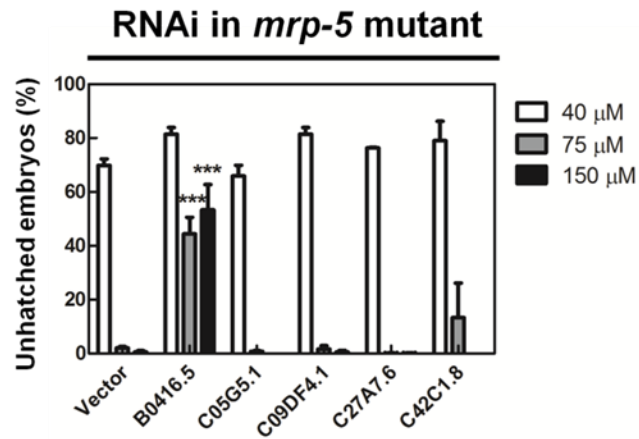
Purpose	Name	Sequence
<i>mrp-5(ok2067)</i> Genotyping	5' Flank (A)	GATGGCTCAAGAAAGGACACG
	5' Internal (B)	TGGTAGCTCCATGAATGACGG
	3' Internal (C)	GGTATTTGTTTCATGCTTCCGTGC
	3' Flank (D)	AGCATGACTGTCAAAAGTGCG
<i>C. elegans</i> qRT-PCR	5' <i>qgpd-2</i>	TGCTCACGAGGGGAGACTAC
	3' <i>qgpd-2</i>	CGGTGGACTCAACGACATAG
	5' <i>qhrp-1</i>	AATGGCAGGATGGTCAGAAAC
	3' <i>qhrp-1</i>	CGATGAATGAAAGGAACGATACG
	5' <i>qmrp-5</i>	CTCTTCTCCTTTGTCACCTACTC
	3' <i>qmrp-5</i>	TTCATCTTCCCATAAACACTTCC
Mouse <i>Mrp5</i> Genotyping	5' <i>Mrp5</i> Genotype	CTAGAGTCTAATCCGTATTGG
	3' <i>Mrp5</i> Genotype	CCCGCAAATACATTCAAACC
	5' Hygromycin Genotype	GCTTTCAGCTTCGATGTAGG
	3' Hygromycin Genotype	CGTCAGGACATTGTTGGAGC
Mouse qRT-PCR	5' <i>mGapdh</i>	CTCCACTCACGGCAAATTCAAC
	3' <i>mGapdh</i>	GTAGACTCCACGACATACTCAGC
	5' <i>mMrp5</i>	GGCTGGACCTCATCAGCATT
	3' <i>mMrp5</i>	GATGCCAGTCTGACGGTGAA
	5' <i>mHrg1</i>	CTTCGTGGGTGCTCTCTTCTC
	3' <i>mHrg1</i>	GACTCTGATGCTGGGTGATGG
	5' <i>mHmox1</i>	TGGTGCAAGAT ACTGCCCT
	3' <i>mHmox1</i>	GTCTGGGATGAGGTAGTGCTGAT

Appendix III

The *mrp-5(ok2067)* allele is an in-frame deletion that results in a dysfunctional protein.

(A) Sequencing chromatogram showing deletion boundaries (arrows) and deleted region (dotted line), respectively, in the wild-type (top) and *mrp-5(ok2067)* (bottom) transcripts after RT-PCR. (B) RNAi of *mrp-5* in *mrp-5(ok2067)* mutant worms causes no added embryonic lethal phenotype. Mutant worms were grown at 500 μ M heme, and their synchronized L1 progeny were grown on vector or *mrp-5(RNAi)* plates and their subsequent progeny were scored for hatching. Error bars represent standard error of the mean; ns, not significant (two-way ANOVA, Bonferroni post-test). (C) RNAi of FLVCR homologs in *mrp-5(ok2067)* background results in no added heme-specific phenotypes. Error bars indicate standard error of the mean. *** $P < 0.001$ when compared to vector control under identical conditions (two-way ANOVA, Bonferroni post-test).

(These experiments were conducted by Simon Beardsley.)

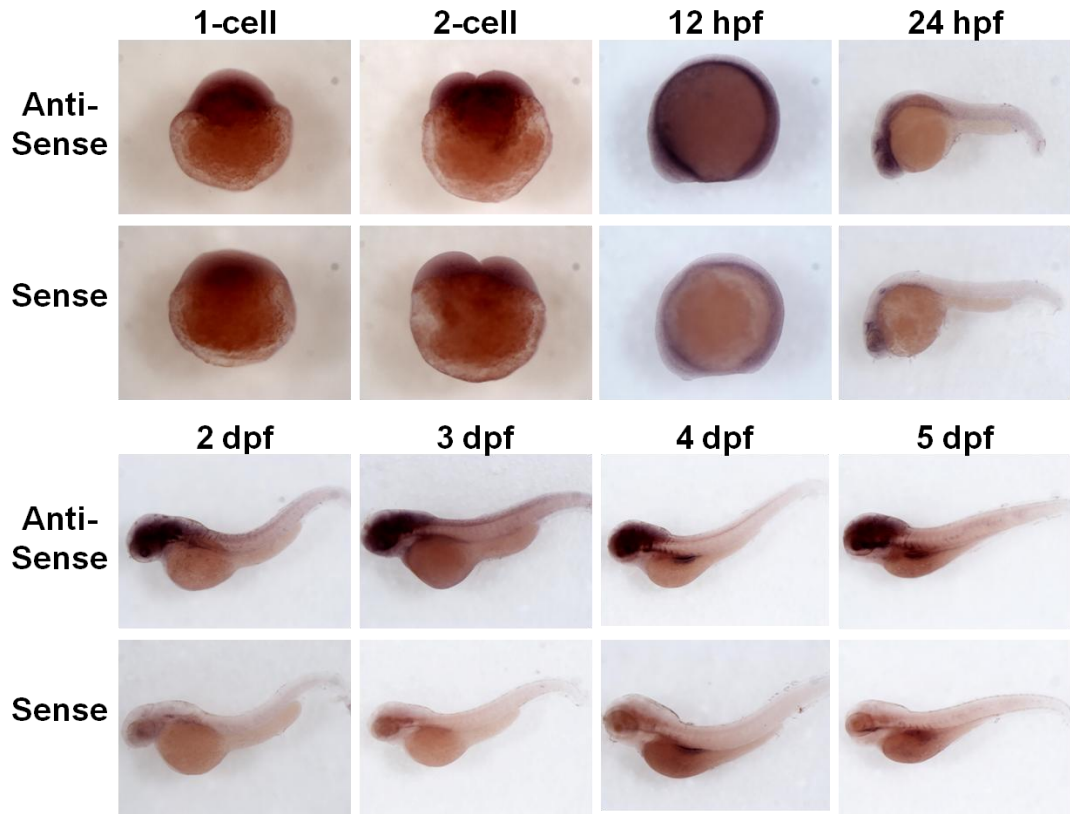
A**B****C**

Appendix IV

***In situ* hybridization reveals tissue specific expression of *mrp5*.**

Zebrafish *mrp5* expression by whole mount *in situ* hybridization using anti-sense probe, at indicated developmental stages. Anterior is to the left. Sense probe image is shown to indicate background staining.

(This experiment was conducted by Jianbing Zhang.)

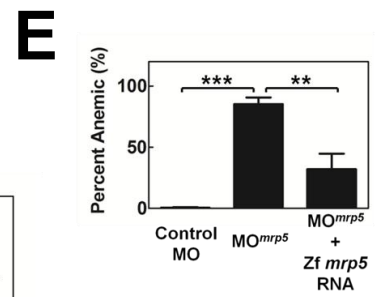
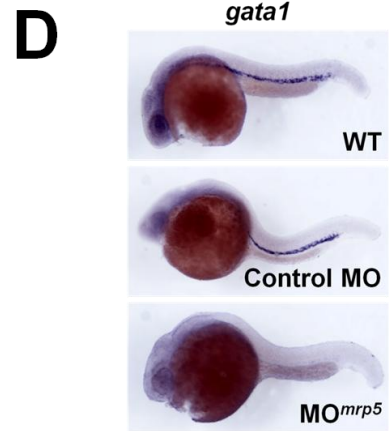
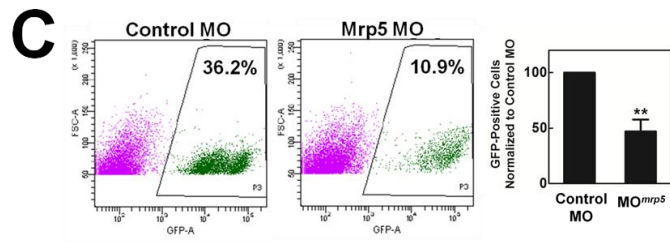
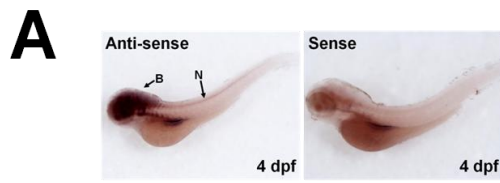


Appendix V

***mrp5* is required for zebrafish erythropoiesis.**

(A) Lateral view of zebrafish *mrp5* expression by whole mount *in situ* hybridization using anti-sense probe, 4 days post-fertilization. Anterior is to the left. Sense probe image is shown to indicate background staining. B, brain, N, neural tube. (B) Knockdown of zebrafish *mrp5* using morpholinos (MO^{mrp5}) results in severe anemia, as indicated by reduced staining of *o*-dianisidine-positive red cells, as indicated by black arrowheads. (C) Transgenic embryos expressing GFP from the globin locus control region (LCR-GFP) were injected with control MO or MO^{mrp5} . LEFT: On day 2 post-fertilization, percent GFP-positive RBCs was analyzed by FACS. X and Y axes measure GFP and forward scatter, respectively; boxed area indicates gate for RBCs. RIGHT: Quantification of morphants shown at left. For MO^{mrp5} injection, n=4. **P<0.01 for MO^{mrp5} morphants compared to control morphants under identical conditions. (One-way ANOVA, Bonferroni post-test.) (D) Lateral view of zebrafish *gata1* expression in wild type, control MO, and MO^{mrp5} morphants by whole mount *in situ* hybridization using anti-sense probe, 24 hpf. Anterior is to the left. (E) Quantification of anemia rescue in zebrafish co-injected with *mrp5* cRNA. ***P<0.001 for MO^{mrp5} morphants compared to control morphants under identical conditions, n=4. **P<0.01 for *mrp5* morphants co-injected with rescue cRNA when compared to *mrp5* morphants with no rescue cRNA under identical conditions, n=3 (One-way ANOVA, Bonferroni post-test.)

(These experiments were performed by Jianbing Zhang.)

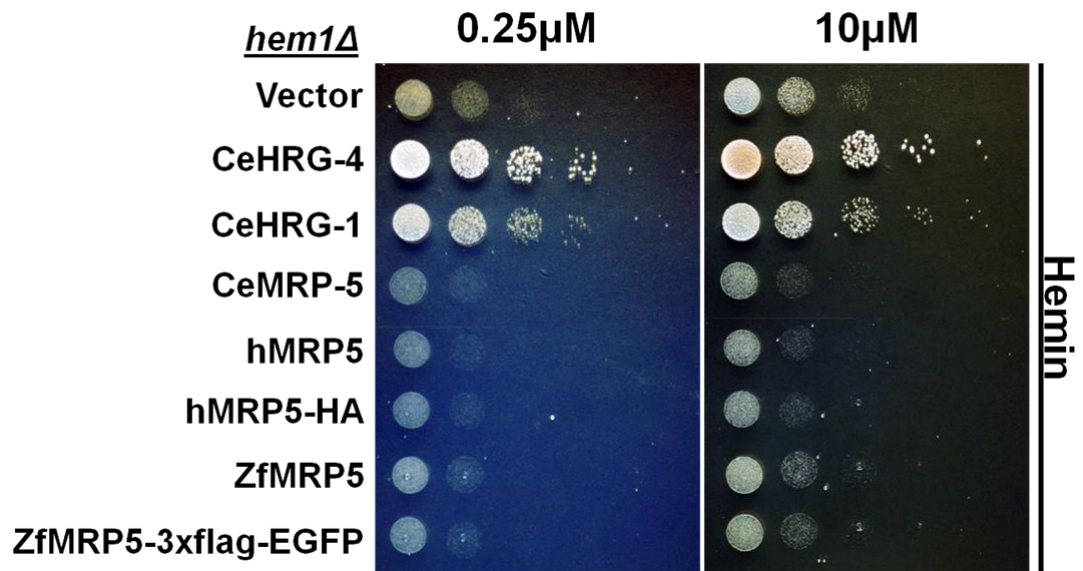


Appendix VI

Zebrafish Mrp5 inhibits heme-dependent growth in *hem1*Δ yeast.

The *hem1*Δ yeast strain was transformed with empty vector, CeHRG-4, CeHRG-1, or MRP5, grown overnight without added heme or ALA and spotted on plates supplemented with 0.25 or 10 μM heme. Plates were incubated at 30°C for 72 h before imaging.

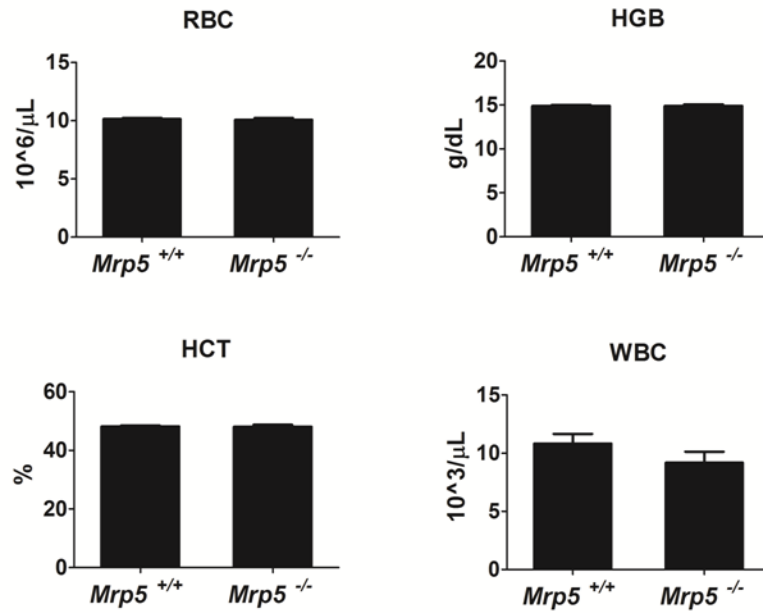
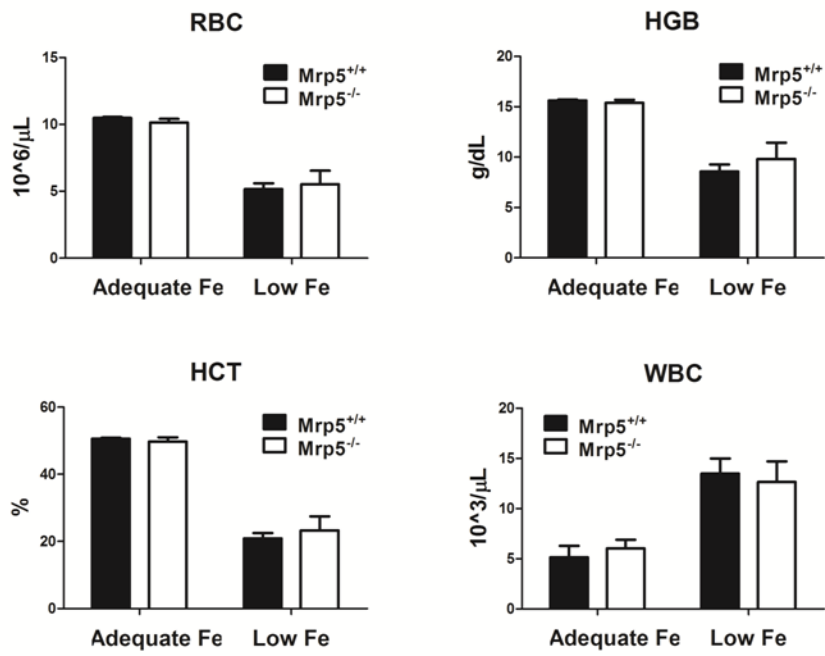
(This experiment was conducted by Jianbing Zhang.)



Appendix VII

Appendix VII. *Mrp5*^{-/-} mice are hematologically normal

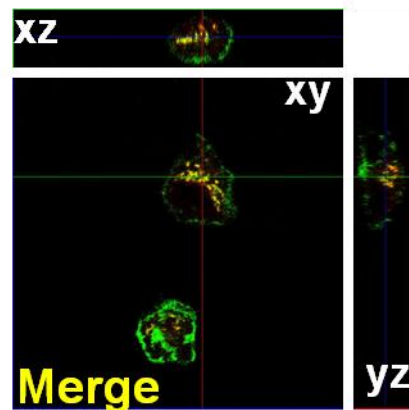
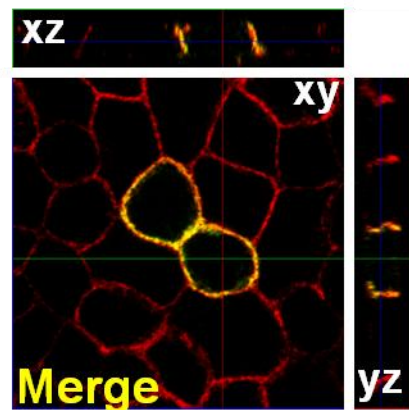
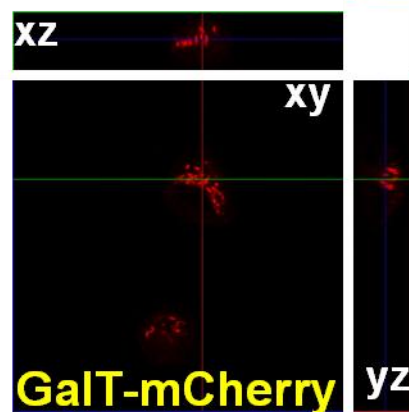
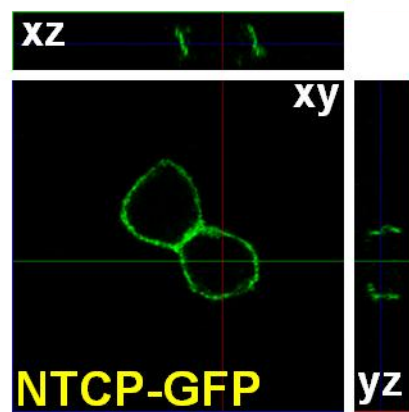
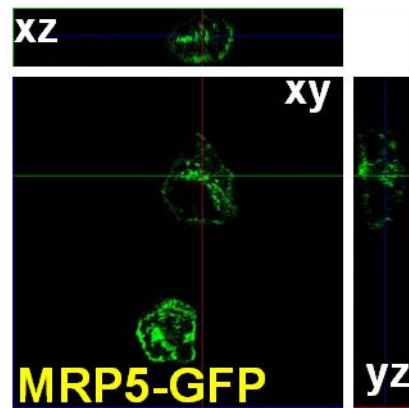
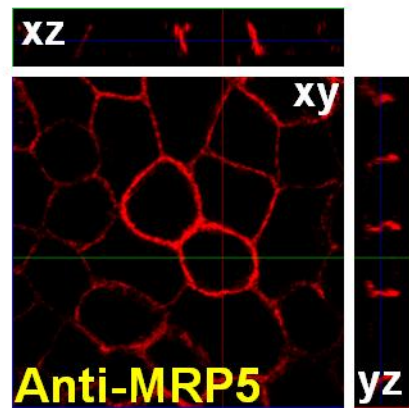
Hematological parameters of **(A)** *Mrp5* wild-type and knockout mice on chow diet [wild-type mice, n=10; knockout mice, n=12] and **(B)** *Mrp5* wild-type and knockout mice weaned onto adequate or low iron diets [wild-type mice on adequate iron, n=4; wild-type mice on low iron, n=5; knockout mice on adequate iron, n=6; knockout mice on low iron, n = 4]. No significant difference was seen between genotypes on chow, adequate iron, or low iron diets. Samples were acquired by retro-orbital bleeding and parameters were analyzed using a ProCyte Dx hematology analyzer (Idexx). RBC, red blood cells, HGB, hemoglobin, HCT, hematocrit, WBC, white blood cells.

A**B**

Appendix VIII

A C-terminal MRP5-GFP fusion is mislocalized to the Golgi apparatus.

GFP-tagged MRP5 mislocalizes to the Golgi in polarized MDCKII cells. MDCKII cells stably expressing human MRP5 were transfected with the basolateral marker NTCP-GFP or the Golgi marker GalT-mCherry and grown to confluency on transwell filters. Polarization of the monolayer was determined by measuring a spike in trans-epithelial electrical resistance. Cells were fixed, stained for MRP5 as necessary, and imaged using confocal microscopy. A single confocal section (xy) is depicted along with composite stacks in side views (yz , xz).



References

1. Green DW, Ingram VM, Perutz MF. The structure of haemoglobin. Sign determination by the isomorphous replacement method. *Proc R Soc Lond A Math Phy.* 1954;225(1162):287-307.
2. Kendrew JC, Bodo G, Dintzis HM, Parrish RG, Wyckoff H, Phillips DC. A three-dimensional model of the myoglobin molecule obtained by x-ray analysis. *Nature.* 1958 Mar 8;181(4610):662-6.
3. Cannon JB, Kuo FS, Pasternack RF, Wong NM, Muller-Eberhard U. Kinetics of the interaction of heme liposomes with heme binding proteins. *Biochemistry.* 1984 Jul 31;23(16):3715-21.
4. Rose MY, Thompson RA, Light WR, Olson JS. Heme transfer between phospholipid membranes and uptake by apohemoglobin. *J Biol Chem.* 1985 Jun 10;260(11):6632-40.
5. Light WR, 3rd, Olson JS. Transmembrane movement of heme. *J Biol Chem.* 1990 Sep 15;265(26):15623-31.
6. Yoda B, Israels LG. Transfer of heme from mitochondria in rat liver cells. *Can J Biochem.* 1972 Jun;50(6):633-7.
7. Vincent SH. Oxidative effects of heme and porphyrins on proteins and lipids. *Semin Hematol.* 1989 Apr;26(2):105-13.
8. Jeney V, Balla J, Yachie A, Varga Z, Vercellotti GM, Eaton JW, et al. Pro-oxidant and cytotoxic effects of circulating heme. *Blood.* 2002;100:879 - 87.

9. Oliveira MF, Timm BL, Machado EA, Miranda K, Attias M, Silva JR, et al. On the pro-oxidant effects of haemozoin. *FEBS Lett.* 2002 Feb 13;512(1-3):139-44.
10. Kumar S, Bandyopadhyay U. Free heme toxicity and its detoxification systems in human. *Toxicol Lett.* 2005;157(3):175-88.
11. Chow JM, Huang GC, Lin HY, Shen SC, Yang LY, Chen YC. Cytotoxic effects of metal protoporphyrins in glioblastoma cells: roles of albumin, reactive oxygen species, and heme oxygenase-1. *Toxicol Lett.* 2008 Mar 15;177(2):97-107.
12. Larsen R, Gouveia Z, Soares MP, Gozzelino R. Heme cytotoxicity and the pathogenesis of immune-mediated inflammatory diseases. *Front Pharmacol.* 2012;3:77.
13. Gonzales DH, Neupert W. Biogenesis of mitochondrial c-type cytochromes. *J Bioenerg Biomembr.* 1990 Dec;22(6):753-68.
14. Hederstedt L. Heme A biosynthesis. *Biochim Biophys Acta.* 2012 Jun;1817(6):920-7.
15. Bowman SE, Bren KL. The chemistry and biochemistry of heme c: functional bases for covalent attachment. *Nat Prod Rep.* 2008 Dec;25(6):1118-30.
16. Kim HJ, Khalimonchuk O, Smith PM, Winge DR. Structure, function, and assembly of heme centers in mitochondrial respiratory complexes. *Biochim Biophys Acta.* 2012 Sep;1823(9):1604-16.
17. Smith PM, Fox JL, Winge DR. Biogenesis of the cytochrome bc(1) complex and role of assembly factors. *Biochim Biophys Acta.* 2012 Feb;1817(2):276-86.

18. Soto IC, Fontanesi F, Liu J, Barrientos A. Biogenesis and assembly of eukaryotic cytochrome c oxidase catalytic core. *Biochim Biophys Acta*. 2012 Jun;1817(6):883-97.
19. Lemarie A, Grimm S. Mutations in the heme b-binding residue of SDHC inhibit assembly of respiratory chain complex II in mammalian cells. *Mitochondrion*. 2009 Jul;9(4):254-60.
20. Xia D, Yu CA, Kim H, Xia JZ, Kachurin AM, Zhang L, et al. Crystal structure of the cytochrome bc₁ complex from bovine heart mitochondria. *Science*. 1997 Jul 4;277(5322):60-6.
21. Iwata S, Lee JW, Okada K, Lee JK, Iwata M, Rasmussen B, et al. Complete structure of the 11-subunit bovine mitochondrial cytochrome bc₁ complex. *Science*. 1998 Jul 3;281(5373):64-71.
22. Lange C, Hunte C. Crystal structure of the yeast cytochrome bc₁ complex with its bound substrate cytochrome c. *Proc Natl Acad Sci U S A*. 2002 Mar 5;99(5):2800-5.
23. Zhang Z, Huang L, Shulmeister VM, Chi YI, Kim KK, Hung LW, et al. Electron transfer by domain movement in cytochrome bc₁. *Nature*. 1998 Apr 16;392(6677):677-84.
24. Brasseur G, Saribas AS, Daldal F. A compilation of mutations located in the cytochrome b subunit of the bacterial and mitochondrial bc₁ complex. *Biochim Biophys Acta*. 1996 Jul 18;1275(1-2):61-9.

25. Bernard DG, Gabilly ST, Dujardin G, Merchant S, Hamel PP. Overlapping specificities of the mitochondrial cytochrome c and c1 heme lyases. *J Biol Chem.* 2003 Dec 12;278(50):49732-42.
26. Khalimonchuk O, Bestwick M, Meunier B, Watts TC, Winge DR. Formation of the redox cofactor centers during Cox1 maturation in yeast cytochrome oxidase. *Mol Cell Biol.* 2010 Feb;30(4):1004-17.
27. Simpson ER, Boyd GS. The cholesterol side-chain cleavage system of bovine adrenal cortex. *Eur J Biochem.* 1967 Oct;2(3):275-85.
28. Strushkevich N, MacKenzie F, Cherkesova T, Grabovec I, Usanov S, Park HW. Structural basis for pregnenolone biosynthesis by the mitochondrial monooxygenase system. *Proc Natl Acad Sci U S A.* 2011 Jun 21;108(25):10139-43.
29. Mast N, Annalora AJ, Lodowski DT, Palczewski K, Stout CD, Pikuleva IA. Structural basis for three-step sequential catalysis by the cholesterol side chain cleavage enzyme CYP11A1. *J Biol Chem.* 2011 Feb 18;286(7):5607-13.
30. Brown SB. Stereospecific haem cleavage. A model for the formation of bile-pigment isomers in vivo and in vitro. *Biochem J.* 1976 Oct 1;159(1):23-7.
31. Santucci R, Ascoli F, La Mar GN, Parish DW, Smith KM. Horse heart myoglobin reconstituted with a symmetrical heme. A circular dichroism study. *Biophys Chem.* 1990 Aug 31;37(1-3):251-5.
32. Black SD. Membrane topology of the mammalian P450 cytochromes. *FASEB J.* 1992 Jan 6;6(2):680-5.

33. Avadhani NG, Sangar MC, Bansal S, Bajpai P. Bimodal targeting of cytochrome P450s to endoplasmic reticulum and mitochondria: the concept of chimeric signals. *FEBS J.* 2011 Nov;278(22):4218-29.
34. Quigley JG, Yang Z, Worthington MT, Phillips JD, Sabo KM, Sabath DE, et al. Identification of a human heme exporter that is essential for erythropoiesis. *Cell.* 2004 Sep 17;118(6):757-66.
35. Keel SB, Doty RT, Yang Z, Quigley JG, Chen J, Knoblauch S, et al. A heme export protein is required for red blood cell differentiation and iron homeostasis. *Science.* 2008 Feb 8;319(5864):825-8.
36. Chiabrando D, Marro S, Mercurio S, Giorgi C, Petrillo S, Vinchi F, et al. The mitochondrial heme exporter FLVCR1b mediates erythroid differentiation. *J Clin Invest.* 2012 Dec 3;122(12):4569-79.
37. Iwahara S-I, Satoh H, Song D-X, Webb J, Burlingame AL, Nagae Y, et al. Purification, characterization, and cloning of a heme-binding protein (23 kDa) in rat liver cytosol. *Biochemistry.* 1995;34(41):13398-406.
38. Taketani S, Adachi Y, Kohno H, Ikehara S, Tokunaga R, Ishii T. Molecular Characterization of a Newly Identified Heme-binding Protein Induced during Differentiation of murine Erythroleukemia Cells. *J Biol Chem.* 1998 November 20, 1998;273(47):31388-94.
39. Zylka MJ, Reppert SM. Discovery of a putative heme-binding protein family (SOUL/HBP) by two-tissue suppression subtractive hybridization and database searches. *Mol Brain Res.* 1999;74(1-2):175-81.

40. Rajagopal A, Rao AU, Amigo J, Tian M, Upadhyay SK, Hall C, et al. Haem homeostasis is regulated by the conserved and concerted functions of HRG-1 proteins. *Nature*. 2008 Jun 19;453(7198):1127-31.
41. Yuan X, Protchenko O, Philpott CC, Hamza I. Topologically conserved residues direct heme transport in HRG-1-related proteins. *J Biol Chem*. 2012 Feb 10;287(7):4914-24.
42. Huynh C, Yuan X, Miguel DC, Renberg RL, Protchenko O, Philpott CC, et al. Heme uptake by *Leishmania amazonensis* is mediated by the transmembrane protein LHR1. *PLoS Pathog*. 2012;8(7):e1002795.
43. White C, Yuan X, Schmidt PJ, Bresciani E, Samuel TK, Campagna D, et al. HRG1 is essential for heme transport from the phagolysosome of macrophages during erythrophagocytosis. *Cell Metab*. 2013 Feb 5;17(2):261-70.
44. O'Callaghan KM, Ayllon V, O'Keefe J, Wang Y, Cox OT, Loughran G, et al. Heme-binding protein HRG-1 is induced by insulin-like growth factor I and associates with the vacuolar H⁺-ATPase to control endosomal pH and receptor trafficking. *J Biol Chem*. 2010 Jan 1;285(1):381-91.
45. Fogarty FM, O'Keefe J, Zhadanov A, Papkovsky D, Ayllon V, O'Connor R. HRG-1 enhances cancer cell invasive potential and couples glucose metabolism to cytosolic/extracellular pH gradient regulation by the vacuolar-H ATPase. *Oncogene*. 2013 Oct 21.
46. Campbell MR, Karaca M, Adamski KN, Chorley BN, Wang X, Bell DA. Novel hematopoietic target genes in the NRF2-mediated transcriptional pathway. *Oxid Med Cell Longev*. 2013;2013:120305.

47. Delaby C, Rondeau C, Pouzet C, Willemetz A, Pilard N, Desjardins M, et al. Subcellular localization of iron and heme metabolism related proteins at early stages of erythrophagocytosis. *PLoS One*. 2012;7(7):e42199.
48. De Matteis MA, Luini A. Exiting the Golgi complex. *Nat Rev Mol Cell Biol*. 2008 Apr;9(4):273-84.
49. Klebanoff SJ, Kettle AJ, Rosen H, Winterbourn CC, Nauseef WM. Myeloperoxidase: a front-line defender against phagocytosed microorganisms. *J Leukoc Biol*. 2013 Feb;93(2):185-98.
50. Hansson M, Olsson I, Nauseef WM. Biosynthesis, processing, and sorting of human myeloperoxidase. *Arch Biochem Biophys*. 2006 Jan 15;445(2):214-24.
51. Nauseef WM, McCormick S, Yi H. Roles of heme insertion and the mannose-6-phosphate receptor in processing of the human myeloid lysosomal enzyme, myeloperoxidase. *Blood*. 1992 November 15, 1992;80(10):2622-33.
52. Nauseef WM, Brigham S, Cogley M. Hereditary myeloperoxidase deficiency due to a missense mutation of arginine 569 to tryptophan. *J Biol Chem*. 1994 Jan 14;269(2):1212-6.
53. DeLeo FR, Goedken M, McCormick SJ, Nauseef WM. A novel form of hereditary myeloperoxidase deficiency linked to endoplasmic reticulum/proteasome degradation. *J Clin Invest*. 1998 Jun 15;101(12):2900-9.
54. Ruby JR, Dyer RF, Skalko RG. Continuities between mitochondria and endoplasmic reticulum in the mammalian ovary. *Z Zellforsch Mikrosk Anat*. 1969;97(1):30-7.

55. Lewis JA, Tata JR. A rapidly sedimenting fraction of rat liver endoplasmic reticulum. *J Cell Sci.* 1973 Sep;13(2):447-59.
56. Vance JE. Phospholipid synthesis in a membrane fraction associated with mitochondria. *J Biol Chem.* 1990 May 5;265(13):7248-56.
57. Kornmann B, Currie E, Collins SR, Schuldiner M, Nunnari J, Weissman JS, et al. An ER-Mitochondria Tethering Complex Revealed by a Synthetic Biology Screen. *Science.* 2009 June 25, 2009:1175088.
58. Kornmann B, Osman C, Walter P. The conserved GTPase Gem1 regulates endoplasmic reticulum-mitochondria connections. *Proc Natl Acad Sci U S A.* 2011 Aug 23;108(34):14151-6.
59. Michel AH, Kornmann B. The ERMES complex and ER-mitochondria connections. *Biochem Soc Trans.* 2012 Apr;40(2):445-50.
60. Zhang A, Williamson CD, Wong DS, Bullough MD, Brown KJ, Hathout Y, et al. Quantitative proteomic analyses of human cytomegalovirus-induced restructuring of endoplasmic reticulum-mitochondrial contacts at late times of infection. *Mol Cell Proteomics.* 2011 Oct;10(10):M111 009936.
61. Poston CN, Duong E, Cao Y, Bazemore-Walker CR. Proteomic analysis of lipid raft-enriched membranes isolated from internal organelles. *Biochem Biophys Res Commun.* 2011 Nov 18;415(2):355-60.
62. Schumann U, Subramani S. Special delivery from mitochondria to peroxisomes. *Trends Cell Biol.* 2008;18(6):253-6.

63. Neuspiel M, Schauss AC, Braschi E, Zunino R, Rippstein P, Rachubinski RA, et al. Cargo-Selected Transport from the Mitochondria to Peroxisomes Is Mediated by Vesicular Carriers. *Curr Biol.* 2008;18(2):102-8.
64. Soubannier V, Rippstein P, Kaufman BA, Shoubridge EA, McBride HM. Reconstitution of mitochondria derived vesicle formation demonstrates selective enrichment of oxidized cargo. *PLoS One.* 2012;7(12):e52830.
65. McLelland GL, Soubannier V, Chen CX, McBride HM, Fon EA. Parkin and PINK1 function in a vesicular trafficking pathway regulating mitochondrial quality control. *EMBO J.* 2014 Jan 20.
66. Knutson M, Wessling-Resnick M. Iron metabolism in the reticuloendothelial system. *Crit Rev Biochem Mol Biol.* 2003;38(1):61-88.
67. Bratosin D, Mazurier J, Tissier JP, Estaquier J, Huart JJ, Ameisen JC, et al. Cellular and molecular mechanisms of senescent erythrocyte phagocytosis by macrophages. A review. *Biochimie.* 1998 Feb;80(2):173-95.
68. Poss KD, Tonegawa S. Heme oxygenase 1 is required for mammalian iron reutilization. *Proc Natl Acad Sci USA.* 1997 September 30, 1997;94(20):10919-24.
69. Kovtunovych G, Eckhaus MA, Ghosh MC, Ollivierre-Wilson H, Rouault TA. Dysfunction of the heme recycling system in heme oxygenase 1-deficient mice: effects on macrophage viability and tissue iron distribution. *Blood.* 2010 Dec 23;116(26):6054-62.
70. Beaumont C, Canonne-Hergaux F. [Erythrophagocytosis and recycling of heme iron in normal and pathological conditions; regulation by hepcidin]. *Transfus Clin Biol.* 2005 Jun;12(2):123-30.

71. Gottlieb Y, Truman M, Cohen LA, Leichtmann-Bardoogo Y, Meyron-Holtz EG. Endoplasmic reticulum anchored heme-oxygenase 1 faces the cytosol. *Haematologica*. 2012 Oct;97(10):1489-93.
72. Liu Y, Ortiz de Montellano PR. Reaction intermediates and single turnover rate constants for the oxidation of heme by human heme oxygenase-1. *J Biol Chem*. 2000 Feb 25;275(8):5297-307.
73. Reed JR, Huber WJ, 3rd, Backes WL. Human heme oxygenase-1 efficiently catabolizes heme in the absence of biliverdin reductase. *Drug Metab Dispos*. 2010 Nov;38(11):2060-6.
74. Kambe T, Weaver BP, Andrews GK. The genetics of essential metal homeostasis during development. *Genesis*. 2008 Apr;46(4):214-28.
75. Magness ST, Maeda N, Brenner DA. An exon 10 deletion in the mouse ferrochelatase gene has a dominant-negative effect and causes mild protoporphyria. *Blood*. 2002 Aug 15;100(4):1470-7.
76. Phillips JD, Bergonia HA, Reilly CA, Franklin MR, Kushner JP. A porphomethene inhibitor of uroporphyrinogen decarboxylase causes porphyria cutanea tarda. *Proc Natl Acad Sci U S A*. 2007 Mar 20;104(12):5079-84.
77. Chen C, Samuel TK, Sinclair J, Dailey HA, Hamza I. An intercellular heme-trafficking protein delivers maternal heme to the embryo during development in *C. elegans*. *Cell*. 2011 May 27;145(5):720-31.
78. Syberg F, Suveyzdis Y, Kotting C, Gerwert K, Hofmann E. Time-resolved Fourier transform infrared spectroscopy of the nucleotide-binding domain from the

ATP-binding Cassette transporter MsbA: ATP hydrolysis is the rate-limiting step in the catalytic cycle. *J Biol Chem*. 2012 Jul 6;287(28):23923-31.

79. Vasiliou V, Vasiliou K, Nebert DW. Human ATP-binding cassette (ABC) transporter family. *Hum Genomics*. 2009 Apr;3(3):281-90.

80. Licht A, Schneider E. ATP binding cassette systems: structures, mechanisms, and functions. *centeurjbiol*. 2011 2011/10/01;6(5):785-801.

81. Jones PM, George AM. Mechanism of the ABC transporter ATPase domains: catalytic models and the biochemical and biophysical record. *Crit Rev Biochem Mol Biol*. 2013 Jan-Feb;48(1):39-50.

82. Ehrenman K, Sehgal A, Lige B, Stedman TT, Joiner KA, Coppens I. Novel roles for ATP-binding cassette G transporters in lipid redistribution in *Toxoplasma*. *Mol Microbiol*. 2010 Jun 1;76(5):1232-49.

83. Wilcox LJ, Balderes DA, Wharton B, Tinkelenberg AH, Rao G, Sturley SL. Transcriptional profiling identifies two members of the ATP-binding cassette transporter superfamily required for sterol uptake in yeast. *J Biol Chem*. 2002 Sep 6;277(36):32466-72.

84. Lee M, Choi Y, Burla B, Kim YY, Jeon B, Maeshima M, et al. The ABC transporter AtABCB14 is a malate importer and modulates stomatal response to CO₂. *Nat Cell Biol*. 2008 Oct;10(10):1217-23.

85. Kang J, Hwang JU, Lee M, Kim YY, Assmann SM, Martinoia E, et al. PDR-type ABC transporter mediates cellular uptake of the phytohormone abscisic acid. *Proc Natl Acad Sci U S A*. 2010 Feb 2;107(5):2355-60.

86. Shitan N, Bazin I, Dan K, Obata K, Kigawa K, Ueda K, et al. Involvement of CjMDR1, a plant multidrug-resistance-type ATP-binding cassette protein, in alkaloid transport in *Coptis japonica*. *Proc Natl Acad Sci U S A*. 2003 Jan 21;100(2):751-6.
87. Jardetzky O. Simple allosteric model for membrane pumps. *Nature*. 1966 Aug 27;211(5052):969-70.
88. Janas E, Hofacker M, Chen M, Gompf S, van der Does C, Tampe R. The ATP hydrolysis cycle of the nucleotide-binding domain of the mitochondrial ATP-binding cassette transporter Mdl1p. *J Biol Chem*. 2003 Jul 18;278(29):26862-9.
89. Chen J, Lu G, Lin J, Davidson AL, Quioco FA. A tweezers-like motion of the ATP-binding cassette dimer in an ABC transport cycle. *Mol Cell*. 2003 Sep;12(3):651-61.
90. Al-Shawi MK, Polar MK, Omote H, Figler RA. Transition state analysis of the coupling of drug transport to ATP hydrolysis by P-glycoprotein. *J Biol Chem*. 2003 Dec 26;278(52):52629-40.
91. Shapiro AB, Ling V. Positively cooperative sites for drug transport by P-glycoprotein with distinct drug specificities. *Eur J Biochem*. 1997 Nov 15;250(1):130-7.
92. Decottignies A, Kolaczowski M, Balzi E, Goffeau A. Solubilization and characterization of the overexpressed PDR5 multidrug resistance nucleotide triphosphatase of yeast. *J Biol Chem*. 1994 Apr 29;269(17):12797-803.
93. Gadsby DC, Vergani P, Csanady L. The ABC protein turned chloride channel whose failure causes cystic fibrosis. *Nature*. 2006 Mar 23;440(7083):477-83.

94. Chen M, Abele R, Tampe R. Functional non-equivalence of ATP-binding cassette signature motifs in the transporter associated with antigen processing (TAP). *J Biol Chem*. 2004 Oct 29;279(44):46073-81.
95. Egner R, Rosenthal FE, Kralli A, Sanglard D, Kuchler K. Genetic separation of FK506 susceptibility and drug transport in the yeast Pdr5 ATP-binding cassette multidrug resistance transporter. *Mol Biol Cell*. 1998 Feb;9(2):523-43.
96. Tutulan-Cunita AC, Mikoshi M, Mizunuma M, Hirata D, Miyakawa T. Mutational analysis of the yeast multidrug resistance ABC transporter Pdr5p with altered drug specificity. *Genes Cells*. 2005 May;10(5):409-20.
97. Gustot A, Smriti, Ruyschaert JM, McHaourab H, Govaerts C. Lipid composition regulates the orientation of transmembrane helices in HorA, an ABC multidrug transporter. *J Biol Chem*. 2010 May 7;285(19):14144-51.
98. Aller SG, Yu J, Ward A, Weng Y, Chittaboina S, Zhuo R, et al. Structure of P-glycoprotein reveals a molecular basis for poly-specific drug binding. *Science*. 2009 Mar 27;323(5922):1718-22.
99. Schumacher MA, Miller MC, Brennan RG. Structural mechanism of the simultaneous binding of two drugs to a multidrug-binding protein. *EMBO J*. 2004 Aug 4;23(15):2923-30.
100. Dawson RJ, Locher KP. Structure of a bacterial multidrug ABC transporter. *Nature*. 2006 Sep 14;443(7108):180-5.
101. Currier SJ, Kane SE, Willingham MC, Cardarelli CO, Pastan I, Gottesman MM. Identification of residues in the first cytoplasmic loop of P-glycoprotein

involved in the function of chimeric human MDR1-MDR2 transporters. *J Biol Chem.* 1992 Dec 15;267(35):25153-9.

102. Cotten JF, Ostedgaard LS, Carson MR, Welsh MJ. Effect of cystic fibrosis-associated mutations in the fourth intracellular loop of cystic fibrosis transmembrane conductance regulator. *J Biol Chem.* 1996 Aug 30;271(35):21279-84.

103. Jin MS, Oldham ML, Zhang Q, Chen J. Crystal structure of the multidrug transporter P-glycoprotein from *Caenorhabditis elegans*. *Nature.* 2012 Oct 25;490(7421):566-9.

104. Allikmets R, Gerrard B, Hutchinson A, Dean M. Characterization of the human ABC superfamily: isolation and mapping of 21 new genes using the expressed sequence tags database. *Hum Mol Genet.* 1996 Oct;5(10):1649-55.

105. Kool M, de Haas M, Scheffer GL, Scheper RJ, van Eijk MJ, Juijn JA, et al. Analysis of expression of cMOAT (MRP2), MRP3, MRP4, and MRP5, homologues of the multidrug resistance-associated protein gene (MRP1), in human cancer cell lines. *Cancer Res.* 1997 Aug 15;57(16):3537-47.

106. Suzuki T, Nishio K, Sasaki H, Kurokawa H, Saito-Ohara F, Ikeuchi T, et al. cDNA cloning of a short type of multidrug resistance protein homologue, SMRP, from a human lung cancer cell line. *Biochem Biophys Res Commun.* 1997 Sep 29;238(3):790-4.

107. Meyer Zu Schwabedissen HE, Grube M, Heydrich B, Linnemann K, Fusch C, Kroemer HK, et al. Expression, localization, and function of MRP5 (ABCC5), a transporter for cyclic nucleotides, in human placenta and cultured human

trophoblasts: effects of gestational age and cellular differentiation. *Am J Pathol.* 2005 Jan;166(1):39-48.

108. Nies AT, Jedlitschky G, König J, Herold-Mende C, Steiner HH, Schmitt HP, et al. Expression and immunolocalization of the multidrug resistance proteins, MRP1-MRP6 (ABCC1-ABCC6), in human brain. *Neuroscience.* 2004;129(2):349-60.

109. Torky AR, Stehfest E, Viehweger K, Taege C, Foth H. Immuno-histochemical detection of MRPs in human lung cells in culture. *Toxicology.* 2005 Feb 28;207(3):437-50.

110. Wijnholds J, Mol CA, van Deemter L, de Haas M, Scheffer GL, Baas F, et al. Multidrug-resistance protein 5 is a multispecific organic anion transporter able to transport nucleotide analogs. *Proc Natl Acad Sci U S A.* 2000 Jun 20;97(13):7476-81.

111. Jedlitschky G, Burchell B, Keppler D. The multidrug resistance protein 5 functions as an ATP-dependent export pump for cyclic nucleotides. *J Biol Chem.* 2000 Sep 29;275(39):30069-74.

112. Nies AT, Rius M, Keppler D. Multidrug Resistance Proteins of the ABCC Subfamily. *Drug Transporters: John Wiley & Sons, Inc.;* 2006. p. 263-318.

113. McAleer MA, Breen MA, White NL, Matthews N. pABC11 (also known as MOAT-C and MRP5), a member of the ABC family of proteins, has anion transporter activity but does not confer multidrug resistance when overexpressed in human embryonic kidney 293 cells. *J Biol Chem.* 1999 Aug 13;274(33):23541-8.

114. Borst P, de Wolf C, van de Wetering K. Multidrug resistance-associated proteins 3, 4, and 5. *Pflugers Arch.* 2007 Feb;453(5):661-73.

115. Guo Y, Kock K, Ritter CA, Chen ZS, Grube M, Jedlitschky G, et al. Expression of ABCC-type nucleotide exporters in blasts of adult acute myeloid leukemia: relation to long-term survival. *Clin Cancer Res.* 2009 Mar 1;15(5):1762-9.
116. Alexiou GA, Goussia A, Ntoulia A, Zagorianakou P, Malamou-Mitsi V, Voulgaris S, et al. Immunohistochemical study of MRP5 expression in meningiomas. *Cancer Chemother Pharmacol.* 2013 Mar;71(3):825-8.
117. Alexiou GA, Goussia A, Voulgaris S, Fotopoulos AD, Fotakopoulos G, Ntoulia A, et al. Prognostic significance of MRP5 immunohistochemical expression in glioblastoma. *Cancer Chemother Pharmacol.* 2012 May;69(5):1387-91.
118. Hamza I, Dailey HA. One ring to rule them all: trafficking of heme and heme synthesis intermediates in the metazoans. *Biochim Biophys Acta.* 2012 Sep;1823(9):1617-32.
119. Severance S, Hamza I. Trafficking of heme and porphyrins in metazoa. *Chem Rev.* 2009 Oct;109(10):4596-616.
120. Rao AU, Carta LK, Lesuisse E, Hamza I. Lack of heme synthesis in a free-living eukaryote. *Proc Natl Acad Sci U S A.* 2005 Mar 22;102(12):4270-5.
121. Nass R, Hamza I. The nematode *C. elegans* as an animal model to explore toxicology in vivo: solid and axenic growth culture conditions and compound exposure parameters. In: Maines MD, Costa LG, Hodgson E, Reed DJ, Sipes IG, editors. *Current Protocols in Toxicology*. New York: John Wiley & Sons, Inc.; 2007. p. 1.9.1-9.17.
122. Epstein HF, Shakes DC, editors. *Caenorhabditis elegans: Modern Biological Analysis of an Organism*. San Diego: Academic Press; 1995.

123. Praitis V, Casey E, Collar D, Austin J. Creation of low-copy integrated transgenic lines in *Caenorhabditis elegans*. *Genetics*. 2001 Mar;157(3):1217-26.
124. Kamath RS, Fraser AG, Dong Y, Poulin G, Durbin R, Gotta M, et al. Systematic functional analysis of the *Caenorhabditis elegans* genome using RNAi. *Nature*. 2003 Jan 16;421(6920):231-7.
125. Reboul J, Vaglio P, Rual JF, Lamesch P, Martinez M, Armstrong CM, et al. *C. elegans* ORFeome version 1.1: experimental verification of the genome annotation and resource for proteome-scale protein expression. *Nat Genet*. 2003 May;34(1):35-41.
126. Protchenko O, Shakoury-Elizeh M, Keane P, Storey J, Androphy R, Philpott CC. Role of PUG1 in inducible porphyrin and heme transport in *Saccharomyces cerevisiae*. *Eukaryot Cell*. 2008 May;7(5):859-71.
127. Kaplan J, McVey Ward D, Crisp RJ, Philpott CC. Iron-dependent metabolic remodeling in *S. cerevisiae*. *Biochim Biophys Acta*. 2006 Jul;1763(7):646-51.
128. Ito H, Fukuda Y, Murata K, Kimura A. Transformation of intact yeast cells treated with alkali cations. *J Bacteriol*. 1983 Jan;153(1):163-8.
129. Adams A GD, Kaiser CA, Stearns T. *Methods in yeast genetics*: Cold Spring Harbor Press; 1997.
130. de Wolf CJ, Yamaguchi H, van der Heijden I, Wielinga PR, Hundscheid SL, Ono N, et al. cGMP transport by vesicles from human and mouse erythrocytes. *FEBS J*. 2007 Jan;274(2):439-50.
131. Spector D L GRD, Leinwand L A, editor. *Cells: A Laboratory Manual* Cold Spring Harbor Lab. Press, Plainview, NY; 1998.

132. Williams DA, Rosenblatt MF, Beier DR, Cone RD. Generation of murine stromal cell lines supporting hematopoietic stem cell proliferation by use of recombinant retrovirus vectors encoding simian virus 40 large T antigen. *Mol Cell Biol.* 1988 Sep;8(9):3864-71.
133. Marim FM, Silveira TN, Lima DS, Jr., Zamboni DS. A method for generation of bone marrow-derived macrophages from cryopreserved mouse bone marrow cells. *PLoS One.* 2010;5(12):e15263.
134. Englen MD, Valdez YE, Lehnert NM, Lehnert BE. Granulocyte/macrophage colony-stimulating factor is expressed and secreted in cultures of murine L929 cells. *J Immunol Methods.* 1995 Aug 18;184(2):281-3.
135. Sassa S, Nagai T. The role of heme in gene expression. *Int J Hematol.* 1996 Apr;63(3):167-78.
136. Burke D, Dawson D, Stearns T. *Methods in Yeast Genetics: A Cold Spring Harbor Laboratory Course Manual.* Cold Spring Harbor: Cold Spring Harbor Laboratory Press; 2000.
137. Tamura K, Peterson D, Peterson N, Stecher G, Nei M, Kumar S. MEGA5: molecular evolutionary genetics analysis using maximum likelihood, evolutionary distance, and maximum parsimony methods. *Mol Biol Evol.* 2011 Oct;28(10):2731-9.
138. Larkin MA, Blackshields G, Brown NP, Chenna R, McGettigan PA, McWilliam H, et al. Clustal W and Clustal X version 2.0. *Bioinformatics.* 2007 Nov 1;23(21):2947-8.
139. Johns SJ. TOPO2, Transmembrane protein display software.

140. Krogh A, Larsson B, von Heijne G, Sonnhammer EL. Predicting transmembrane protein topology with a hidden Markov model: application to complete genomes. *J Mol Biol.* 2001 Jan 19;305(3):567-80.
141. Chen C, Samuel TK, Krause M, Dailey HA, Hamza I. Heme utilization in the *Caenorhabditis elegans* hypodermal cells is facilitated by heme-responsive gene-2. *J Biol Chem.* 2012 Mar 16;287(12):9601-12.
142. Severance S, Rajagopal A, Rao AU, Cerqueira GC, Mitreva M, El-Sayed NM, et al. Genome-wide analysis reveals novel genes essential for heme homeostasis in *Caenorhabditis elegans*. *PLoS Genet.* 2010;6(7):e1001044.
143. Sinclair J, Hamza I. A novel heme response element mediates transcriptional regulation in *Caenorhabditis elegans*. *J Biol Chem.* 2010 Oct 11.
144. Lipovich L, Hughes AL, King MC, Abkowitz JL, Quigley JG. Genomic structure and evolutionary context of the human feline leukemia virus subgroup C receptor (hFLVCR) gene: evidence for block duplications and de novo gene formation within duplicons of the hFLVCR locus. *Gene.* 2002 Mar 20;286(2):203-13.
145. Borst P, Evers R, Kool M, Wijnholds J. A family of drug transporters: the multidrug resistance-associated proteins. *J Natl Cancer Inst.* 2000 Aug 16;92(16):1295-302.
146. Edgley ML, Baillie DL, Riddle DL, Rose AM. Genetic balancers. *WormBook.* 2006:1-32.
147. McGhee JD, Sleumer MC, Bilenky M, Wong K, McKay SJ, Goszczynski B, et al. The ELT-2 GATA-factor and the global regulation of transcription in the *C. elegans* intestine. *Dev Biol.* 2007 Feb 15;302(2):627-45.

148. Contrino S, Smith RN, Butano D, Carr A, Hu F, Lyne R, et al. modMine: flexible access to modENCODE data. *Nucleic Acids Res.* 2012 Jan;40(Database issue):D1082-8.
149. Oka T, Toyomura T, Honjo K, Wada Y, Futai M. Four subunit a isoforms of *Caenorhabditis elegans* vacuolar H⁺-ATPase. Cell-specific expression during development. *J Biol Chem.* 2001 Aug 31;276(35):33079-85.
150. Chen B, Jiang Y, Zeng S, Yan J, Li X, Zhang Y, et al. Endocytic sorting and recycling require membrane phosphatidylserine asymmetry maintained by TAT-1/CHAT-1. *PLoS Genet.* 2010;6(12):e1001235.
151. Qadota H, Inoue M, Hikita T, Koppen M, Hardin JD, Amano M, et al. Establishment of a tissue-specific RNAi system in *C. elegans*. *Gene.* 2007 Oct 1;400(1-2):166-73.
152. Kos V, Ford RC. The ATP-binding cassette family: a structural perspective. *Cell Mol Life Sci.* 2009 Oct;66(19):3111-26.
153. Kim BE, Nevitt T, Thiele DJ. Mechanisms for copper acquisition, distribution and regulation. *Nat Chem Biol.* 2008 Mar;4(3):176-85.
154. Toyoda Y, Hagiya Y, Adachi T, Hoshijima K, Kuo MT, Ishikawa T. MRP class of human ATP binding cassette (ABC) transporters: historical background and new research directions. *Xenobiotica.* 2008 Jul;38(7-8):833-62.
155. Yabuuchi H, Shimizu H, Takayanagi S, Ishikawa T. Multiple splicing variants of two new human ATP-binding cassette transporters, ABCC11 and ABCC12. *Biochem Biophys Res Commun.* 2001 Nov 9;288(4):933-9.

156. Shafizadeh E, Paw BH. Zebrafish as a model of human hematologic disorders. *Curr Opin Hematol.* 2004 Jul;11(4):255-61.
157. Paik EJ, Zon LI. Hematopoietic development in the zebrafish. *Int J Dev Biol.* 2010;54(6-7):1127-37.
158. Protchenko O, Rodriguez-Suarez R, Androphy R, Bussey H, Philpott CC. A screen for genes of heme uptake identifies the FLC family required for import of FAD into the endoplasmic reticulum. *J Biol Chem.* 2006 Jul 28;281(30):21445-57.
159. Schuller HJ. Transcriptional control of nonfermentative metabolism in the yeast *Saccharomyces cerevisiae*. *Curr Genet.* 2003 Jun;43(3):139-60.
160. Hon T, Dodd A, Dirmeier R, Gorman N, Sinclair PR, Zhang L, et al. A mechanism of oxygen sensing in yeast. Multiple oxygen-responsive steps in the heme biosynthetic pathway affect Hap1 activity. *J Biol Chem.* 2003 Dec 12;278(50):50771-80.
161. Dancis A, Klausner RD, Hinnebusch AG, Barriocanal JG. Genetic evidence that ferric reductase is required for iron uptake in *Saccharomyces cerevisiae*. *Mol Cell Biol.* 1990 May;10(5):2294-301.
162. Paumi CM, Chuk M, Snider J, Stagljar I, Michaelis S. ABC transporters in *Saccharomyces cerevisiae* and their interactors: new technology advances the biology of the ABCC (MRP) subfamily. *Microbiol Mol Biol Rev.* 2009 Dec;73(4):577-93.
163. Yang Z, Philips JD, Doty RT, Giraudi P, Ostrow JD, Tiribelli C, et al. Kinetics and specificity of feline leukemia virus subgroup C receptor (FLVCR) export function and its dependence on hemopexin. *J Biol Chem.* 2010 Sep 10;285(37):28874-82.

164. Chen W, Dailey HA, Paw BH. Ferrochelatase forms an oligomeric complex with mitoferrin-1 and Abcb10 for erythroid heme biosynthesis. *Blood*. 2010 Jul 29;116(4):628-30.
165. Suzuki T, Sasaki H, Kuh HJ, Agui M, Tatsumi Y, Tanabe S, et al. Detailed structural analysis on both human MRP5 and mouse *mrp5* transcripts. *Gene*. 2000 Jan 25;242(1-2):167-73.
166. Wang F, Paradkar PN, Custodio AO, McVey Ward D, Fleming MD, Campagna D, et al. Genetic variation in *Mon1a* affects protein trafficking and modifies macrophage iron loading in mice. *Nat Genet*. 2007 Aug;39(8):1025-32.
167. Scheffer GL, Kool M, Heijn M, de Haas M, Pijnenborg AC, Wijnholds J, et al. Specific detection of multidrug resistance proteins MRP1, MRP2, MRP3, MRP5, and MDR3 P-glycoprotein with a panel of monoclonal antibodies. *Cancer Res*. 2000 Sep 15;60(18):5269-77.
168. Micronutrient deficiencies. Battling iron deficiency anaemia: The challenge. 2003. <http://www.who.int/nut/ida.htm>. 2003.
169. Iron deficiency anaemia: assessment, prevention and control. A guide for programme managers. Geneva, World Health Organization, (Document WHO/NHD/01.3). 2001.
170. Uzel C, Conrad ME. Absorption of heme iron. *Semin Hematol*. 1998 Jan;35(1):27-34.
171. Fleming MD, Hamza I. Mitochondrial heme: an exit strategy at last. *J Clin Invest*. 2012 Dec 3;122(12):4328-30.

172. Tammur J, Prades C, Arnould I, Rzhetsky A, Hutchinson A, Adachi M, et al. Two new genes from the human ATP-binding cassette transporter superfamily, ABCC11 and ABCC12, tandemly duplicated on chromosome 16q12. *Gene*. 2001 Jul 25;273(1):89-96.
173. Kruh GD, Guo Y, Hopper-Borge E, Belinsky MG, Chen ZS. ABCC10, ABCC11, and ABCC12. *Pflugers Arch*. 2007 Feb;453(5):675-84.
174. Ono N, Van der Heijden I, Scheffer GL, Van de Wetering K, Van Deemter E, De Haas M, et al. Multidrug resistance-associated protein 9 (ABCC12) is present in mouse and boar sperm. *Biochem J*. 2007 Aug 15;406(1):31-40.
175. Bonifacino JS, Traub LM. Signals for sorting of transmembrane proteins to endosomes and lysosomes. *Annu Rev Biochem*. 2003;72:395-447.
176. Lutsenko S, Petris MJ. Function and regulation of the mammalian copper-transporting ATPases: insights from biochemical and cell biological approaches. *J Membr Biol*. 2003 Jan 1;191(1):1-12.
177. Lagace TA, Ridgway ND. The role of phospholipids in the biological activity and structure of the endoplasmic reticulum. *Biochim Biophys Acta*. 2013 Nov;1833(11):2499-510.
178. Frelet A, Klein M. Insight in eukaryotic ABC transporter function by mutation analysis. *FEBS Lett*. 2006 Feb 13;580(4):1064-84.
179. Ernst R, Kueppers P, Stindt J, Kuchler K, Schmitt L. Multidrug efflux pumps: substrate selection in ATP-binding cassette multidrug efflux pumps--first come, first served? *FEBS J*. 2010 Feb;277(3):540-9.

180. Wheeler DL, Church DM, Federhen S, Lash AE, Madden TL, Pontius JU, et al. Database resources of the National Center for Biotechnology. *Nucleic Acids Res.* 2003 Jan 1;31(1):28-33.
181. Sherry ST, Ward MH, Kholodov M, Baker J, Phan L, Smigielski EM, et al. dbSNP: the NCBI database of genetic variation. *Nucleic Acids Res.* 2001 Jan 1;29(1):308-11.
182. Wolters DA, Washburn MP, Yates JR, 3rd. An automated multidimensional protein identification technology for shotgun proteomics. *Anal Chem.* 2001 Dec 1;73(23):5683-90.
183. Washburn MP, Wolters D, Yates JR, 3rd. Large-scale analysis of the yeast proteome by multidimensional protein identification technology. *Nat Biotechnol.* 2001 Mar;19(3):242-7.
184. Brennan ML, Anderson MM, Shih DM, Qu XD, Wang X, Mehta AC, et al. Increased atherosclerosis in myeloperoxidase-deficient mice. *J Clin Invest.* 2001 Feb;107(4):419-30.
185. Mahler JF, Davis BJ, Morham SG, Langenbach R. Disruption of cyclooxygenase genes in mice. *Toxicol Pathol.* 1996 Nov-Dec;24(6):717-9.
186. Dailey HA. Terminal steps of haem biosynthesis. *Biochem Soc Trans.* 2002 Aug;30(4):590-5.
187. Tsiftoglou AS, Tsamadou AI, Papadopoulou LC. Heme as key regulator of major mammalian cellular functions: Molecular, cellular, and pharmacological aspects. *Pharmacol Ther.* 2006;111(2):327-45.

188. Drakesmith H, Prentice AM. Heparin and the iron-infection axis. *Science*. 2012 Nov 9;338(6108):768-72.
189. Ji C, Juarez-Hernandez RE, Miller MJ. Exploiting bacterial iron acquisition: siderophore conjugates. *Future Med Chem*. 2012 Mar;4(3):297-313.
190. Silva-Gomes S, Vale-Costa S, Appelberg R, Gomes MS. Iron in intracellular infection: to provide or to deprive? *Front Cell Infect Microbiol*. 2013;3:96.